

Arnold Diffusion, Quantitative Estimates and Stochastic Behavior in the Three-Body Problem

Maciej J. Capiński

Faculty of Applied Mathematics
AGH University of Science and Technology
al. Mickiewicza 30, 30-059 Kraków, Poland

Marian Gidea

Department of Mathematical Sciences
Yeshiva University
New York, NY 10016, USA

October 19, 2020

Abstract

We consider a class of autonomous Hamiltonian systems subject to small, time-periodic perturbations. When the perturbation parameter is set to zero, the energy of the system is preserved. This is no longer the case when the perturbation parameter is non-zero.

We describe a topological method to establish orbits which diffuse in energy for every suitably small perturbation parameter $\varepsilon > 0$. The method yields quantitative estimates: (i) The existence of orbits along which the energy drifts by an amount independent of ε . The time required by such orbits to drift is $O(1/\varepsilon)$; (ii) The existence of orbits along which the energy makes chaotic excursions; (iii) Explicit estimates for the Hausdorff dimension of the set of such chaotic orbits; (iv) The existence of orbits along which the time evolution of energy approaches a stopped diffusion process (Brownian motion with drift), as ε tends to 0. For each ε fixed, the set of initial conditions of the orbits that yield the diffusion process has positive Lebesgue measure, and in the limit the measure of these sets approaches zero.

Moreover, we can obtain any desired values of the drift and variance for the limiting Brownian motion, for appropriate sets of initial conditions.

A key feature of our topological method is that it can be implemented in computer assisted proofs. We give an application to a concrete model of the planar elliptic restricted three-body problem, on the motion of an infinitesimal body relative to the Neptune-Triton system.

Contents

1	Introduction	2
2	Statement of the main theorem	7
3	Tools	11
4	Master theorems	17
5	Proof of the main theorem	21
6	Propagation of discs	36
7	Existence of diffusing orbits	38
8	Symbolic dynamics	40
9	Hausdorff dimension	44
10	Stochastic behavior	46
11	Appendix	55

1 Introduction

1.1 Motivation

The Arnold diffusion problem concerns global instability in Hamiltonian systems under arbitrarily small perturbations, which yield the existence of orbits undergoing large effects over time. While Arnold illustrated such an instability mechanism in a particular example [1], he conjectured that it “*is applicable to the general case (for example, to the problem of three bodies)*”. Quantitative properties of Arnold’s mechanism were first explored by Chirikov [2], who conjectured that the energy of perturbed orbits can follow a diffusion process. For this reason he coined the term “Arnold diffusion” to describe this behaviour.

In this paper, we develop a topological method to study Arnold diffusion in concrete models, under verifiable conditions. We consider an autonomous Hamiltonian system, in which the energy is preserved, and study its dynamics under small, time dependent perturbations. We show that for every value of the perturbation parameter within some range, there exist orbits that drift in energy, as well as orbits that undergo chaotic excursions in energy, over an explicit energy range which is independent of the size of the perturbation. We will refer to them as ‘diffusing orbits’. Further, we extract quantitative information on the diffusing orbits: an explicit estimate on the diffusion time; an explicit estimate on the Lebesgue measure of orbits that drift in energy for every fixed perturbation parameter; an explicit estimate on the Hausdorff dimension of chaotic orbits; and an explicit description of the limiting stochastic process – as the perturbation parameter tends to zero – associated to diffusing orbits.

Some of the existing results on Arnold diffusion are devoted to arbitrarily small perturbations of ‘generic type’ in ‘generic systems’. The novelty of our work is that we obtain a mechanism of diffusion that can also be applied to concrete systems, for concrete perturbations, and for perturbation parameters from arbitrarily close to zero up to some physically relevant value.

Besides deriving our results via a traditional mathematical proof, we produce a method that is implementable in computer assisted proofs which use validated numerical methods. We develop a topological method which allows us to obtain – by verifying only a finite number of explicit conditions up to finite precision – asymptotic results for infinitely many parameter values (an interval with one endpoint at zero), and for infinite sets of initial conditions (of positive Lebesgue measure, or of large Hausdorff dimension).

We apply this method to study diffusion in the elliptic restricted three-body problem (PER3BP), on the motion of a small body (e.g., asteroid or spaceship) under the gravity exerted by two larger bodies moving on Keplerian ellipses. We regard the eccentricity of the orbits of the large bodies as a perturbation parameter, where the unperturbed case corresponds to the planar circular restricted three-body problem (PCR3BP). We consider the PER3BP for physically relevant values of the mass ratio of the large bodies and of the eccentricity of their orbits. In particular, our results hold for the observed values in the Neptune-Triton system (which has the smallest eccentricity in the Solar System). We expect that with extra work we can extend the range of applicability. For simplicity, in the rest of the paper we will describe results for the PER3BP with the same mass ratio and eccentricity as the Neptune-Triton system. Of course, since our results are quite robust, it is to be expected that they also apply to models that incorporate more small effects (such as, the unrestricted three body problem with small mass of the small body).

While in this work we focus on the PER3BP, the underlying topological method can be applied to other models, for instance, to time-dependent, generic perturbations of the geodesic flow, the so called “Mather acceleration” problem.

1.2 Brief description of the main results

Consider a class of Hamiltonian systems of the form

$$H_\varepsilon(x, y, I, \theta) = H_0(x, y, I, \theta) + \varepsilon H_1(x, y, I, \theta, t; \varepsilon),$$

where (x, y, I, θ) takes values in some sub-domain of $\mathbb{R}^{n_u} \times \mathbb{R}^{n_s} \times \mathbb{R}^{n_c} \times \mathbb{T}^{n_c}$, $n_u = n_s > 0$, $n_c > 0$, and $t \in \mathbb{T}^1$. Here \mathbb{T}^k , $k \geq 1$, stands for the k -dimensional torus, and the symplectic form is $\omega = dy \wedge dx + dI \wedge d\theta$.

Suppose that, for the unperturbed system, when $\varepsilon = 0$, there exists a $(2n_c)$ -dimensional normally hyperbolic invariant manifold Λ_0 , corresponding to $x = y = 0$, which can be described via action-angle coordinates (I, θ) , where I is an integral of motion; that is, $I = \text{const.}$ along each trajectory in Λ_0 . Suppose that the stable and unstable manifolds $W^s(\Lambda_0)$ and $W^u(\Lambda_0)$ of Λ_0 intersect transversally. The energy H_0 is preserved along trajectories; in particular, each homoclinic orbit is bi-asymptotic to the same action level set $I = \text{const.}$ in Λ_0 . There is no diffusion in the action variable I .

When we add the perturbation, i.e., we let $\varepsilon \in (0, \varepsilon_0]$, with ε_0 sufficiently small, we have persistence of the normally hyperbolic invariant manifold Λ_0 to some manifold

Λ_ε . The stable and unstable manifolds $W^s(\Lambda_\varepsilon)$ and $W^u(\Lambda_\varepsilon)$ of Λ_ε continue intersecting transversally. Take a neighborhood of Λ_ε where the action variable I is well defined, and a family of return maps to that neighborhood. To show the existence of diffusing orbits, that is, orbits along which I changes by $O(1)$, as well as symbolic dynamics relative to I , it is sufficient to show that these properties can be achieved by iterating the return maps in suitable ways.

The class of systems considered above, when the unperturbed Hamiltonian has periodic/quasiperiodic orbits whose stable and unstable manifolds intersect transversally, is sometimes referred to as *a priori chaotic*.

When we let $\varepsilon > 0$ small, the system is not autonomous, so the energy is no longer preserved. There exist diffusing orbits that follow $W^u(\Lambda_\varepsilon)$, $W^s(\Lambda_\varepsilon)$ and return to a neighborhood of Λ_ε with an $O(\varepsilon)$ -change in the action coordinate I , and implicitly an $O(\varepsilon)$ -change in their energy. The effects of the small perturbation can accumulate over time. The existence of orbits whose I -coordinate explores a $O(1)$ -region of the action-space amounts to the Arnold diffusion phenomenon in this setting.

Our methods allow us to prove the following results:

- There exists an explicit constant $C_{h_0} > 0$, independent of the perturbation, such that, for each $\varepsilon \in (0, \varepsilon_0]$, there exist orbits for which $\|I(t(\varepsilon)) - I(0)\| \geq C_{h_0}$, for some $t(\varepsilon) > 0$. We provide estimates on the Lebesgue measure of such orbits. Moreover, we show that the corresponding diffusion time $t(\varepsilon)$ satisfies $t(\varepsilon) \leq T/\varepsilon$ for some explicit constant $T > 0$. This order of time for diffusion is optimal for the class of a priori chaotic systems considered in this paper.
- Given a sequence of action level sets $(I^\sigma)_{\sigma \geq 0}$, with $\|I^{\sigma+1} - I^\sigma\| > 2\eta\varepsilon$, for some suitable $\eta > 0$, there exists an orbit with $\|I(t^\sigma) - I^\sigma\| < \eta\varepsilon$, for some increasing sequence of times $t^\sigma > 0$ and all $\sigma \geq 0$;
- The set of all initial points whose orbits $(\eta\varepsilon)$ -shadow, in terms of the action variable I , any prescribed sequence of action level sets $(I^\sigma)_{\sigma \geq 0}$ as above, has Hausdorff dimension strictly greater than 4.
- Consider the stochastic process $X_t^\varepsilon(z)$ given by the energy path along an orbit starting from z , with appropriately rescaled time t . Then, for every choice of $\mu \in \mathbb{R}$, $\sigma \in \mathbb{R}^+$, there exists a set of points $z \in \Omega_\varepsilon$, of positive Lebesgue measure, such that X_t^ε converges to $\mu t + \sigma W_t$ as $\varepsilon \rightarrow 0$, where W_t is the standard Brownian motion. The convergence is in the sense of the functional central limit theorem (see Section 10).

The situation described above is present in the PER3BP. In this case $n_u = n_s = n_c = 1$. The PER3BP can be described as a time-periodic Hamiltonian perturbation of the autonomous Hamiltonian associated to the PCR3BP, with the perturbation parameter ε equal to the eccentricity of the orbits of the primaries. In the PCR3BP, we choose one of the equilibrium points of center-saddle type. The typical geometric picture is the following. There is a family of Lyapunov periodic orbits around this point that forms a 2-dimensional normally hyperbolic invariant manifold (NHIM) Λ_0 . The dynamics restricted to Λ_0 is integrable and can be described in action-angle coordinates (I, θ) on Λ_0 ; each Lyapunov orbit corresponds to a unique value of I . The action coordinate I is uniquely

determined by the energy of the PCR3BP. The stable and unstable manifolds $W^s(\Lambda_0)$ and $W^u(\Lambda_0)$ turn around the main bodies and intersect along transverse homoclinic orbits. After the perturbation Λ_0 is perturbed to Λ_ε , with a Cantor set of Lyapunov orbits surviving as KAM tori in the extended phase space [3].

1.3 Methodology

Our argument has several components that involve different tools. We first use topological methods to identify a mechanism that, given some conditions verifiable by finite computations in a concrete system, leads to the existence of orbits which diffuse and for which we have symbolic dynamics in energy. We also use some stochastic analysis and geometry to show that the topological description leads to a set of orbits – with initial conditions of positive Lebesgue measure for finite time approximation and a fixed perturbation parameter, and of positive Hausdorff dimension for arbitrarily long time – whose dynamics can be described as a stochastic process. In other words, we use traditional mathematical methods to show that some structures verifiable with finite precision, lead to dynamical, stochastic and geometric consequences.

In a second part, we use computer assisted proofs to verify these conditions in a concrete model of astronomical interest, namely the Neptune-Triton system. The code and the documentation for the computer assisted proof is available on the web page of the first author.

1.4 Overview

Our argument relies on topological methods and their implementation into computer assisted proofs. The main topological tool is *correctly aligned windows with cone conditions*; see [4, 5].

A window is a multidimensional rectangle with some distinguished ‘topologically unstable’ and ‘topologically stable’ directions. Two windows are correctly aligned under some mapping if the image of the first window stretches across the second window along its ‘topologically unstable’ directions. Given a family of cones, a mapping is said to satisfy a cone condition if it maps cones in the family inside cones in the family. The correct alignment of windows with cone conditions can be validated using rigorous numerics with interval arithmetic.

We construct windows inside some surfaces of sections along the NHIM and along its hyperbolic stable and unstable manifolds mentioned in Section 1.2. The NHIM and its hyperbolic stable and unstable manifolds induce stable and unstable hyperbolic coordinates as well as centre coordinates on the aforementioned surfaces of sections. The constructed windows have their ‘topologically unstable’ directions aligned with the hyperbolic unstable directions, and their ‘topologically stable’ directions aligned with the hyperbolic stable directions and centre directions combined. The correct alignment of windows is achieved by the appropriate section-to-section mappings.

To control the behavior of the windows in the centre directions, in our theoretical arguments we consider topological discs inside the windows, which are aligned with their ‘topologically unstable’ directions. These discs also satisfy cone conditions, they are uniformly bounded in the centre directions. Given a finite sequence of correctly aligned windows with cone conditions, for every such disc inside the first window there exists a

disc inside the last window, which is the image of a subset of the first disc. Consequently, there exist orbits that ‘shadow’ the given sequence of windows. If the resulting disc in the last window of a sequence can be fitted inside the first window of another sequence of windows, the ‘shadowing’ can be continued through this new sequence of windows. In our constructions, we continue this ‘shadowing’ process indefinitely by concatenating only a finite collection of finite sequences of correctly aligned windows. Using these discs is a novel contribution to the method of correctly aligned windows, which allows us to obtain infinite ‘shadowing’ for systems with center coordinates by using only finitely many windows.

In our construction for our diffusion results, certain sequences of correctly aligned windows from the collection yield a growth in the action variable by $O(\varepsilon)$. Other sequences yield a decay in the action by $O(\varepsilon)$. Checking the growth (resp. decay) in action by $O(\varepsilon)$ is done by computing the derivative with respect to ε of the action along the underlying composition of section-to-section mappings, and showing that this derivative is larger than some positive constant (resp. smaller than some negative constant). The verification can be done via rigorous numerics. This is the key step that allows us to quantify the change in action along sequences of correctly aligned windows, for all ε (including values arbitrarily close to 0).

We can follow repeatedly the sequences of windows that yield growth in action until we obtain a growth of order $O(1)$. We can also alternate sequences of windows that yield growth in action with sequences that achieve decay in action to obtain symbolic dynamics, hence chaotic orbits. The conclusion is the existence of diffusing orbits and symbolic dynamics, for every value of the perturbation parameter $\varepsilon \in (0, \varepsilon_0]$. We emphasize that our procedure involves the construction of only finitely many windows, and the rigorous verification of only finitely many correct alignments with cone conditions.

The orbits that achieve diffusion and symbolic dynamics have initial points lying on C^0 -families of discs. This allows us to obtain information about the Lebesgue measure and the Hausdorff dimension of such orbits.

Moreover, we use the symbolic dynamics to show the existence of orbits whose time-evolution of the action variable follows a random walk. For $\varepsilon > 0$ fixed, the set of initial points that follow such a random walk for finitely many steps has positive Lebesgue measure. When we let $\varepsilon \rightarrow 0$, we obtain in the limit a stopped diffusion process (Brownian motion with drift). Moreover, we can obtain any Brownian motion with drift that we wish, for suitable choices of sets of initial points.

1.5 Related works

In the recent years, the Arnold diffusion problem has taken a central role in the study of Hamiltonian dynamics. Significant works, using variational methods or geometric methods, include, e.g., [6–34]. There are also numerical approaches, including, e.g., [35–43]. Part of the interest in Arnold diffusion is owed to the seminal work of John Mather in the field [44, 45], as well as to possible applications to celestial mechanics, dynamical astronomy, particle accelerators, and plasma confinement; see, e.g., [46–48].

In particular, various mechanisms for Arnold diffusion in the N -body problem have been examined in several papers, including, e.g., [3, 49–56]. The present work is closely related to [3], in which Arnold diffusion is shown in the PERTBP, using a shadowing

lemma for NHIM's ([34]) and numerical arguments. The paper [3] assumes the existence of a NHIM, and does not provide quantitative estimates on diffusion; also, the numerical experiments are non-rigorous. In the present paper we develop an entirely new methodology, which does not need to assume or to verify the existence of a NHIM. Moreover, we provide quantitative estimates via computer assisted proofs. In particular, we show that diffusing orbits exist in the concrete system under consideration, with the given mass parameter and up to the true value of the eccentricity.

Several works, including e.g. [11, 17, 18, 23, 57–63], obtain estimates on the diffusion time. A novelty of our results is that we provide optimal estimates on the diffusing time with explicit constants, and for the full range of parameters under consideration.

Estimates on the Hausdorff dimension of the set of initial conditions for unstable orbits appear for example in [64], where they study oscillatory motions in the Sitnikov problem and in the PCR3BP. In this paper we provide estimates on the Lebesgue measure of the set of initial conditions for orbits that drift on energy, and on the Hausdorff dimension of the set of initial conditions for orbits undergoing symbolic dynamics.

Related works that provide analytic results on the stochastic process followed by diffusing orbits in random iterations of the maps appear in, e.g., [65–68]. There are also heuristic arguments and numerical work, e.g., [2, 69, 70]. A novelty of this paper is that we provide rigorous results, via a computer assisted proof, on the stochastic process underlying diffusing orbits, as the perturbation parameter tends to zero. Moreover, we can obtain in the limit *any Brownian motion with drift*, that is, any value of the drift and variance.

2 Statement of the main theorem

Our results on Arnold diffusion in the PER3BP are stated in Theorem 1. They are derived from the general results obtained in this paper – Theorems 2, 3, 4 and 5. These general results and the underlying methodology can be applied to other models, for instance to time-dependent, generic perturbations of the geodesic flow [13, 16, 62].

2.1 Model

We first briefly introduce the model and then state the main result. Our model describes the motion of a massless particle (e.g., an asteroid or a spaceship), under the gravitational pull of two large bodies, which we call primaries. The primaries rotate in a plane along Keplerian elliptical orbits with eccentricity ε , while the massless particle moves in the same plane and has no influence on the orbits of the primaries. We use normalized units, in which the masses of the primaries are μ and $1 - \mu$. We consider a frame of ‘pulsating’ coordinates that rotates together with the primaries, making their position fixed on the horizontal axis [71]. The motion of the massless particle is described via the Hamiltonian

$H_\varepsilon : \mathbb{R}^4 \times \mathbb{T} \rightarrow \mathbb{R}$

$$\begin{aligned}
H_\varepsilon(X, Y, P_X, P_Y, \theta) &= \frac{(P_X + Y)^2 + (P_Y - X)^2}{2} - \frac{\Omega(X, Y)}{1 + \varepsilon \cos(\theta)}, \\
\Omega(X, Y) &= \frac{1}{2}(X^2 + Y^2) + \frac{(1 - \mu)}{r_1} + \frac{\mu}{r_2}, \\
r_1^2 &= (X - \mu)^2 + Y^2, \\
r_2^2 &= (X - \mu + 1)^2 + Y^2.
\end{aligned} \tag{1}$$

The corresponding Hamilton equations are:

$$\begin{aligned}
\frac{dX}{d\theta} &= \frac{\partial H_\varepsilon}{\partial P_X}, & \frac{dP_X}{d\theta} &= -\frac{\partial H_\varepsilon}{\partial X}, \\
\frac{dY}{d\theta} &= \frac{\partial H_\varepsilon}{\partial P_Y}, & \frac{dP_Y}{d\theta} &= -\frac{\partial H_\varepsilon}{\partial Y},
\end{aligned} \tag{2}$$

where $X, Y \in \mathbb{R}$ are the position coordinates of the massless particle, and $P_X, P_Y \in \mathbb{R}$ are the associated linear momenta. The variable $\theta \in \mathbb{T}$ is the true anomaly of the Keplerian orbits of the primaries, where \mathbb{T} denotes the 1-dimensional torus. The system is non-autonomous, thus we consider it in the extended phase space, of dimension 5, which includes θ as an independent variable. We use the notation Φ_t^ε to denote the flow of (2) in the extended phase space, which includes $\theta \in \mathbb{T}$.

When $\varepsilon = 0$ the corresponding Hamiltonian H_0 describes the PCR3BP, and the variable θ represents the physical time. An important feature of our model is that the Hamiltonian H_0 is autonomous, hence the energy is preserved. The energy H_0 is no longer preserved when $\varepsilon > 0$. The main objective of this paper is to investigate the changes in the energy when $\varepsilon > 0$.

There are certain geometric structures that organize the dynamics. The Hamiltonian vector field of H_0 has 5 equilibrium points. One of these points, denoted by L_1 , is located between the primaries, and is of center-stable linear stability type. There exists a family of Lyapunov periodic orbits about L_1 . Each Lyapunov periodic orbit is uniquely characterized by some fixed value of the energy H_0 . The family of Lyapunov orbits form a normally hyperbolic invariant manifold (NHIM) with boundary in the phase space, which we denote as Λ_0 . The NHIM has associated stable and unstable manifolds, $W^s(\Lambda_0)$, $W^u(\Lambda_0)$, respectively. For certain values of the mass ratio and energy, one can observe numerically that $W^s(\Lambda_0)$ and $W^u(\Lambda_0)$ intersect transversally.

The NHIM Λ_0 and the homoclinic orbits to Λ_0 are the geometric objects on which the computer assisted proof is based. We emphasize that in the computer assisted proof we do not need an explicit knowledge of these objects. We only use numerical approximations of these objects to construct the tools – correctly aligned windows with cone condition – which are used in the computer assisted proof.

2.2 Main theorem

Below we state our main theorem.

Theorem 1 Consider the Neptune-Triton PER3BP, with mass ratio $\mu = 2.089 \cdot 10^{-4}$, and orbit eccentricity $\varepsilon_0 = 1.6 \cdot 10^{-5}$. Let h_0 be a fixed energy level, specified below, and $I = H_0 - h_0$ be the rescaled energy. We have the following results:

- (1) (Diffusing orbits) There exist $C_{h_0} > 0$ and $T > 0$ such that for every $\varepsilon \in (0, \varepsilon_0]$, there exists a point $z(\varepsilon)$ and a time $t(\varepsilon) \in (0, T/\varepsilon)$, such that

$$I\left(\Phi_{t(\varepsilon)}^\varepsilon(z(\varepsilon))\right) - I(z(\varepsilon)) > C_{h_0}. \quad (3)$$

The Lebesgue measure of the set of points z satisfying (3) has a lower bound given by Theorem 2, where the respective constants are defined in Theorem 8 and (50).

- (2) (Symbolic dynamics) There exists $\eta > 0$ such that for every $\varepsilon \in (0, \varepsilon_0]$ and every sequence $\{I^n\}_{n \in \mathbb{N}}$, $I^n \in [2\eta\varepsilon, C_{h_0} - 2\eta\varepsilon]$ with $|I^{n+1} - I^n| > 2\eta\varepsilon$ there exists a point z and an increasing sequence of times $t^n > 0$, for $n \in \mathbb{N}$, such that

$$|I(\Phi_{t^n}^\varepsilon(z)) - I^n| < \eta\varepsilon \quad \text{for all } n \in \mathbb{N}.$$

- (3) (Hausdorff dimension) Given $\{I^n\}_{n \in \mathbb{N}}$ as in (2), the Hausdorff dimension of the set

$$\{z : \exists (t^n)_{n \in \mathbb{N}} \text{ positive and increasing, s.t. } \forall n \in \mathbb{N}, |I(\Phi_{t^n}^\varepsilon(z)) - I^n| < \eta\varepsilon\}$$

is strictly greater than 4 (in the 5 dimensional extended phase space).

- (4) (Stochastic behavior) Let $\gamma > \frac{3}{2}$. For each $X_0 \in (0, C_{h_0})$, $\mu \in \mathbb{R}$, $\sigma > 0$, consider the stochastic processes

$$X_t^0 := X_0 + \mu t + \sigma W_t, \quad \text{for } t \in [0, 1].$$

For $\varepsilon > 0$ and a given point z define the energy path ¹

$$X_t^\varepsilon(z) := I(\Phi_{t\varepsilon^{-\gamma}}^\varepsilon(z)), \quad \text{for } t \in [0, 1].$$

Define the stopping time

$$\tau = \tau(X^\varepsilon) := \inf \{t : X_t^\varepsilon \geq C_{h_0} \text{ or } X_t^\varepsilon \leq 0\}.$$

Then for every $0 < \varepsilon < \varepsilon_0$ there exists a set Ω_ε of positive Lebesgue measure, such that the process $X_t^\varepsilon : \Omega_\varepsilon \rightarrow \mathbb{R}$, for $t \in [0, 1]$, has the following limit

$$\lim_{\varepsilon \rightarrow 0} X_{t \wedge \tau}^\varepsilon = X_{t \wedge \tau}^0,$$

where $t \wedge \tau = \min(t, \tau)$. Above, Ω_ε is endowed with with the sigma field of Borel sets and the normalized Lebesgue measure (i.e., $\mathbb{P}_\varepsilon(\Omega_\varepsilon) = 1$), and the limit is in the sense of the functional central limit theorem (see Section 10).

¹Alternatively we could define the energy paths as $X_t^\varepsilon(z) := I(\Phi_{\gamma\varepsilon^{-3/2}t}^\varepsilon(z))$, by taking sufficiently large $\gamma > 0$. The explicit size of such γ and the related details are outlined in the footnotes in Section 10.

The constants in the statements (1)-(4) above can be chosen as

$$h_0 = -1.5050906397016, \quad C_{h_0} = 10^{-6}, \quad T = \frac{1}{4}, \quad \eta = 10^{-2}.$$

Remark 1 In the statement of Theorem 1, $\varepsilon_0 = 1.6 \cdot 10^{-5}$ represents the true value of the eccentricity of the orbit of Triton. This is among the lowest values of orbital eccentricities among the planets and moons in our solar system. Triton is believed to have been captured by Neptune about 1 billion years ago in a highly eccentric orbit, which decayed in time to the currently observed value [72].

The PRE3BP is a simplified model, which neglects the effects of the other bodies in the solar system on the small particle. In the case of the Neptune-Triton system such effects are non-negligible. We therefore do not claim that our results are fully physical. They should be viewed as a mathematical model of some planet-moon or star-planet system, which is isolated from other effects. We have chosen the Neptune-Triton system due to its small eccentricity. When eccentricity is small, it is hard to observe diffusion directly by integrating the system and measuring the change in energy along the trajectory.

Remark 2 The constant h_0 in the statement of Theorem 1 is the energy of some Lyapunov orbit, depicted in Figure 2. This is merely a choice of convenience.

Statement (1) of Theorem 1 shows the existence of orbits that diffuse in energy for the whole range of eccentricities from zero up to the current value of the eccentricity of the orbit of Triton. In particular, there exist orbits whose energy changes by at least $C_{h_0} = 10^{-6}$, in a time at most $T/\varepsilon_0 = \frac{5}{32} \cdot 10^5$, in normalized units. In real units these values are physically significant. Indeed, the energy drift C_{h_0} corresponds to a distance of order 1 km between two Lyapunov orbits whose energy differs by C_{h_0} . Since the orbital period of Triton is 6 days, which corresponds to 2π in our model, the time T/ε_0 needed to achieve this change is under 42 years. Yet the Lebesgue measure of the set of initial points of diffusing orbits which we establish is exponentially small in ε .

Statement (2) of Theorem 1 shows that any sequence of energy levels within the range $(0, C_{h_0})$ can be $O(\varepsilon)$ -shadowed by true orbits. There is a mild condition that these level sets should be chosen $O(\varepsilon)$ apart from one another as well as from the endpoints of the energy range.

Statement (4) of Theorem 1 shows that for any prescribed Brownian motion with drift, there exist sets of initial conditions Ω_ε for which the corresponding energy paths approach asymptotically, as $\varepsilon \rightarrow 0$, the given Brownian motion with drift. This fact is consistent with Chirikov's empirical observations in [2] that different sets of initial conditions yield different stochastic processes. The obtained sets Ω_ε have positive Lebesgue measure which goes to 0 as $\varepsilon \rightarrow 0$. The broader question on characterizing the limiting stochastic process for a fixed set of initial points of positive measure is an open question.

We emphasize that the methodology in this paper can be used to obtain results similar to those in Theorem 1 for other concrete three-body problems, with higher values of the eccentricity.

Remark 3 The diffusion time of order $O(1/\varepsilon)$ in (1) is optimal for a priori chaotic Hamiltonian systems, in the sense that the energy $H_0(z(t))$, hence the action I , cannot grow in time faster than $O(\varepsilon)$ (see, e.g., [17, 62]). Indeed, if $z(t)$ is a solution of a

Hamiltonian of the form

$$H_\varepsilon(z, t) = H_0(z) + \varepsilon H_1(z, t; \varepsilon),$$

then we have

$$\frac{d}{dt}H_0(z(t)) = \varepsilon[H_0, H_1](z(t), t; \varepsilon),$$

where $[\cdot, \cdot]$ denotes the Poisson bracket. In our setting, both H_0 and H_1 and their derivatives are bounded since we restrict to z in a compact neighborhood of some homoclinic orbit, $t \in \mathbb{T}^1$, and $\varepsilon \in [0, \varepsilon_0]$; see Section 5, and in particular Figure 2. This implies that there is a constant $A > 0$ such that

$$|H_0(z(t)) - H_0(z(0))| \leq \varepsilon A t, \quad \text{for all } t \geq 0,$$

hence the energy $H_0(z(t))$ cannot grow faster than linearly in time, with an $O(\varepsilon)$ growth rate.

3 Tools

Our diffusion mechanism will be based on some abstract topological results – Theorems 2, 3, 4 and 5, – from which the proof of Theorem 1 will follow. These results are formulated in the general context of a non-autonomous, parameter dependent C^r -smooth Hamiltonian $H_\varepsilon : \mathbb{R}^{n_u+n_s+2n_c} \times \mathbb{T} \rightarrow \mathbb{R}$ of the form

$$H_\varepsilon(z, t) = H_0(z) + \varepsilon H_1(z, t; \varepsilon), \tag{4}$$

where $r \geq 3$, $n_u = n_s \geq 1$, $n_c \geq 1$, and $\varepsilon \in [0, \varepsilon_0]$. The associated ODE is

$$z'(t) = J\nabla H_\varepsilon(z(t), t), \tag{5}$$

where J is the standard almost complex structure on $\mathbb{R}^{n_u+n_s+2n_c}$. Although $n_u = n_s$, we will keep the two notations separate for convenience. (In the sequel, n_u will play the role of the dimension of the ‘unstable’ variables, n_s of the ‘stable’ variables, and $2n_c$ of the ‘center’ ones).

We denote by $\Phi_t^\varepsilon(z, \theta)$ the flow induced by (5) in the extended phase space, where $(z, \theta) \in \mathbb{R}^{n_u+n_s+2n_c} \times \mathbb{T}$, and $\theta'(t) = 1$. Note that for $\varepsilon = 0$ the system (4) is autonomous, so H_0 is preserved along the solutions.

In the context of the PER3BP it is enough to consider $n_u = n_s = n_c = 1$, but we formulate the general results in the higher dimensional setting when $n_u = n_s \geq 1$ and $n_c = 1$, since this can be done at no expense. The results can also be generalized to $n_c \geq 1$. We refrain from doing so here since the statements become too technical. We comment on such generalization in Sections 7, 8, 9 and 10 where we prove the four general results.

3.1 Iterated function systems

In our general results which lead to the proof of the Main Theorem 1, we use a system of maps as defined below, rather than the flow.

Let

$$\{(\Sigma_{\ell,0}, \dots, \Sigma_{\ell,k_\ell})\}_{\ell \in L} \quad (6)$$

be a finite collection of sections in the extended phase space $\mathbb{R}^{n_u+n_s+2} \times \mathbb{T}$, where L is a finite set, and $k_\ell \geq 0$ for each $\ell \in L$. We assume that each section $\Sigma_{\ell,i}$ is (locally) transverse to the flow Φ_t^ε , and is homeomorphic to $\mathbb{R}^{n_u} \times \mathbb{R}^{n_s} \times \mathbb{R} \times \mathbb{T}$,

$$\Sigma_{\ell,i} \simeq \mathbb{R}^{n_u} \times \mathbb{R}^{n_s} \times \mathbb{R} \times \mathbb{T}, \quad (7)$$

with local coordinates

$$v = (x, y, I, \theta), \quad x \in \mathbb{R}^{n_u}, \quad y \in \mathbb{R}^{n_s}, \quad (I, \theta) \in \mathbb{R} \times \mathbb{T}^1. \quad (8)$$

The coordinate I on each section $\Sigma_{\ell,i}$ is defined by $I = H_0 - h_0$, where H_0 is the energy of the unperturbed Hamiltonian when $\varepsilon = 0$ in (4), and h_0 is some initial level of the energy H_0 .

Further, we assume that

$$\Sigma_{\ell,0} = \Sigma_{\ell,k_\ell} = \Sigma_0,$$

where Σ_0 is a fixed section for all $\ell \in L$. The sections are assumed to be independent of ε .

For a given $\ell \in L$ and $i \in \{1, \dots, k_\ell\}$ we define $\tau_{\ell,i} : \Sigma_{\ell,i-1} \rightarrow \mathbb{R}$ by

$$\tau_{\ell,i}(z, \theta) := \inf \{t > 0 : (z, \theta) \in \Sigma_{\ell,i-1} \text{ and } \Phi_t^\varepsilon(z, \theta) \in \Sigma_{\ell,i}\}.$$

Then we define the family of maps $f_{\ell,i,\varepsilon} : \Sigma_{\ell,i-1} \rightarrow \Sigma_{\ell,i}$, for $i \in \{1, \dots, k_\ell\}$, to be the section-to-section mappings along the flow, i.e., $f_{\ell,i,\varepsilon} = \Phi_{\tau_{\ell,i}}^\varepsilon$.

Note that $\tau_{\ell,i}$ and $f_{\ell,i,\varepsilon}$ are only locally defined.

We use the section-to-section mappings to define return maps $F_{\ell,\varepsilon} : \Sigma_0 \rightarrow \Sigma_0$ associated to each family of sections associated to $\ell \in L$, i.e.,

$$F_{\ell,\varepsilon} = f_{\ell,k_\ell,\varepsilon} \circ \dots \circ f_{\ell,1,\varepsilon}. \quad (9)$$

The dynamics of primary interest is that of the iterated function system (IFS)

$$\mathcal{F}_\varepsilon = \{F_{\ell,\varepsilon}\}_{\ell \in L}, \quad (10)$$

that depends on $\varepsilon \in [0, \varepsilon_0]$. For a fixed ε , an orbit of a point z_0 under the IFS is given by

$$z_n = F_{\ell_n,\varepsilon} \circ \dots \circ F_{\ell_1,\varepsilon}(z_0), \quad (11)$$

for some choice of $\ell_1, \dots, \ell_n \in L$. Note that the same point z_0 can yield different orbits depending on the choice of successive maps that are applied.

We express the maps $f_{\ell,i,\varepsilon}$ as well as $F_{\ell,\varepsilon}$ in the local coordinates of the sections, i.e.,

$$\begin{aligned} f_{\ell,i,\varepsilon} &: \mathbb{R}^{n_u} \times \mathbb{R}^{n_s} \times \mathbb{R} \times \mathbb{T} \rightarrow \mathbb{R}^{n_u} \times \mathbb{R}^{n_s} \times \mathbb{R} \times \mathbb{T}, & \text{for } i \in \{1, \dots, k_\ell\}, \\ F_{\ell,\varepsilon} &: \mathbb{R}^{n_u} \times \mathbb{R}^{n_s} \times \mathbb{R} \times \mathbb{T} \rightarrow \mathbb{R}^{n_u} \times \mathbb{R}^{n_s} \times \mathbb{R} \times \mathbb{T}, & \text{for } \ell \in L. \end{aligned}$$

Since I is defined by $I = H_0 - h_0$, it is a first integral of the Hamiltonian vector field of H_0 . A change in I is equivalent to a change in the energy H_0 . We will refer to I as the

‘action variable’ and to the θ as the ‘angle’ variable. We point out that we do not require the coordinate systems (x, y, I, θ) to be symplectic though.

For the unperturbed system, with $\varepsilon = 0$, the ODE which drives our IFS is autonomous, and hence the energy H_0 , and implicitly the action I , are both preserved by the maps, i.e.,

$$\pi_I f_{\ell, i, \varepsilon=0}(z) = \pi_I z.$$

Remark 4

1. In the case of the PER3BP, in the definition of the action $I = H_0 - h_0$, the energy h_0 is chosen as the energy level of some Lyapunov orbit.
2. In the case of the PER3BP, for each index $\ell \in L$, we construct a sequence of sections $(\Sigma_{\ell, 0} \dots, \Sigma_{\ell, k_\ell})$ so that some of the sections are positioned along a homoclinic orbit to Λ_0 , and some other sections are positioned along the NHIM Λ_0 itself. In our constructions we will always use the same number of sections along the homoclinic orbit, but we will use a varying number of sections along the NHIM. (For example, after a homoclinic excursion we can cross different numbers of sections around the normally hyperbolic invariant manifold in order to return to the manifold at different angles.) Different sequences of sections, corresponding to different indices ℓ , may share some common sections. Overall there is a finite number of sections, therefore a finite number of sequences of sections that we use.

The index ℓ plays the role of a selector for which particular sequence of sections we use to achieve a desired effect on the dynamics.

More generally, if we use more than one homoclinic orbit, we can associate different sets of indices ℓ to sequences of sections associated to different homoclinic orbits.

For the general results, we consider the case of using more than one homoclinic orbit, therefore we allow multiple sets of sections, corresponding to different homoclinics.

3. The dynamics of interest for establishing diffusion is that of the maps $F_{\ell, \varepsilon}$ in the IFS. The section-to-section maps $f_{\ell, i, \varepsilon}$ play a technical role in the computer assisted proof. They allow for shorter integration times between respective sections. This helps in the setting of strong expansion along the unstable coordinate and improves the accuracy of the estimates.

3.2 Cone conditions

Let $\mathbb{R}^n = \mathbb{R}^{n_1} \times \mathbb{R}^{n_2}$, and $Q : \mathbb{R}^{n_1} \times \mathbb{R}^{n_2} \rightarrow \mathbb{R}$ be a function given by

$$Q(z_1, z_2) = \|z_1\|_{n_1}^2 - \|z_2\|_{n_2}^2, \tag{12}$$

where $\|\cdot\|_{n_i}$, are some norms on \mathbb{R}^{n_i} , for $i = 1, 2$. For a point $z \in \mathbb{R}^n$ we define the Q -cone at z as the set $\{z' \in \mathbb{R}^n : Q(z - z') > 0\}$.

Definition 1 Let $Q_1, Q_2 : \mathbb{R}^{n_1} \times \mathbb{R}^{n_2} \rightarrow \mathbb{R}$ be cones of the form (12). We say that a continuous map $f : \mathbb{R}^n \rightarrow \mathbb{R}^n$ satisfies a (Q_1, Q_2) -cone condition if

$$Q_1(z - z') > 0 \quad \text{implies} \quad Q_2(f(z) - f(z')) > 0 \tag{13}$$

for all z, z' .

When $Q_1 = Q_2 = Q$, then we will simply say that f satisfies a Q -cone condition.

Condition (13) means that if z' is inside the Q_1 -cone based at z , then $f(z')$ is inside the Q_2 -cone based at $f(z)$.

For the general results, in (12) we will take $n_1 = n_u$, $n_2 = n_s + 2$, $z = (z_1, z_2) \in \mathbb{R}^{n_u + n_s + 2}$ with $z_1 = x \in \mathbb{R}^{n_u}$, $z_2 = (y, I, \theta) \in \mathbb{R}^{n_s + 2}$, and the norms

$$\|z_1\|_{n_1} = \|x\| \text{ and } \|z_2\|_{n_2} = \max \left\{ \frac{1}{a_y} \|y\|, \frac{1}{\varepsilon a_I} \|I\|, \frac{1}{a_\theta} \|\theta\| \right\},$$

where $\|\cdot\|$ denotes the Euclidean norm and $a_y, a_\theta, a_I > 0$ are constants independent of ε . Then the mapping defining the corresponding cone is given by

$$Q^\varepsilon(x, y, I, \theta) = \|x\|^2 - \left(\max \left\{ \frac{1}{a_y} \|y\|, \frac{1}{\varepsilon a_I} \|I\|, \frac{1}{a_\theta} \|\theta\| \right\} \right)^2. \quad (14)$$

Note that Q^ε represents a family of functions, parameterized by $\varepsilon > 0$. If we also want to emphasize the dependence on $a = (a_y, a_I, a_\theta) \in \mathbb{R}_+^3$, we write Q_a^ε instead of Q^ε .

We shall keep in mind that $Q^\varepsilon(x, y, I, \theta) > 0$ implies

$$a_y \|x\| \geq \|y\|, \quad a_\theta \|x\| \geq \|\theta\|, \quad \varepsilon a_I \|x\| \geq \|I\|. \quad (15)$$

3.3 Correctly aligned windows

We shall write $B^n(z, r)$ to denote a ball in \mathbb{R}^n of radius r centered at z , $\bar{B}^n(z, r)$ for its closure, $\partial B^n(z, r)$ for its boundary, and B^n for a unit ball in \mathbb{R}^n centered at 0. Here the balls are considered under some norms on \mathbb{R}^n .

A window in $\mathbb{R}^n = \mathbb{R}^{n_1} \times \mathbb{R}^{n_2}$ is a set of the form $N = \bar{B}^{n_1}(z_1, r_1) \times \bar{B}^{n_2}(z_2, r_2) \subseteq \mathbb{R}^n$ with a choice of an ‘exit set’ and ‘entry set’ respectively given by

$$\begin{aligned} N^- &:= \partial \bar{B}^{n_1}(z_1, r_1) \times \bar{B}^{n_2}(z_2, r_2), \\ N^+ &:= \bar{B}^{n_1}(z_1, r_1) \times \partial \bar{B}^{n_2}(z_2, r_2). \end{aligned}$$

Definition 2 ([5, Definition 6]) *Assume that N and M are windows in \mathbb{R}^n , and let $f : N \rightarrow \mathbb{R}^n$ be a continuous mapping.*

We say that N is correctly aligned with M , and write

$$N \xrightarrow{f} M$$

if the following conditions are satisfied:

1. *There exists a continuous homotopy $\chi : [0, 1] \times N \rightarrow \mathbb{R}^{n_1} \times \mathbb{R}^{n_2}$, such that the following conditions hold true*

$$\begin{aligned} \chi_0 &= f, \\ \chi([0, 1], N^-) \cap M &= \emptyset, \\ \chi([0, 1], N) \cap M^+ &= \emptyset. \end{aligned}$$

2. There exists a linear map $A : \mathbb{R}^{n_1} \rightarrow \mathbb{R}^{n_1}$ such that

$$\begin{aligned}\chi_1(z_1, z_2) &= (Az_1, 0), \quad \text{for all } (z_1, z_2) \in N \subset \mathbb{R}^{n_1} \times \mathbb{R}^{n_2}, \\ A(\partial B^{n_1}) &\subset \mathbb{R}^{n_1} \setminus \bar{B}^{n_1}.\end{aligned}$$

Intuitively, Definition 2 states that $f(N)$ is topologically aligned with M as in Figure 1. The coordinate z_1 corresponds to the ‘topologically unstable’ directions, and z_2 to the ‘topologically stable’ directions.

The terminology of a ‘window’ and ‘correctly aligned windows’ was introduced by Easton in [73]. An alternative terminology which refers to ‘windows’ as ‘h-sets’, and to ‘correct alignment’ as ‘covering relation’, has been introduced in [5], where the method of [73] has been generalized.

Definition 3 *If N is correctly aligned with M , and the function f also satisfies a (Q_1, Q_2) -cone condition, then we say that we have a correct alignment with cone conditions, and denote this by*

$$(N, Q_1) \xrightarrow{f} (M, Q_2).$$

Remark 5 *Correct alignment of windows and cone conditions are robust. When they hold for f , then they will also hold for functions that are sufficiently C^1 -close to f .*

For the general results we will consider windows of the form:

$$N = \bar{B}^{n_u} \times \bar{B}^{n_s} \times [I^1, I^2] \times [\theta^1, \theta^2] \subset \mathbb{R}^{n_u} \times \mathbb{R}^{n_s} \times \mathbb{R} \times \mathbb{T}^1,$$

where $I^1, I^2 \in \mathbb{R}$, $I^1 < I^2$, $\theta^1, \theta^2 \in [0, 2\pi)$, $\theta^1 < \theta^2$.

In terms of coordinates, $z = (z_1, z_2) \in N$ if $z_1 = x \in \bar{B}^{n_u}$, $z_2 = (y, I, \theta)$, where $y \in \bar{B}^{n_s}$, $I \in [I^1, I^2]$, and $\theta \in [\theta^1, \theta^2]$. The coordinate x is the topologically unstable coordinate, and y, I, θ the topologically stable coordinates.

The exit set of N is defined by

$$N^- = \partial(\bar{B}^{n_u}) \times \bar{B}^{n_s} \times [I^1, I^2] \times [\theta^1, \theta^2],$$

and the entry set by

$$N^+ = \bar{B}^{n_u} \times \partial(\bar{B}^{n_s} \times [I^1, I^2] \times [\theta^1, \theta^2]).$$

Remark 6 *In the context of the PER3BP, we will construct windows contained in the Poincaré sections $\Sigma_{\ell, i}$, which are correctly aligned under the section-to-section mappings $f_{\ell, i, \varepsilon} : \Sigma_{\ell, i-1} \rightarrow \Sigma_{\ell, i}$. The sections and the section-to-section mappings are as in Section 3.1. Via the local coordinates of the sections, the windows are given as subsets of $\mathbb{R}^{n_u+n_s+2}$ and the section-to-section mappings as maps $f_{\ell, i, \varepsilon} : \mathbb{R}^{n_u+n_s+2} \rightarrow \mathbb{R}^{n_u+n_s+2}$. Relative to these local coordinates, we will verify that the coordinate x is expanded and the coordinate y is contracted by the maps $f_{\ell, i, \varepsilon}$. The coordinates I, θ play the role of centre coordinates, as they remain ‘neutral’ under the maps $f_{\ell, i, \varepsilon}$, which means that the expansion and contraction rates in I, θ are dominated by those in x, y . In the context of the windowing method, we treat the x -coordinate as topologically unstable, and the (y, I, θ) as topologically stable. In order to achieve topological stability in (I, θ) , at each step of the correct alignment we choose the successive windows N and M such that the (I, θ) -component of M contains inside it the projection of the image of N onto the (I, θ) -coordinates.*

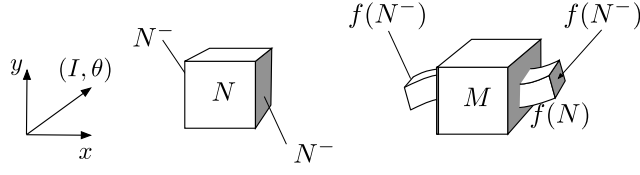


Figure 1: The correct alignment of windows $N \xrightarrow{f} M$.

3.4 Connecting sequences

We work in the framework of the IFS introduced in Section 3.1.

Consider two sets in Σ_0 , which we shall refer to as energy strips:

$$\mathbf{S}^u = \bar{B}^{n_u} \times \bar{B}^{n_s} \times \mathbb{R} \times S_\theta^u \quad \text{and} \quad \mathbf{S}^d = \bar{B}^{n_u} \times \bar{B}^{n_s} \times \mathbb{R} \times S_\theta^d, \quad (16)$$

where

$$S_\theta^u = [\theta_1^u, \theta_2^u] \quad \text{and} \quad S_\theta^d = [\theta_1^d, \theta_2^d].$$

The indices u, d are meant to suggest that when an orbit starts from \mathbf{S}^u and returns to \mathbf{S}^u , the action variable I goes up, and when it starts from \mathbf{S}^d and returns to \mathbf{S}^d , the action variable I goes down.

Definition 4 (*Connecting sequence*)

1. A connecting sequence consists of a sequence of windows

$$N_{\ell,0}, N_{\ell,1}, \dots, N_{\ell,k_\ell-1}, N_{\ell,k_\ell},$$

a sequence of cones

$$Q_{\ell,0}^\varepsilon, Q_{\ell,1}^\varepsilon, \dots, Q_{\ell,k_\ell-1}^\varepsilon, Q_{\ell,k_\ell}^\varepsilon,$$

and a sequence of maps

$$f_{\ell,i,\varepsilon}, \quad i = 1, \dots, k_\ell,$$

for some $\ell \in L$, such that the following correct alignments with cone conditions hold:

$$(N_{\ell,0}, Q_{\ell,0}^\varepsilon) \xrightarrow{f_{\ell,1,\varepsilon}} (N_{\ell,1}, Q_{\ell,1}^\varepsilon) \xrightarrow{f_{\ell,2,\varepsilon}} \dots \xrightarrow{f_{\ell,k_\ell,\varepsilon}} (N_{\ell,k_\ell}, Q_{\ell,k_\ell}^\varepsilon). \quad (17)$$

Above, we assume that the cone $Q_{\ell,0}^\varepsilon$ corresponding to the initial window $N_{\ell,0}$ and the cone $Q_{\ell,k}^\varepsilon$ corresponding to the final window $N_{\ell,k}$ are the same cone, i.e.,

$$Q_{\ell,0}^\varepsilon = Q_{\ell,k}^\varepsilon = Q^\varepsilon \quad (18)$$

with Q^ε independent of $\ell \in L$.

2. Let $\kappa_1, \kappa_2 \in \{u, d\}$. A connecting sequence from \mathbf{S}^{κ_1} to \mathbf{S}^{κ_2} is a connecting sequence as above, such that

$$N_{\ell,0} \subseteq \mathbf{S}^{\kappa_1}, \quad N_{\ell,k_\ell} \subseteq \mathbf{S}^{\kappa_2}, \quad \pi_{x,y} N_{\ell,0} = \pi_{x,y} \mathbf{S}^{\kappa_1}, \quad \text{and} \quad \pi_{x,y} N_{\ell,k_\ell} = \pi_{x,y} \mathbf{S}^{\kappa_2}.$$

To simplify notation we refer to a connecting sequence (17) by writing out the sequence of sets $(N_{\ell,0}, \dots, N_{\ell,k_\ell})$.

Definition 5 We will say that the orbit of a point $z \in N_{\ell,0}$ passes through a connecting sequence $(N_{\ell,0}, \dots, N_{\ell,k_\ell})$, for $\ell \in L$, if

$$f_{\ell,i,\varepsilon} \circ \dots \circ f_{\ell,1,\varepsilon}(z) \in N_{\ell,i}, \quad \text{for } i = 1, \dots, k_\ell.$$

For each connecting sequence as in (17), we have a map $F_{\ell,\varepsilon}$ in the IFS defined as in (9). Each $F_{\ell,\varepsilon}$ is associated with a connecting sequence from \mathbf{S}^{κ_1} to \mathbf{S}^{κ_2} for some $\kappa_1, \kappa_2 \in \{u, d\}$. Note that $F_{\ell,\varepsilon}(z)$ is well defined for any z which passes through the connecting sequence. For a fixed ε , an orbit of the IFS starting from a point z_0 can be expressed using the functions $F_{\ell,\varepsilon}$ as in (11).

4 Master theorems

4.1 Master theorem for establishing diffusion

Consider an energy strip \mathbf{S}^u as in (16), and assume that we have an IFS with a finite set L of connecting sequences of the form (17), satisfying (18), with Q^ε independent of $\ell \in L$.

We will assume below that the following condition holds:

Condition C1.

(C1.i) For each $\ell \in L$ and $\varepsilon \in (0, \varepsilon_0]$ there is a connecting sequence $(N_{\ell,0}, \dots, N_{\ell,k_\ell})$ from \mathbf{S}^u to \mathbf{S}^u ;

(C1.ii) The projection of the initial windows $N_{\ell,0}$ onto the (I, θ) -coordinates covers $[0, 1] \times S_\theta^u$, i.e.,

$$\bigcup_{\ell \in L} \pi_{I,\theta}(N_{\ell,0}) = [0, 1] \times S_\theta^u; \quad (19)$$

(C1.iii) Whenever $N_{\ell,0} \cap N_{\ell',0} \neq \emptyset$, for every $(I^*, \theta^*) \in \pi_{I,\theta}(N_{\ell,0} \cap N_{\ell',0})$ the multi-dimensional rectangle

$$\bar{B}^{n_u} \times \bar{B}^{n_s} \times (\bar{B}(I^*, \varepsilon_0 a_I) \cap [0, 1]) \times (\bar{B}(\theta^*, a_\theta) \cap S_\theta^u)$$

is contained in $N_{\ell,0}$ or in $N_{\ell',0}$, where a_I, a_θ are associated to $Q^\varepsilon = Q_a^\varepsilon$;

(C1.iv) There exists a fixed constant $c > 0$ such that, for each $z \in N_{\ell,0}$ which passes through the connecting sequence we have

$$\varepsilon \cdot c < \pi_I F_{\ell,\varepsilon}(z) - \pi_I(z). \quad (20)$$

Remark 7 In the above, we require that the constant c from condition (20) is independent from the choice of a connecting sequence.

Also, in condition (C1.iii), when \bar{B}^{n_u} and \bar{B}^{n_s} are balls of radius r instead of unit balls, then we require that $\bar{B}^{n_u} \times \bar{B}^{n_s} \times (\bar{B}(I^*, \varepsilon_0 a_I r) \cap [0, 1]) \times (\bar{B}(\theta^*, a_\theta r) \cap S_\theta^u)$ is contained in $N_{\ell,0}$ or $N_{\ell',0}$.

Theorem 2 (Existence of diffusing orbits) *Assume that condition C1 holds. Then for each $\varepsilon \in (0, \varepsilon_0]$, there exist $z \in \mathbf{S}^u$ and a sequence of functions $F_{\ell_1, \varepsilon}, \dots, F_{\ell_m, \varepsilon}$ of the form (9), such that $\tilde{z} = (F_{\ell_m, \varepsilon} \circ \dots \circ F_{\ell_1, \varepsilon})(z) \in \mathbf{S}^u$ satisfies*

$$\|\pi_I(\tilde{z}) - \pi_I(z)\| \geq 1, \quad (21)$$

for some

$$m \leq \frac{1}{\varepsilon c}.$$

In other words, there exists an orbit of the IFS with a change in I of order $O(1)$.

Moreover, if $\alpha \in \mathbb{R}$ is a number such that

$$\alpha > \sup_{\ell \in L, \varepsilon \in [0, \varepsilon_0]} \{\|DF_{\ell, \varepsilon}(z)\| : z \in N_{\ell, 0}\}, \quad (22)$$

then for every $\varepsilon \in (0, \varepsilon_0]$ the set

$$\Omega := \left\{ z : \pi_I z \in [0, 1/3] \text{ and } \|\pi_I(F_{\ell_m, \varepsilon} \circ \dots \circ F_{\ell_1, \varepsilon})(z) - \pi_I(z)\| \geq \frac{1}{3} \right\}$$

has positive Lebesgue measure $\mu(\Omega)$ lower bounded by

$$\mu(\Omega) \geq \alpha^{-2n_u/(3\varepsilon c)} \mu(\mathbf{S}^u \cap \{I \in [0, 1/3]\}).$$

The proof is given in section 7.

Remark 8 *The second part of Theorem 2 provides an explicit lower bound estimate for the Lebesgue measure of a set of points whose action changes by $O(1)$. This lower bound is clearly positive but exponentially small in ε .*

4.2 Master theorem for establishing symbolic dynamics

Consider two energy strips \mathbf{S}^u and \mathbf{S}^d as in (16).

We assume that there is a finite collection of connecting sequences as in (17), with ℓ from a set of labels $L = L^{uu} \cup L^{ud} \cup L^{du} \cup L^{dd}$, with $L^{\alpha\beta}$, $\alpha, \beta \in \{u, d\}$, mutually disjoint. We assume that the connecting sequences for $\ell \in L^{\alpha\beta}$ are from \mathbf{S}^α to \mathbf{S}^β for $\alpha, \beta \in \{u, d\}$, and satisfy (18), with Q^ε independent of $\ell \in L$.

We assume the following condition:

Condition C2.

(C2.i) For each $\ell \in L^{\alpha\beta}$, $\alpha, \beta \in \{u, d\}$, and each $\varepsilon \in (0, \varepsilon_0]$, there is a connecting sequence $(N_{\ell, 0}, \dots, N_{\ell, k_\ell})$ from \mathbf{S}^α to \mathbf{S}^β ;

(C2.ii) We have

$$\bigcup_{\ell \in L^{\alpha\beta}} \pi_{I, \theta}(N_{\ell, 0}) = [0, 1] \times S_\theta^\alpha, \quad \text{for } \alpha, \beta \in \{u, d\};$$

(C2.iii) Whenever $N_{\ell, 0} \cap N_{\ell', 0} \neq \emptyset$ for $\ell, \ell' \in L^{\alpha\beta}$, for every $(I^*, \theta^*) \in \pi_{I, \theta}(N_{\ell, 0} \cap N_{\ell', 0})$ the multi-dimensional rectangle

$$\bar{B}^{n_u} \times \bar{B}^{n_s} \times (\bar{B}(I^*, \varepsilon_0 a_I) \cap [0, 1]) \times (\bar{B}(\theta^*, a_\theta) \cap S_\theta^\alpha)$$

is contained in $N_{\ell, 0}$ or $N_{\ell', 0}$;

(C2.iv) There exists a constant $C > 0$, such that, if the orbit of z passes through a connecting sequence then

$$|\pi_I F_{\ell, \varepsilon}(z) - \pi_I(z)| < \varepsilon \cdot C \quad \text{for } \ell \in L^{uu}, L^{ud}, L^{du}, L^{dd};$$

(C2.v) There exists a $c > 0$ such that, if the orbit of z passes through a connecting sequence then

$$\begin{aligned} \varepsilon \cdot c &< \pi_I F_{\ell, \varepsilon}(z) - \pi_I(z) && \text{if } \ell \in L^{uu}, \\ \varepsilon \cdot c &< \pi_I(z) - \pi_I F_{\ell, \varepsilon}(z) && \text{if } \ell \in L^{dd}. \end{aligned}$$

Remark 9 *In the above, we require that the constant c and C are independent of the choice of a connecting sequence.*

Also, in condition (C2.iii), when \bar{B}^{n_u} and \bar{B}^{n_s} are balls of radius r instead of unit balls, then we require that $\bar{B}^{n_u} \times \bar{B}^{n_s} \times (\bar{B}(I^, \varepsilon_0 a_I r) \cap [0, 1]) \times (\bar{B}(\theta^*, a_{\theta r}) \cap S_{\theta}^{\alpha})$ is contained in $N_{\ell, 0}$ or $N_{\ell', 0}$.*

Theorem 3 (Symbolic dynamics) *Let $\eta > 0$ be a constant satisfying $\eta \geq 2a_I + C$. Assume that condition **C2** holds. Then, for every $\varepsilon \in (0, \varepsilon_0]$ and every infinite sequence of I -level sets $(I^n)_{n \in \mathbb{N}}$ with $2\eta\varepsilon \leq I^n \leq 1 - 2\eta\varepsilon$ and $|I^{n+1} - I^n| > 2\eta\varepsilon$, there exist an orbit $(z_n)_{n \in \mathbb{N}}$ of the IFS (11),*

$$z_n = F_{\ell_n, \varepsilon} \circ \dots \circ F_{\ell_1, \varepsilon}(z_0), \quad (23)$$

where $\{\ell_i\}_{i \in \mathbb{N}} \subset L$, and an increasing sequence k_n such that, for every $n \in \mathbb{N}$ we have

$$|\pi_I z_{k_n} - I^n| < \eta\varepsilon. \quad (24)$$

The proof is given in section 8.

Remark 10 *In Theorem 3, when \bar{B}^{n_u} and \bar{B}^{n_s} are balls of radius r instead of unit balls, it is enough that $\eta \geq 2ra_I + C$ (instead of $\eta \geq 2a_I + C$).*

4.3 Master theorem for estimating the Hausdorff dimension of orbits that undergo symbolic dynamics

Condition C3. If

$$\ell_1, \ell_2 \in L^{uu}, \ell'_1 \in L^{ud}, \ell'_2 \in L^{du}, \quad \text{or} \quad \ell_1, \ell_2 \in L^{dd}, \ell'_1 \in L^{du}, \ell'_2 \in L^{ud},$$

then the domain of $F_{\ell_2, \varepsilon} \circ F_{\ell_1, \varepsilon}$ is disjoint from the domain of $F_{\ell'_2, \varepsilon} \circ F_{\ell'_1, \varepsilon}$.

The theorem below gives us the lower bound on the Hausdorff dimension of a set of orbits which follow the symbolic dynamics from Theorem 3.

Theorem 4 (Hausdorff dimension) *Assume that condition **C2** holds, $\eta \geq 2a_I + C$, and $(I^n)_{n \in \mathbb{N}}$ is such that $2\eta\varepsilon \leq I^n \leq 1 - 2\eta\varepsilon$ and $|I^{n+1} - I^n| > 2\eta\varepsilon$.*

Then the set

$$\{z_0 : \exists (z_n)_{n \in \mathbb{N}} \text{ as in (23)}, \exists (k_n)_{n \in \mathbb{N}} \text{ increasing s.t. } \forall n, |\pi_I z_{k_n} - I^n| < \eta\varepsilon\} \quad (25)$$

has Hausdorff dimension greater or equal to $n_s + 2$.

If in addition $n_u = n_s = 1$ and condition **C3** holds, then the Hausdorff dimension of the set (25) is strictly greater than $n_s + 2 = 3$.

The proof is given in section 9. Note that different points z_0 in the set (25) correspond to different orbits of the IFS that achieve the shadowing of the prescribed level sets of the action.

Remark 11 We can divide $(0, \varepsilon_0]$ into finitely many subintervals

$$(0, \varepsilon_0] = (0, \varepsilon_1] \cup [\varepsilon_1, \varepsilon_2] \cup \dots \cup [\varepsilon_{k-1}, \varepsilon_k]$$

with $\varepsilon_k = \varepsilon_0$, and validate **C1**, **C2**, **C3** on each sub-interval. In the computer assisted proof the connecting sequences used for each subinterval $[\varepsilon_{k-1}, \varepsilon_k]$ are independent of ε , but may be different from one subinterval to another.

4.4 Master theorem for establishing stochastic behavior

We start by introducing some notation. We write W_t for the standard Brownian motion and assume that it is defined on a probability space $(\Omega, \mathbb{F}, \mathbb{P})$. By $C[0, 1]$ we denote the space of continuous real functions on $[0, 1]$. We endow $C[0, 1]$ with the Borel σ -field denoted as \mathcal{C} , generated by open sets with topology induced by the supremum norm.

Recall that for a stochastic process $X_t : \Omega \rightarrow \mathbb{R}$ and for $\omega \in \Omega$, a path is the function $t \mapsto X_t(\omega)$, for $t \in [0, 1]$. All stochastic processes which we shall deal with have continuous paths. We can therefore view a stochastic process X_t as $X : \Omega \rightarrow C[0, 1]$ by assigning to $\omega \in \Omega$ the corresponding path. See [74].

Let $(\Omega_\varepsilon, \mathbb{F}_\varepsilon, \mathbb{P}_\varepsilon)$ be a family of probability spaces parameterized by $\varepsilon \in (0, \varepsilon_0]$. We say that stochastic processes $X^\varepsilon : \Omega_\varepsilon \rightarrow C[0, 1]$ converge to $X : \Omega \rightarrow C[0, 1]$ in distribution on $C[0, 1]$ as $\varepsilon \rightarrow 0$, if for every $A \in \mathcal{C}$ with $\mathbb{P}(X \in \partial A) = 0$, we have $\mathbb{P}_\varepsilon(X^\varepsilon \in A) \rightarrow \mathbb{P}(X \in A)$ as $\varepsilon \rightarrow 0$. (In our setting all considered $X^\varepsilon : \Omega_\varepsilon \rightarrow C[0, 1]$ and $X : \Omega \rightarrow C[0, 1]$ will be measurable.)

We now state our theorem concerning the convergence of energy paths to a diffusion process.

Theorem 5 (Stochastic behaviour) Let $\gamma > \frac{3}{2}$. For every $X_0 \in (0, 1)$, $\mu \in \mathbb{R}$ and $\sigma > 0$, consider the stochastic processes

$$X_t^0 := X_0 + \mu t + \sigma W_t, \quad \text{for } t \in [0, 1].$$

Let $I = H_0 - h_0$. For $\varepsilon > 0$ and a given point z define the energy path ²

$$X_t^\varepsilon(z) := I(\Phi_{t\varepsilon}^\varepsilon - \gamma(z)), \quad \text{for } t \in [0, 1].$$

Define the stopping times

$$\tau = \tau(X^\varepsilon) := \inf \{t : X_t^\varepsilon \geq 1 \text{ or } X_t^\varepsilon \leq 0\}.$$

If the condition **C2** is satisfied, then for every $0 < \varepsilon \leq \varepsilon_0$ there exists a set $\Omega_\varepsilon \subset \mathbb{R}^{n_u + n_s + 2} \times \mathbb{T}$ of positive Lebesgue measure such that

²Alternatively we could define the energy paths as $X_t^\varepsilon(z) := I(\Phi_{\gamma\varepsilon^{-3/2}t}^\varepsilon(z))$, by taking sufficiently large $\gamma > 0$. The explicit size of such γ and the related details are outlined in the footnotes in Section 10.

1. Ω_ε projects onto the y, I, θ coordinates as $\pi_{y,I,\theta}\Omega_\varepsilon = \pi_{y,I,\theta}(\mathbf{S}^u \cup \mathbf{S}^d) \cap \{I \in [X_0 - \varepsilon, X_0 + \varepsilon]\}$.
2. Let Ω_ε be endowed with with the sigma field of Borel sets and the normalized Lebesgue measure (i.e., $\mathbb{P}_\varepsilon(\Omega_\varepsilon) = 1$). Then the family of processes $X^\varepsilon : \Omega_\varepsilon \rightarrow C[0, 1]$ has the following limit in distribution on $C[0, 1]$

$$\lim_{\varepsilon \rightarrow 0} X_{t \wedge \tau}^\varepsilon = X_{t \wedge \tau}^0, \quad (26)$$

where $t \wedge \tau = \min(t, \tau)$.

The proof is given in Section 10.

5 Proof of the main theorem

5.1 Computer assisted proofs

It is well known that numerical integration of differential equations inherently carries numerical errors, due to computer rounding or to the numerical methods involved. Therefore, the results obtained through numerical experiments are in general non-rigorous. Computer assisted proofs provide methods that use numerical experiments to produce rigorous results. Instead of a numerical computation of an approximate solution, the computer is utilized to return an enclosure, which is a set containing the true solution.

One basic tool that we use in this paper is interval arithmetic. This involves enclosing numbers in intervals that account for round-off errors, and performing arithmetic operation on these intervals. The output of these operations are intervals as well, which account for the numerical error and contain the true result. Interval arithmetic methods have been extended to operations with elementary functions, to solving linear systems, and to computing high order derivatives of functions [75]. Combined with the Lohner algorithm [76–78] interval arithmetic can be used to obtain rigorous enclosures of solutions of ordinary differential equations, together with their partial derivatives with respect to initial conditions, up to any given order. These methods can also be used to obtain enclosures of images of Poincaré maps as well as of their partial derivatives. All these have been implemented in the CAPD³ library [79], which is our tool of choice for our computer assisted proof⁴.

To obtain a computer assisted proof, we use interval arithmetic methods to validate the assumptions of the mathematical theorems. This is done by a finite number of computations. The use of interval arithmetic eliminates the problem of having to control rounding errors resulting from numerical methods or from the floating point computer representation of numbers.⁵

Computer assisted proofs are usually conducted in a two-step procedure:

- first, one computes via standard (non-rigorous) numerical experiments some geometric objects of interest, in order to obtain an intuitive understanding of the properties of the system,

³Computer Assisted Proofs in Dynamics: <http://capd.ii.uj.edu.pl/>

⁴The code and the documentation for the computer assisted proof is available on the web page of the first author.

⁵This methodology was also used to obtain a computer assisted proof of Smale’s 14th Problem in [80]

- second, one performs rigorous, interval arithmetic-based estimates to validate the assumptions of the appropriate theorems that establish the properties observed in the non-rigorous numerical experiments.

For the computer assisted proof in this paper we verify rigorously the conditions **C1** and **C2**, which are sufficient for Theorems 2, 3, 4, 5. These conditions are formulated in terms of:

- correctly aligned windows,
- cone conditions,
- estimates on the change of energy along orbits.

In the subsequent sections we discuss in detail how these are validated. Here we just mention that correct alignment of windows can be validated by checking inequalities between various projections of images of sets by section-to-section maps. Our validation of cone conditions and of (C1.iv), (C2.iv–C2.v) is based on the enclosures of partial derivatives of section-to-section maps, with respect to the initial conditions and with respect to the parameter. Computation of enclosures of both the images and partial derivatives of such maps with respect to the initial conditions are a part of the CAPD library. Partial derivatives which include the parameter can also be automatically obtained in CAPD by adding the parameter as one of the variables of the system.

5.2 Outline of the proof

In Section 5.3 we give the theoretical tools which we use for the validation of correct alignment of windows, for validation of cone conditions, and for establishing estimates on the change of energy along orbits.

In the next three subsections we describe how we choose the local maps for the connecting sequences used in the proof of the main theorem. We choose these maps to be section-to-section maps along the flow, expressed in appropriate local coordinates. Section 5.4 describes how we choose the local coordinates. In Section 5.5 we discuss how we choose the sections along the flow. In Section 5.6 we describe how we choose our connecting sequences.

It is important to emphasize that our computer assisted proof is conducted in the two-step procedure outlined in Section 5.1. The choices described in Sections 5.4, 5.5, 5.6 are associated with the first step (non-rigorous numerics). The local maps for connecting sequences are chosen based on the non-rigorous numerical investigation of the properties of the system. Once these choices are made, we conduct rigorous, interval arithmetic-based estimates to validate **C1** and **C2**, which leads to the proof of our main theorem. This is done in Section 5.7.

5.3 Tools for validating correct alignment of windows, cone conditions and changes of energy along trajectories

We start by introducing some notation. For $E \subset \mathbb{R}$ and $N \subset \mathbb{R}^n$ consider a family of $(k \times n)$ -matrices $B(\varepsilon, x)$, with $\varepsilon \in E$ and $x \in N$. We will use the following notation for

the following subsets of $\mathbb{R}^{k \times n}$

$$[B(E, N)] = \left\{ B : B_{ji} \in \left[\inf_{\varepsilon \in E, x \in N} B(\varepsilon, x), \sup_{\varepsilon \in E, x \in N} B(\varepsilon, x) \right] \right\}, \quad (27)$$

$$[B(E, N)] = \left\{ B : B_{ji} \in \left[\inf_{\varepsilon \in E, x \in N} B(\varepsilon, x), \sup_{\varepsilon \in E, x \in N} B(\varepsilon, x) \right] \right\}. \quad (28)$$

We refer to a subset of $\mathbb{R}^{k \times n}$ which on each projection is a closed interval as an interval matrix. For an interval matrix $\mathbf{A} \subset \mathbb{R}^{k \times n}$ we shall write

$$\|\mathbf{A}\| = \sup \{ \|A\| : A \in \mathbf{A} \}.$$

For a matrix $A \in \mathbb{R}^{k \times k}$ we write

$$m(A) = \begin{cases} \inf_{\|x\|=1} \|Ax\| = \|A^{-1}\|^{-1} & \text{if } \det(A) \neq 0, \\ 0 & \text{otherwise.} \end{cases}$$

For an interval matrix $\mathbf{A} \subset \mathbb{R}^{k \times k}$ we define

$$m(\mathbf{A}) = \inf \{ m(A) : A \in \mathbf{A} \}.$$

We now describe how we validate correct alignment of windows. To simplify the discussion, here we restrict to the simple case when the dimension of expanding coordinate is 1. (This is the setting we encounter in the PER3BP.)

For $z = (z_1, z_2) \in \mathbb{R}^{n_1} \times \mathbb{R}^{n_2}$ we shall write π_{z_1} and π_{z_2} for the projections onto the coordinate z_1 and z_2 , respectively. To validate correct alignment, in our computer assisted proof we use the following lemma.

Lemma 1 *Let N, M be two windows in $\mathbb{R}^{n_1} \times \mathbb{R}^{n_2}$, with $n_1 = 1$, of the form*

$$N = M = [-1, 1] \times \bar{B}^{n_2}.$$

If $\pi_{z_2} f_\varepsilon(N) \subset B^{n_2}$, $\pi_{z_1} f_\varepsilon(\{-1\} \times \bar{B}^{n_2}) < -1$ and $\pi_{z_1} f_\varepsilon(\{1\} \times \bar{B}^{n_2}) > 1$, then $N \xrightarrow{f_\varepsilon} M$.

Proof. Let $\chi : [0, 1] \times N \rightarrow \mathbb{R}^{n_1} \times \mathbb{R}^{n_2}$ be defined as

$$\chi(\lambda, z_1, z_2) = (1 - \lambda) f_\varepsilon(z_1, z_2) + (\lambda z_1, 0).$$

It follows directly that χ satisfies the conditions from Definition 2. ■

For the case when $n_1 > 1$ there are established methods for the validation of correct alignment, and we direct the reader to [4, 5].

We now describe the method with which we validate cone conditions. Consider cones Q_a^ε defined as in (14) with $a = (a_y, a_I, a_\theta)$. Let E be an interval of parameters in \mathbb{R} . We consider a C^2 -function

$$f : E \times \mathbb{R}^u \times \mathbb{R}^s \times \mathbb{R} \times \mathbb{T} \rightarrow \mathbb{R}^u \times \mathbb{R}^s \times \mathbb{R} \times \mathbb{T}.$$

(Here it will be more convenient to write $f(\varepsilon, z)$ than $f_\varepsilon(z)$; for $\varepsilon \in E$.) We consider

$$N = \bar{B}^u \times \bar{B}^s \times J \times S,$$

where J is a closed interval in \mathbb{R} and S is a closed interval in $[0, 2\pi)$. Our objective will be to find $b = (b_y, b_I, b_\theta)$ so that $Q_a^\varepsilon(z - z') > 0$ will imply $Q_b^\varepsilon(f(\varepsilon, z) - f(\varepsilon, z')) > 0$.

We use the following notation (below are interval matrices defined as in (27–28))

$$\left[\frac{\partial f_\kappa}{\partial h} \right] = \left[\frac{\partial f_\kappa}{\partial h}(E, N) \right], \quad \left[\frac{\partial^2 f_\kappa}{\partial \varepsilon \partial h} \right] = \left[\frac{\partial^2 f_\kappa}{\partial \varepsilon \partial h}(E, N) \right], \quad \text{for } h, \kappa \in \{x, y, I, \theta\}.$$

Below lemma is the main tool for validating cone conditions.

Lemma 2 *If for $b = (b_y, b_I, b_\theta) \in \mathbb{R}_+^3$ we have*

$$\begin{aligned} 0 &< \frac{\left\| \left[\frac{\partial f_\kappa}{\partial x} \right] \right\| + \left\| \left[\frac{\partial f_\kappa}{\partial y} \right] \right\| a_y + \varepsilon_0 \left\| \left[\frac{\partial f_\kappa}{\partial I} \right] \right\| a_I + \left\| \left[\frac{\partial f_\kappa}{\partial \theta} \right] \right\| a_\theta}{m \left(\frac{\partial f_x}{\partial x} \right) - \left\| \left[\frac{\partial f_x}{\partial y} \right] \right\| a_y - \varepsilon_0 \left\| \left[\frac{\partial f_x}{\partial I} \right] \right\| a_I - \left\| \left[\frac{\partial f_x}{\partial \theta} \right] \right\| a_\theta} < b_\kappa \quad \text{for } \kappa \in \{y, \theta\}, \\ 0 &< \frac{\left\| \left[\frac{\partial f_I}{\partial \varepsilon \partial x} \right] \right\| + \left\| \left[\frac{\partial f_y}{\partial \varepsilon \partial y} \right] \right\| a_y + \left(1 + \varepsilon_0 \left\| \left[\frac{\partial f_I}{\partial \varepsilon \partial I} \right] \right\| \right) a_I + \left\| \left[\frac{\partial f_I}{\partial \varepsilon \partial \theta} \right] \right\| a_\theta}{m \left(\frac{\partial f_x}{\partial x} \right) - \left\| \left[\frac{\partial f_x}{\partial y} \right] \right\| a_y - \varepsilon_0 \left\| \left[\frac{\partial f_x}{\partial I} \right] \right\| a_I - \left\| \left[\frac{\partial f_x}{\partial \theta} \right] \right\| a_\theta} < b_I. \end{aligned}$$

then

$$Q_a^\varepsilon(z - z') > 0 \quad \implies \quad Q_b^\varepsilon(f(\varepsilon, z) - f(\varepsilon, z')) > 0. \quad (29)$$

Proof. The proof is given in the Appendix. ■

Lemma 2 is used as follows. When validating cone conditions for a connecting sequence $(N_{\ell,0}, \dots, N_{\ell,k_\ell})$, for some $\ell \in L$, we start with the cone Q_a^ε in $N_{\ell,0}$. We recall that by (18) we take the same $a = (a_y, a_I, a_\theta)$ for all $\ell \in L$. We take $b_0 = a$ and validate the cone conditions for the maps $f_{\ell,i,\varepsilon}$, for $i = 1, \dots, k_\ell$, by inductively applying Lemma 2. This way we obtain a sequence $b_i = (b_{i,y}, b_{i,I}, b_{i,\theta})$, for $i = 0, \dots, k_\ell$, which imply that if $z, z' \in N_{\ell,i-1}$ and $Q_{b_{i-1}}^\varepsilon(z - z') > 0$ then

$$Q_{b_i}^\varepsilon(f_{\ell,i,\varepsilon}(z) - f_{\ell,i,\varepsilon}(z')) > 0, \quad \text{for } i = 1, \dots, k_\ell.$$

Our objective is to return back to the cone Q_a^ε in N_{ℓ,k_ℓ} . This is established when $b_{k_\ell,y} \leq a_y$, $b_{k_\ell,I} \leq a_I$, and $b_{k_\ell,\theta} \leq a_\theta$, since in such case $Q_{b_{k_\ell}}^\varepsilon(z - z') > 0$ implies $Q_a^\varepsilon(z - z') > 0$.

We now give two lemmas which we use to verify conditions (C1.iv), (C2.iv–C2.v).

Lemma 3 *Consider two families of functions $f_{1,\varepsilon}, f_{0,\varepsilon}$ for $\varepsilon \in [0, \varepsilon_0]$. Consider also two windows N_0 and N_1 . If for any $q_0 \in N_0$ and $q_1 \in N_1$ and any $\varepsilon \in [0, \varepsilon_0]$*

$$\begin{aligned} \pi_I q_0 + \varepsilon c_0 &< \pi_I f_{0,\varepsilon}(q_0) < \pi_I q_0 + \varepsilon C_0 \\ \pi_I q_1 + \varepsilon c_1 &< \pi_I f_{1,\varepsilon}(q_1) < \pi_I q_1 + \varepsilon C_1, \end{aligned}$$

then for any $q_0 \in N_0$, for which $f_{0,\varepsilon}(q_0) \in N_1$, and for any $\varepsilon \in [0, \varepsilon_0]$,

$$\pi_I q_0 + \varepsilon c_0 + \varepsilon c_1 < \pi_I f_{1,\varepsilon} \circ f_{0,\varepsilon}(q_0) < \pi_I q_0 + \varepsilon C_0 + \varepsilon C_1.$$

Proof. Taking $q_1 = f_{0,\varepsilon}(q_0)$ we have

$$\begin{aligned} \pi_I f_{1,\varepsilon} \circ f_{0,\varepsilon}(q_0) &= \pi_I f_{1,\varepsilon}(q_1) > \pi_I q_1 + \varepsilon c_1 \\ &= \pi_I f_{0,\varepsilon}(q_0) + \varepsilon c_1 > \pi_I q_0 + \varepsilon c_0 + \varepsilon c_1. \end{aligned}$$

The upper bound follows from mirror computation, but with reversed inequalities and by using C_0 and C_1 instead of c_0 and c_1 , respectively. ■

Lemma 3 can be iterated by passing through a connecting sequence. One can verify assumptions of Lemma 3 as follows (denoting $f_i(\varepsilon, q) := f_{i,\varepsilon}(q)$):

Lemma 4 *Assume that*

$$c < \left[\min_{(\varepsilon, q) \in [0, \varepsilon_0] \times N} \frac{\partial \pi_I f}{\partial \varepsilon}(\varepsilon, q), \max_{(\varepsilon, q) \in [0, \varepsilon_0] \times N} \frac{\partial \pi_I f}{\partial \varepsilon}(\varepsilon, q) \right] < C, \quad (30)$$

then for every $q \in N$ and every $\varepsilon \in [0, \varepsilon_0]$

$$\pi_I q + \varepsilon c < \pi_I f(\varepsilon, q) < \pi_I q + \varepsilon C.$$

Proof. For any $q \in N$ and any $\varepsilon \in [0, \varepsilon_0]$

$$\begin{aligned} \pi_I f(\varepsilon, q) &= \pi_I f(0, q) + \int_0^1 \frac{d}{ds} \pi_I f(s\varepsilon, q) ds = \pi_I q + \varepsilon \int_0^1 \frac{\partial}{\partial \varepsilon} \pi_I f(s\varepsilon, q) ds \\ &\in \pi_I q + \varepsilon \left[\frac{\partial \pi_I f}{\partial \varepsilon}([0, \varepsilon_0], N) \right] \in (\pi_I q + \varepsilon c, \pi_I q + \varepsilon C), \end{aligned}$$

which completes the proof. ■

5.4 Construction of local coordinates

Here we discuss the local coordinates which we use for our maps. At any given point $q^* = (X^*, Y^*, P_X^*, P_Y^*, \theta^*) \in \mathbb{R}^4 \times \mathbb{T}$, we define a 4-dimensional section $\Sigma = \Sigma(q^*) \subset \mathbb{R}^4 \times \mathbb{T}$ as in (7). Let $F_Y^* := P_X^* + Y^*$, $F_X^* := P_Y^* - X^*$, which correspond to the vector field (2) at q^* along the X, Y coordinates, respectively. We consider two cases:

Case 1. If $|F_X^*| > |F_Y^*|$, let $a := -F_Y^*/F_X^*$ and define

$$\Sigma := \{(X(Y), Y, P_X, P_Y, \theta) \mid X(Y) = a(Y - Y^*) + X^*\}. \quad (31)$$

This means that Σ is parameterized by (Y, P_X, P_Y, θ) . On this section we define local coordinates $v = (x, y, I, \theta) \in \mathbb{R}^3 \times \mathbb{T}$ as in (8). These are given by

$$(X, Y, P_X, P_Y, \theta) = \Psi_\varepsilon(v) := R_1(p + \varepsilon w + Av), \quad (32)$$

where $p, w \in \mathbb{R}^3 \times \mathbb{T}$ and A is a suitable 4×4 matrix (the particular choices of p, w and A we make are given by (39), (40), and (41)), and where

$$\begin{aligned} R_1(Y, P_Y, h, \theta) &:= \begin{cases} (X(Y), Y, \psi_1(Y, P_Y, h) - Y, P_Y, \theta) & \text{if } F_X^* > 0, \\ (X(Y), Y, -\psi_1(Y, P_Y, h) - Y, P_Y, \theta) & \text{otherwise,} \end{cases} \\ \psi_1(Y, P_Y, h) &:= \sqrt{2(h + \Omega(X(Y), Y)) - (P_Y - X(Y))^2}. \end{aligned}$$

Note that the inverse of R_1 is $R_1^{-1} : \Sigma \rightarrow \mathbb{R}^3 \times \mathbb{T}$

$$R_1^{-1}(X, Y, P_X, P_Y, \theta) = (Y, P_Y, H_0(X, Y, P_X, P_Y), \theta). \quad (33)$$

Case 2. If $|F_X^*| \leq |F_Y^*|$ then we let $a := -F_X^*/F_Y^*$ and define the section as

$$\Sigma = \{(X, Y(X), P_X, P_Y, \theta) \mid Y(X) = a(X - X^*) + Y^*\}. \quad (34)$$

This means that Σ is parameterized by (X, P_X, P_Y, θ) . We define local coordinates $v = (x, y, I, \theta)$ on Σ as

$$(X, Y, P_X, P_Y, \theta) = \Psi_\varepsilon(v) := R_2(p + \varepsilon w + Av), \quad (35)$$

where A is some 4×4 matrix, p, w are some points in $\mathbb{R}^3 \times \mathbb{T}$ and

$$R_2(X, P_X, h, \theta) := \begin{cases} (X, Y(X), P_X, \psi_2(X, P_X, h) + X, \theta) & \text{if } F_Y^* > 0, \\ (X, Y(X), P_X, -\psi_2(X, P_X, h) + X, \theta) & \text{otherwise,} \end{cases}$$

$$\psi_2(X, P_X, h) := \sqrt{2(h + \Omega(X, Y(X))) - (P_X + Y(X))^2}.$$

Note that the inverse of R_2 is $R_2^{-1} : \Sigma \rightarrow \mathbb{R}^3 \times \mathbb{T}$

$$R_2^{-1}(X, Y, P_X, P_Y, \theta) = (X, P_X, H_0(X, Y, P_X, P_Y), \theta). \quad (36)$$

When dealing with Case 1, the section Σ is transverse to the flow at q^* since the vector (F_X^*, F_Y^*) is orthogonal to the line $(X(Y), Y)$ in the (X, Y) -plane. The coordinate change $R_1(Y, P_Y, h, \theta)$ allows us to use the energy h instead of the coordinate P_X . The function R_1 was chosen so that

$$H_0(R_1(Y, P_Y, h, \theta)) = h. \quad (37)$$

Similarly, when dealing with Case 2, the section Σ is transverse to the flow since (F_X^*, F_Y^*) is orthogonal to $(X, Y(X))$, and $R_2(X, P_X, h, \theta)$ allows us to use h instead of P_Y . We also have

$$H_0(R_2(X, P_X, h, \theta)) = h. \quad (38)$$

Remark 12 *We stress that a section Σ as in (31) (resp. (34)) is rigorously defined, as it is obtained by fixing one coordinate Y (resp. X) and solving for the remaining coordinates X, P_X, P_Y, θ (resp. Y, P_X, P_Y, θ). These coordinates are later transformed into the coordinates $v = (x, y, I, \theta)$, which are then used in the numerical computations.*

In all of our coordinate changes, we will always choose

$$p = \begin{cases} (Y^*, P_Y^*, H_0(q^*), \theta^*) & \text{if } q^* \text{ is as in Case 1,} \\ (X^*, P_X^*, H_0(q^*), \theta^*) & \text{if } q^* \text{ is as in Case 2,} \end{cases} \quad (39)$$

always take w of the form

$$w = (w_x, w_y, 0, 0) \quad (40)$$

and always choose A of the form

$$A = \begin{pmatrix} a_{11} & a_{12} & a_{13} & 0 \\ a_{21} & a_{22} & a_{23} & 0 \\ 0 & 0 & 1 & 0 \\ 0 & 0 & 0 & 1 \end{pmatrix}. \quad (41)$$

Lemma 5 *If p , w and A are of the form (39–41) then*

$$H_0(\Psi_\varepsilon(x, y, I, \theta)) = H_0(q^*) + I.$$

Proof. In Case 1, by (32), (39) and (41) we have

$$\pi_I R_1^{-1}(\Psi_\varepsilon(x, y, I, \theta)) = \pi_I(p + \varepsilon w + A(x, y, I, \theta)) = H_0(q^*) + 0 + I,$$

and the result follows from (33). In Case 2 the proof is identical, using R_2 instead of R_1 and (36) instead of (33). ■

From now on we assume that all subsequent coordinate changes defined by (32) or (35), involving p , w and A , take them of the form (39–41). The choice of the coefficients of w and A can depend on the choice of q^* .

Theorem 6 *Consider a sequence of points q_0^*, \dots, q_k^* with $q_k^* = q_0^*$ at which we position sections $\Sigma_0, \dots, \Sigma_k$, with $\Sigma_k = \Sigma_0$. Consider section-to-section maps along the flow $\mathcal{P}_i^\varepsilon : \Sigma_{i-1} \rightarrow \Sigma_i$ together with local maps $f_{i,\varepsilon} = \Psi_{i,\varepsilon}^{-1} \circ \mathcal{P}_i^\varepsilon \circ \Psi_{i-1,\varepsilon}$, for $i = 1, \dots, k$. If $w_k = w_0$ and $A_k = A_0$, then for $q = \Psi_{0,\varepsilon}(v)$*

$$H_0(\mathcal{P}_k^\varepsilon \circ \dots \circ \mathcal{P}_1^\varepsilon(q)) - H_0(q) = \pi_I f_{k,\varepsilon} \circ \dots \circ f_{1,\varepsilon}(v) - \pi_I v.$$

Proof. Since $q_k^* = q_0^*$, $w_k = w_0$ and $A_k = A_0$ we see that $\Psi_{k,\varepsilon} = \Psi_{0,\varepsilon}$, so from the definition of the maps $f_{i,\varepsilon}$ it follows that

$$\Psi_{0,\varepsilon} \circ f_{k,\varepsilon} \circ \dots \circ f_{1,\varepsilon}(v) = \mathcal{P}_k^\varepsilon \circ \dots \circ \mathcal{P}_1^\varepsilon \circ \Psi_{0,\varepsilon}(v).$$

From the fact that $q = \Psi_{0,\varepsilon}(v)$ and by applying Lemma 5 we see that

$$\begin{aligned} H_0(\mathcal{P}_k^\varepsilon \circ \dots \circ \mathcal{P}_1^\varepsilon(q)) - H_0(q) &= H_0(\Psi_{0,\varepsilon}(f_{k,\varepsilon} \circ \dots \circ f_{1,\varepsilon}(v))) - H_0(\Psi_{0,\varepsilon}(v)) \\ &= H_0(q_0^*) + \pi_I f_{k,\varepsilon} \circ \dots \circ f_{1,\varepsilon}(v) - H_0(q_0^*) - \pi_I v \\ &= \pi_I f_{k,\varepsilon} \circ \dots \circ f_{1,\varepsilon}(v) - \pi_I v, \end{aligned}$$

as required. ■

Remark 13 *Theorem 6 ensures that regardless of the choices of the particular coefficients of w_i and A_i , if we return to the same local coordinates, then the change in I in the local coordinates corresponds precisely to the change in H_0 in the original coordinates.*

Let q_1^* and q_2^* be two points which lie on a trajectory of the flow. Let Σ_1 and Σ_2 be two sections at q_1^* and q_2^* , respectively, and let $\mathcal{P}^\varepsilon : \Sigma_1 \rightarrow \Sigma_2$ be a section-to-section map along the flow. We will choose the matrices A_1, A_2 of the form (41) to define local coordinate changes $\Psi_{1,\varepsilon}, \Psi_{2,\varepsilon}$ respectively, to have coefficients so that for the local map

$$f_\varepsilon := \Psi_{2,\varepsilon}^{-1} \circ \mathcal{P}^\varepsilon \circ \Psi_{1,\varepsilon}, \quad (42)$$

we obtain

$$Df_{\varepsilon=0}(0) = \begin{pmatrix} \lambda & 0 & 0 & 0 \\ 0 & \frac{1}{\lambda} & 0 & 0 \\ 0 & 0 & 1 & 0 \\ \Theta_1 & \Theta_2 & \Theta_3 & 1 \end{pmatrix}, \quad (43)$$

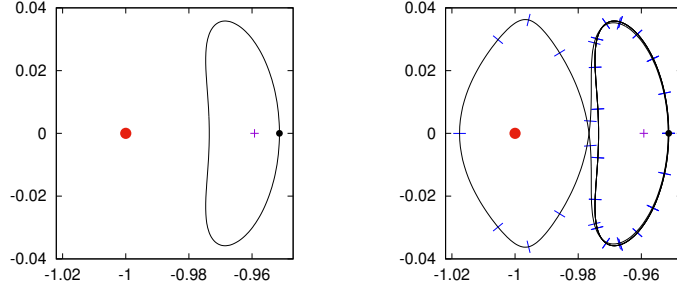


Figure 2: The Lyapunov orbit to the left, and its homoclinic orbit to the right. The point L_1 is depicted with a cross and the smaller primary is depicted with a dot. Along the homoclinic we have a sequence of points, at which we position sections, which are transversal to the flow. The dot on the Lyapunov orbit indicates where the strips S_u and S_d are positioned.

where $\lambda > 1$ and $\Theta_1, \Theta_2, \Theta_3$, are some numbers. (The presence of $\Theta_1, \Theta_2, \Theta_3$ is a result of having zeros in the lower left part of the matrices (41).)

A good choice of w_1, w_2 of the form (40) is one for which

$$\frac{d}{d\varepsilon} \pi_{x,y} f_\varepsilon(0)|_{\varepsilon=0} = 0, \quad (44)$$

or, if this is not possible, one that makes the left hand side of (44) as close to zero as possible.

The reason for (43) and (44) is that then for $v = (x, y, I, \theta)$ which is close to zero and for ε also close to zero we will have $\pi_{x,y} f_\varepsilon(v) \approx (\lambda x, y/\lambda)$. This is useful for the validation of correct alignment of windows.

Remark 14 We choose A_i and w_i , for $i = 1, 2$, by solving (43) and (44). We do not need though to solve these equations analytically. It is sufficient to find their solutions by means of non-rigorous numerical computations. It is then important to compute rigorous enclosures of $\Psi_{i,\varepsilon}$ and $\Psi_{i,\varepsilon}^{-1}$ (for the particular choices of w_i and A_i which we decide on) when performing rigorous, interval arithmetic based validation of the needed conditions.

5.5 Construction of sections and energy strips

In this section we describe how we choose a sequence of points at which we position sections. The section $\Sigma = \{Y = 0\}$ will play a special role in our construction, since on this section we shall position our energy strips \mathbf{S}^u and \mathbf{S}^d as in (16). We define the local coordinates on $\Sigma = \{Y = 0\}$ by choosing

$$q^* = (-0.9513385, 0, 0, -1.02124587611, 0), \quad (45)$$

$$p = (\pi_X q^*, \pi_{P_X} q^*, H_0(q^*), 0), \quad (46)$$

$$w = (0, 0, 0, 0), \quad (47)$$

and taking

$$A = \begin{pmatrix} 0.377372287914 & 0.377372287914 & 1.53559852923 & 0 \\ 0.926061637427 & -0.926061637427 & 0 & 0 \\ 0 & 0 & 1 & 0 \\ 0 & 0 & 0 & 1 \end{pmatrix}. \quad (48)$$

At q^* the vector field in the direction X is zero, which means that at the section $\Sigma = \{Y = 0\}$ we associate the local coordinates from Case 2. This way we obtain a change to local coordinates at $\Sigma = \{Y = 0\}$ defined as

$$\Psi(v) = R_2(p + Av). \quad (49)$$

We note that since we take $w = 0$ to define Ψ , it is independent of ε . (This will not always be the case and on other sections which are used in our construction we can choose w to be non zero.) The particular coefficients of A in (48) have been chosen so that we obtain (43) for the local maps used in the connecting sequences, which are introduced in Section 5.6.

We consider two energy strips in the local coordinates given by Ψ_ε as

$$\begin{aligned} \mathbf{S}^u &= [-r, r] \times [-r, r] \times \mathbb{R} \times [\theta_1^u, \theta_2^u], \\ \mathbf{S}^d &= [-r, r] \times [-r, r] \times \mathbb{R} \times [\theta_1^d, \theta_2^d], \end{aligned} \quad (50)$$

where $r = 10^{-6}$ and

$$\begin{aligned} \theta_1^u &= \frac{1}{2}\pi - 0.08, & \theta_2^u &= \frac{1}{2}\pi + 0.08, \\ \theta_1^d &= \frac{3}{2}\pi - 0.08, & \theta_2^d &= \frac{3}{2}\pi + 0.08. \end{aligned}$$

The coordinates in the above Cartesian product represent: expansion, contraction, energy, angle, respectively. (In this case $n_u = n_s = n_c = 1$.)

Both strips lie on the same section $\Sigma = \{Y = 0\}$. We shall make a distinction though and write

$$\Sigma_u := \{Y = 0\} \cap \{\theta \in [\theta_1^u, \theta_2^u]\} \quad \text{and} \quad \Sigma_d := \{Y = 0\} \cap \{\theta \in [\theta_1^d, \theta_2^d]\}.$$

The remainder of the points around which we position the sections are on a homoclinic orbit to the Lyapunov orbit of the PCR3BP. The homoclinic orbit is computed via non-rigorous numerics, and the corresponding points are depicted in the right hand plot in Figure 2. We will take sequences of points $\{q_i\}_{i=0}^n$ on the homoclinic, with $q_0 \in \Sigma = \{Y = 0\}$, and define a sequence of sections $\{\Sigma_i\}_{i=0}^n$ and corresponding local coordinates as discussed in Cases 1 and 2 from Section 5.4. The sections Σ_i are rigorously defined as per Remark 12.

If we consider the homoclinic orbit in the extended phase space which includes θ , then we can observe the change of θ along $\{q_i\}_{i=0}^n$. We shall use the notation

$$\theta_0 = \pi_\theta q_0.$$

We have chosen our Lyapunov orbit and its homoclinic from Figure 2 so that for any choice of $\theta_0 \in [0, 2\pi)$ we have the following properties. (The discussion below is complemented by Figure 3, which corresponds to the case when $\theta_0 = \pi/2$.)

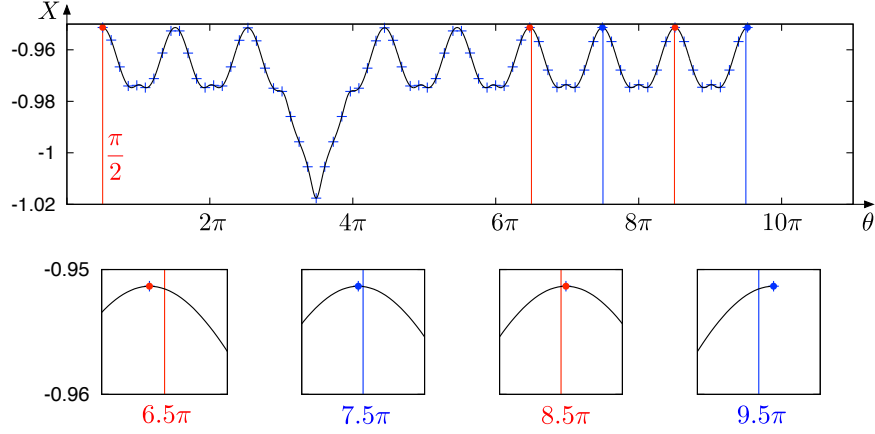


Figure 3: The homoclinic orbit which starts from Σ_u . The crosses depict the points where the orbit intersects the sections (compare with Figure 2). The red and blue dots are where it intersects with $\{Y = 0\}$. The red lines are at $\theta = \frac{1}{2}\pi$ and the blue lines are at $\theta = \frac{3}{2}\pi$, modulo 2π .

Depending on the number of turns the homoclinic orbit makes around the Lyapunov orbit, it returns to $\Sigma = \{Y = 0\}$ at a different angle. If we start from $q_0 \in \Sigma = \{Y = 0\}$ and take 2 turns around the Lyapunov orbit, go around the smaller primary, and make 2 turns around the Lyapunov orbit again, then we arrive at a point $q_{50} \in \Sigma = \{Y = 0\}$, for

$$\pi_\theta q_{50} = \theta_0 - 0.0750229. \quad (51)$$

which (For the case when $\theta_0 = \pi/2$, this feature is depicted in Figure 3. On the plot, the points q_i are depicted by the crosses. The red and blue vertical lines represent the positions of center angles of strips \mathbf{S}^u and \mathbf{S}^d , respectively. The projection of the point q_{50} onto the θ, X coordinates is depicted by the red dot above 6.5π .)

When we take another turn along the homoclinic, we return to a point $q_{58} \in \Sigma = \{Y = 0\}$, for which

$$\pi_\theta q_{58} = \theta_0 + \pi - 0.0249904. \quad (52)$$

(For the case when $\theta_0 = \pi/2$ the projection of the point q_{58} onto the θ, X coordinates is depicted by the blue dot above 7.5π in Figure 3.)

After another turn around the Lyapunov orbit we arrive at $q_{66} \in \Sigma = \{Y = 0\}$, for which

$$\pi_\theta q_{66} = \theta_0 + 0.0250421. \quad (53)$$

(Red dot above 8.5π in Figure 3.)

Yet another turn around the Lyapunov orbit results in $q_{74} \in \Sigma = \{Y = 0\}$, for which

$$\pi_\theta q_{74} = \theta_0 + \pi + 0.0750746. \quad (54)$$

(Blue dot above 9.5π in Figure 3.)

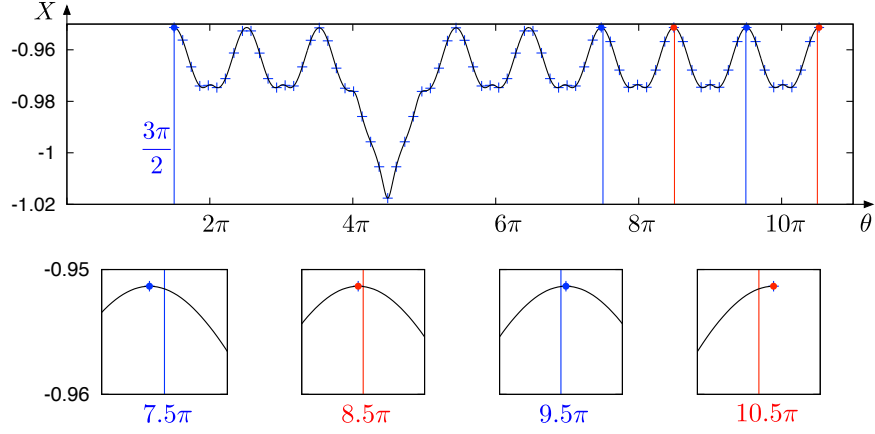


Figure 4: The homoclinic orbit starting from Σ_d . (Compare with Figures 2 and 3). The red and blue dots are where the orbit intersects with $\{Y = 0\}$. The red lines are at $\theta = \frac{1}{2}\pi$ and the blue lines are at $\theta = \frac{3}{2}\pi$, modulo 2π .

From (51), (52), (53), and (54) and looking at Figure 3, we can see that for $q_0 \in \Sigma_u$ we will have:

- When $\theta_0 \geq \pi/2$, the composition of $n_1^{uu} := 50$ section-to-section maps takes the point $q_0 \in \Sigma_u$ to $q_{n_1^{uu}} \in \Sigma_u$.
- When $\theta_0 \geq \pi/2$, the composition of $n_1^{ud} := 58$ section-to-section maps takes the point $q_0 \in \Sigma_u$ to $q_{n_1^{ud}} \in \Sigma_d$.
- When $\theta_0 \leq \pi/2$, the composition of $n_2^{uu} := 66$ section-to-section maps takes the point $q_0 \in \Sigma_u$ to $q_{n_2^{uu}} \in \Sigma_u$.
- When $\theta_0 \leq \pi/2$, the composition of $n_2^{ud} := 74$ section-to-section maps takes the point $q_0 \in \Sigma_u$ to $q_{n_2^{ud}} \in \Sigma_d$.

The choices of the superscripts in n_1^{ui}, n_2^{ui} , for $i \in \{u, d\}$ are to indicate that it takes such numbers of section-to-section maps to get from Σ_u to Σ_i .

The above was possible because we have chosen our Lyapunov orbit carefully. Our Lyapunov orbit has a homoclinic orbit such that after we pass through an excursion along it from $\{Y = 0\}$ to $\{Y = 0\}$ we “move with the angle to the left”. Our Lyapunov orbit has a period slightly longer than π so by making turns around it from $\{Y = 0\}$ to $\{Y = 0\}$, we “move with the angle to the right”.

We can also choose $q_0 \in \Sigma_d$. (The case of $\theta_0 = 3\pi/2$ is depicted in Figure 4.) Then from (51), (52), (53) and (54) and looking at Figure 4 we see that:

- When $\theta_0 \geq 3\pi/2$, the composition of $n_1^{dd} := 50$ section-to-section maps takes the point $q_0 \in \Sigma_d$ to $q_{n_1^{dd}} \in \Sigma_d$.

- When $\theta_0 \geq 3\pi/2$, the composition of $n_1^{du} := 58$ section-to-section maps takes the point $q_0 \in \Sigma_d$ to $q_{n_1^{du}} \in \Sigma_u$.
- When $\theta_0 \leq 3\pi/2$, the composition of $n_2^{dd} := 66$ section-to-section maps takes the point $q_0 \in \Sigma_d$ to $q_{n_2^{dd}} \in \Sigma_d$.
- When $\theta_0 \leq 3\pi/2$, the composition of $n_2^{du} := 74$ section-to-section maps takes the point $q_0 \in \Sigma_d$ to $q_{n_2^{du}} \in \Sigma_u$.

Remark 15 *In the language of the scattering map theory [81], the above construction can be expressed by saying that we obtain pseudo-orbits generated by composing the scattering map from the Lyapunov NHIM (consisting of a family of Lyapunov orbits over some energy interval) to itself, with iterates of inner map restricted the Lyapunov NHIM. Following the scattering map yields a shift of the angle θ to the left, while following the inner dynamics along the Lyapunov NHIM yields a shift of the angle θ to the right. These pseudo-orbits are shadowed by true orbits [34]. In this paper we find these latter orbits directly, without constructing the underlying pseudo-orbits.*

Remark 16 *Our construction admits many generalizations. Here we have chosen to work with a single homoclinic orbit and to combine it with the inner dynamics. For instance, we could combine several homoclinic orbits instead of just one, as it was done for instance in [3].*

Remark 17 *We have chosen \mathbf{S}^u and \mathbf{S}^d to be at particular angles for the following reason. It turns out that for $\varepsilon > 0$ following the homoclinic orbit from \mathbf{S}^u to \mathbf{S}^u yields a gain in energy. Following the homoclinic orbit from \mathbf{S}^d to \mathbf{S}^d yields a reduction in the energy. We establish this rigorously in our computer assisted proof in Section 5.7. The change of energy happens as a trajectory goes around the primary. This part of the excursion is the lowest ‘wedge’ from the plots in Figures 3 and 4. If the tip is at $2k\pi - \pi/2$, $k \in \mathbb{Z}$, then we are gaining energy; when it is at $2k\pi + \pi/2$, $k \in \mathbb{Z}$, then we are losing energy. Traveling along the Lyapunov orbits does not yield significant energy changes.*

5.6 Construction of connecting sequences

Around the homoclinic points for PCRTBP described in Section 5.5 we construct connecting sequences. As the corresponding homoclinic orbit results from an intersection of a 2-dimensional unstable manifold and a 2-dimensional stable manifold of a Lyapunov orbit, there are well defined unstable and stable directions along the homoclinic orbit. These are given by the corresponding tangent vectors to the unstable and stable leaves from of the foliations of the manifolds. In the sequel, we only need approximations of the unstable/stable directions which are obtained via non-rigorous numerics.

We fix a sequence of points q_0^*, \dots, q_n^* along the homoclinic orbit, and along these points we position sections $\Sigma_0, \dots, \Sigma_n$, as discussed in Section 5.5; see Figure 2. We choose this orbit in the extended phase space which includes θ , by selecting $\pi_\theta q_0^* = 0$. Recall that $q_0^* \in \Sigma = \{Y = 0\}$ and also that we have chosen our points along the homoclinic so that for $k \in \{50, 58, 66, 74\}$ we have $q_k^* \in \Sigma = \{Y = 0\}$.

Each connecting sequence will always start with a window on the section $\Sigma = \{Y = 0\}$ and finish also with a window on $\Sigma = \{Y = 0\}$. At the section $\Sigma = \{Y = 0\}$ we use the

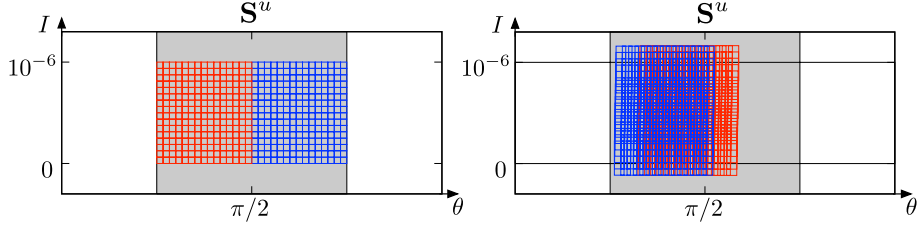


Figure 5: Transition from \mathbf{S}^u to \mathbf{S}^u . The strip \mathbf{S}^u is in grey. On the left hand side plot we see the windows $N_{\ell,0}$, for $\ell \in L_1^{uu}$ in blue and for $\ell \in L_2^{uu}$ in red. On the right hand side we have the windows N_{ℓ,k_ℓ} . For $\ell \in L_1^{uu}$ we take $k_\ell = n_1^{uu} = 50$ and for $\ell \in L_2^{uu}$ we take $k_\ell = n_2^{uu} = 66$ as the length of the connecting sequences.

local coordinate change Ψ given by (49). In our connecting sequences we allow the local coordinates $\Psi_{\ell,i,\varepsilon}$ on the intermediate sections Σ_i , for $i = 1, \dots, k_\ell - 1$, to be dependent on the choice of ℓ, i, ε , but we always start and finish at $\Sigma = \{Y = 0\}$, and always in the same local coordinates given by Ψ . The $A_{\ell,i}$ and $w_{\ell,i}$ for the coordinates $\Psi_{\ell,i,\varepsilon}$ at the sections Σ_i for $i = 1, \dots, k_\ell - 1$ are chosen so that we obtain (43) and (44) along the connecting sequence for the local maps of the form (42). (Our choices of $A_{\ell,i}$ and $w_{\ell,i}$ for such local coordinates are established numerically, by using non-rigorous computations.)

On the strips \mathbf{S}^u and \mathbf{S}^d at $\Sigma = \{Y = 0\}$ (see Section 5.5) we consider cones Q_a^ε as in (14), with $a = (a_y, a_I, a_\theta)$,

$$a_y = 10^{-3}, \quad a_I = 1, \quad a_\theta = 10.$$

We construct connecting sequences from \mathbf{S}^u to \mathbf{S}^u by subdividing $\mathbf{S}^u \cap \{I \in [0, 10^{-6}]\}$ into $16 \times 30 = 480$ windows $N_{\ell,0}$, overlapping along the I, θ coordinates. Their projections onto I, θ are depicted on the left hand side plot in Figure 5. We ensure that the windows overlap so that conditions (C1.iii) and (C2.iii) are fulfilled⁶. We take the windows $N_{\ell,0}$ on the x, y coordinates to be $[-r, r] \times [-r, r]$, the same as for the strip \mathbf{S}^u . We label the window with $\theta > \pi/2$ with a set of labels denoted L_1^{uu} and the windows with $\theta < \pi/2$ with a set of labels denoted L_2^{uu} . For each $\ell \in L_j^{uu}$ we consider a connecting sequence of length n_j^{uu} , for $j \in \{1, 2\}$ and construct a connecting sequences

$$(N_{\ell,0}, Q_a^\varepsilon) \xrightarrow{f_{\ell,1,\varepsilon}} \dots \xrightarrow{f_{\ell,n_j^{uu},\varepsilon}} (N_{\ell,n_j^{uu}}, Q_a^\varepsilon), \quad \ell \in L_j^{uu}, j \in \{1, 2\}. \quad (55)$$

In a similar way we construct connecting sequences from \mathbf{S}^d to \mathbf{S}^d . These sequences are of the lengths n_1^{dd} and n_2^{dd} , for L_1^{dd} and L_2^{dd} , respectively; see Figure 6.

We construct connecting sequences from \mathbf{S}^u to \mathbf{S}^d by subdividing $\mathbf{S}^u \cap \{I \in [0, 10^{-6}]\}$ into $16 \times 4 = 64$ windows $N_{\ell,0}$ as in Figure 7. (The reason why we construct fewer windows than for previous transitions will be explained in Section 5.7). We also construct connecting sequences from \mathbf{S}^d to \mathbf{S}^u in an analogous fashion; see Figure 8.

⁶Since $r = 10^{-6}$, $\varepsilon_0 = 1.6 \cdot 10^{-5}$ are very small, the required overlap of size $\varepsilon_0 a_I r$ and $a_\theta r$ (see Remarks 7 and 9) along I and θ , respectively, is so small that it is not visible on the plots at this resolution.

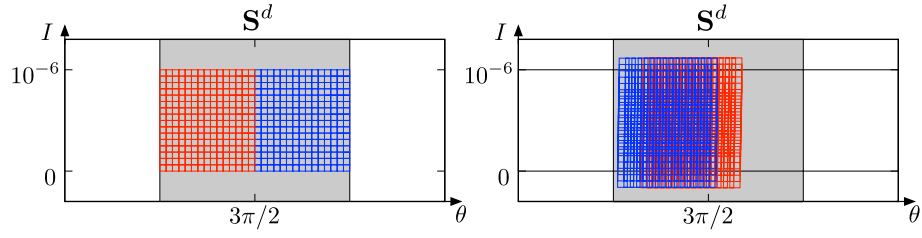


Figure 6: Transition from \mathbf{S}^d to \mathbf{S}^d . On the left we have the windows $N_{\ell,0}$, for $\ell \in L_1^{dd}$ in blue, and for $\ell \in L_2^{dd}$ in red. On the right are the respective windows N_{ℓ,k_ℓ} .

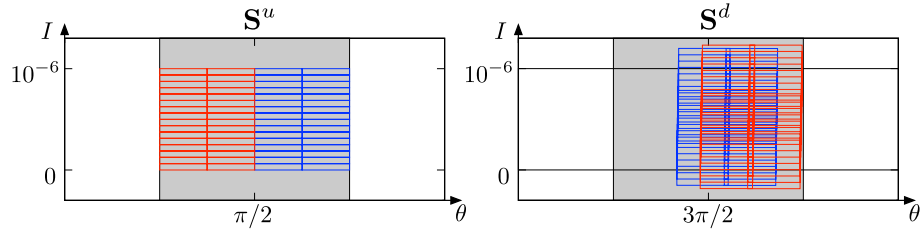


Figure 7: Transition from \mathbf{S}^u to \mathbf{S}^d . On the left we have the windows $N_{\ell,0}$, for $\ell \in L_1^{du}$ in blue, and for $\ell \in L_2^{du}$ in red. On the right are the respective windows N_{ℓ,k_ℓ} .

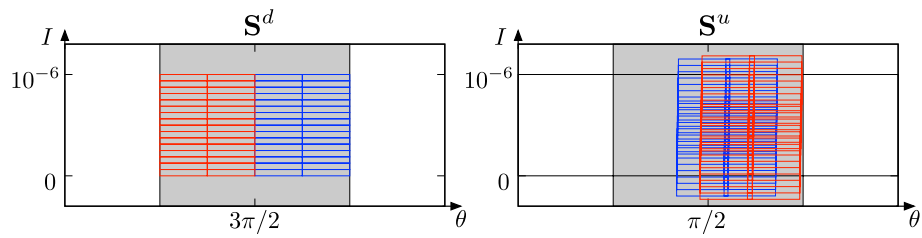


Figure 8: Transition from \mathbf{S}^d to \mathbf{S}^u . On the left we have the windows $N_{\ell,0}$, for $\ell \in L_1^{du}$ in blue, and for $\ell \in L_2^{du}$ in red. On the right are the respective windows N_{ℓ,k_ℓ} .

5.7 Proof of Theorem 1

Here we start the rigorous, interval-arithmetic validation of conditions **C1** and **C2** which lead to the proof of the main theorem.

Earlier sections provided a description of the choices of local maps (42) we use in our program. The key issue is that due to the form of the coordinate changes we consider, regardless of the particular choices of the coefficients for our local maps, we are sure that the change in I reflects precisely the change of the energy H_0 . This is ensured by Theorem 6 and the fact that our connecting sequences always start and finish in the same section $\Sigma = \{Y = 0\}$, with the same local coordinates Ψ .

In the computer assisted proof, for each map $f_{\ell,i,\varepsilon}$ involved in conditions **C1** and **C2** our program validates the correct alignment of windows, cone conditions, and establishes estimates on the change in energy. If at any point one of the required conditions would not be fulfilled, our program would stop and report an error.

Using Lemmas 1 and 2, we validate the correct alignment and cone condition along each step of the connecting sequences constructed in Section 5.6. We do this by subdividing the parameter interval $[0, \varepsilon_0]$ into eight smaller subintervals of equal length, and on each of them we perform the validation separately, as described in Remark 11. The plots from Figure 5, 6, 7, 8 show in fact the results obtained through the computer assisted proof and have been validated using rigorous interval arithmetic computations. Note that the windows which pass through n_1^{uu} sections shift in the angle θ to the left (blue), and those passing through n_2^{uu} sections (red) shift in the angle θ to the right, just as discussed in Section 5.5.

Thus we obtain a computer assisted proof of the following result.

Theorem 7 *In the Neptune-Triton system, for every $\varepsilon \in (0, \varepsilon_0]$, with $\varepsilon_0 = 1.6 \cdot 10^{-5}$, for every $\kappa, r \in \{u, d\}$, there exist connecting sequences from \mathbf{S}^κ to \mathbf{S}^r*

$$(N_{\ell,0}, Q_a^\varepsilon) \xrightarrow{f_{\ell,1,\varepsilon}} \dots \xrightarrow{f_{\ell,n_j^{\kappa r},\varepsilon}} (N_{\ell,n_j^{\kappa r}}, Q_a^\varepsilon), \quad l \in L_j^{\kappa r}, j \in \{1, 2\},$$

which fulfill the conditions (C1.i–C1.iii) and (C2.i–C2.iii).

To estimate the change of I along the connecting sequences, we need to obtain estimates on the derivative of the return map with respect to the parameter $\varepsilon \in (0, \varepsilon_0]$. For this we use Lemmas 3, 4, which together with computer assisted validation allows us to prove the following theorem.

Theorem 8 *Let*

$$c = 0.00012, \quad \text{and} \quad C = 0.0076.$$

In the Neptune-Triton system, for every $\varepsilon \in (0, \varepsilon_0]$, with $\varepsilon_0 = 1.6 \cdot 10^{-5}$, for every z which passes through the corresponding connecting sequence we have the following bounds:

$$\begin{aligned} c\varepsilon < \pi_I F_{\ell,\varepsilon}(z) - \pi_I(z) &< C\varepsilon && \text{for } \ell \in L_1^{uu} \cup L_2^{uu}, \\ c\varepsilon < \pi_I(z) - \pi_I F_{\ell,\varepsilon}(z) &< C\varepsilon && \text{for } \ell \in L_1^{dd} \cup L_2^{dd}, \\ |\pi_I F_{\ell,\varepsilon}(z) - \pi_I(z)| &< C\varepsilon && \text{for } \ell \in L_1^{ud} \cup L_2^{ud} \cup L_1^{du} \cup L_2^{du}. \end{aligned}$$

The main difficulty in the computer assisted validation of above theorem was obtaining the lower bound c . This is the reason why we needed more subdivisions of the strips for the transitions from \mathbf{S}^u to \mathbf{S}^u and from \mathbf{S}^d to \mathbf{S}^d than for \mathbf{S}^u to \mathbf{S}^d and \mathbf{S}^d to \mathbf{S}^u . (The smaller the sets the sharper the interval arithmetic bounds.)

We are ready to prove the main theorem.

Proof of Theorem 1. The initial level of the energy h_0 is the energy of the Lyapunov orbit of the PCR3BP, which passes through q^* from (45),

$$h_0 = H_0(q^*) = -1.5050906397016.$$

By Theorems 7, 8 conditions **C1** and **C2** are satisfied, which by the Theorems 2, 3, and 5 gives (1), (2) and (4), respectively.

We will now show that **C3** is satisfied. Let $\ell_1, \ell_2 \in L^{uu}$ and $\ell'_1 \in L^{ud}$, $\ell'_2 \in L^{du}$. Trajectories starting from points from the domain of $F_{\ell_2, \varepsilon} \circ F_{\ell_1, \varepsilon}$ make different numbers of turns around the Lyapunov orbit between the homoclinic excursions than trajectories starting from the domain of $F_{\ell'_2, \varepsilon} \circ F_{\ell'_1, \varepsilon}$ (see Figures 3, 4), hence the domains are disjoint. The same argument can be applied when $\ell_1, \ell_2 \in L^{dd}$ and $\ell'_1 \in L^{du}$, $\ell'_2 \in L^{ud}$, which means that condition **C3** is fulfilled. By Theorem 4 the Hausdorff dimension of the set of initial points for orbits that shadow a given energy sequence is strictly greater than 3 in the four dimensional section $\{Y = 0\}$. Due to the smooth dependence of solutions on initial conditions, we know that cone conditions, covering relations and energy change bounds will also hold for connecting sequences which start and finish at sections $\{Y = \mathcal{Y}\}$, for all $|\mathcal{Y}| < \mathcal{Y}_0$, for sufficiently small $\mathcal{Y}_0 > 0$. This means that in the full phase space the Hausdorff dimension of the sets of orbits that shadow an energy sequence is strictly greater than 4.

Now we verify the choice of T and η from Theorem 1. From Theorem 2 we know that to diffuse the distance of 1 along I we need no more than $1/(c\varepsilon)$ transitions between strips. Here we diffuse over a shorter distance $C_{h_0} = 10^{-6}$, so the number of needed transitions is $C_{h_0}/(c\varepsilon)$. Each transition takes less time than $(9 + \frac{1}{10})\pi$ (see Figures 3, 4). This means that the time needed to diffuse over the distance C_{h_0} is less than

$$\frac{(9 + \frac{1}{10})\pi C_{h_0}}{c\varepsilon} < \frac{1}{4\varepsilon} = \frac{1}{\varepsilon} T.$$

From Theorem 3 (see also Remark 10) we know that we need

$$\eta \geq 2ra_I + C = 2 \cdot 10^{-6} \cdot 1 + 0.0076.$$

Clearly $\eta = 10^{-2}$ satisfies this condition. ■

The total CPU time of the computer assisted proof was 186406 seconds. The proof was conducted using a parallel computation on eight threads of an iMac desktop computer with four 3.1 GHz Intel i7 cores. Running it once takes under six and a half hours.

6 Propagation of discs

In this section we introduce the notion of horizontal discs which satisfy Q^ε -cone condition. Such discs will be the main building blocks used for the proofs of Theorems 2, 3, 4 and 5.

We stress that discs are not directly used in the computer assisted proof of Theorem 1. That proof relies on the construction of connecting sequences.

Definition 6 A continuous map $h : \bar{B}^{n_u} \rightarrow \mathbb{R}^{n_u} \times \mathbb{R}^{n_s+2}$ that satisfies a graph condition that $h(x) = (x, \pi_{y,I,\theta} h(x))$, for all $x \in \bar{B}^{n_u}$ will be referred to as a horizontal disc. If $h(\bar{B}^{n_u}) \subseteq N$ then h is said to be a horizontal disc in N .

Recall that in (14) we have considered $Q^\varepsilon : \mathbb{R}^{n_u} \times \mathbb{R}^{n_s} \times \mathbb{R} \times \mathbb{R} \rightarrow \mathbb{R}$ which define cones, and that we have assumed that Q^ε satisfy condition (15).

Definition 7 Given a cone $Q^\varepsilon : \mathbb{R}^{n_u} \times \mathbb{R}^{n_s+2} \rightarrow \mathbb{R}$, a horizontal disc $h : \bar{B}^{n_u} \rightarrow \mathbb{R}^{n_u} \times \mathbb{R}^{n_s+2}$ is said to satisfy a Q^ε -cone condition if $Q^\varepsilon(h(x) - h(x')) > 0$, for all $x, x' \in \bar{B}^{n_u}$ with $x \neq x'$. We shall refer to such h as a Q^ε -disc.

The image $h(\bar{B}^{n_u})$ of a Q^ε -disc is a n_u -dimensional topological disc. In the sequel we will use the same notation h for the image $h(\bar{B}^{n_u})$ of the map h as for the map itself. From now in the case of a Q^ε -disc, we shall add a superscript and write h^ε .

Remark 18 Definition 6 is an analogue of the definition of a ‘horizontal disc’ from [4]. It is slightly simplified compared to [4]. A horizontal disc in the sense of [4], which satisfies the cone condition, is a Q^ε -disc in the sense of Definition 6; and vice versa. (See [4, Lemma 5].)

Remark 19 An important feature is that the length of a Q^ε -disc h^ε is bounded along the θ, I directions, with the bound in I of order $O(\varepsilon)$. This is because by (15) for any $x, x' \in \bar{B}^{n_u}$ from $Q^\varepsilon(h^\varepsilon(x) - h^\varepsilon(x')) > 0$ it follows that

$$\begin{aligned} \|\pi_\theta(h^\varepsilon(x) - h^\varepsilon(x'))\| &\leq a_\theta \|\pi_x(x - x')\| \leq 2a_\theta, \\ \|\pi_I(h^\varepsilon(x) - h^\varepsilon(x'))\| &\leq \varepsilon a_I \|\pi_x(x - x')\| \leq 2\varepsilon a_I. \end{aligned}$$

Let us now turn to our IFS (10) from Section 3.1. Let us assume that for this IFS we have a finite collection of connecting sequences indexed by L as in Section 3.4.

Theorem 9 [4, Theorem 7] Given $\ell \in L$, for every connecting sequence (17) and for every Q^ε -disc h^ε in $N_{\ell,0}$ there exists a topological disc $\mathcal{D} \subset h^\varepsilon$ such that for all $z \in \mathcal{D}$ holds

$$(f_{\ell,m,\varepsilon} \circ f_{\ell,m-1,\varepsilon} \circ \dots \circ f_{\ell,1,\varepsilon})(z) \in N_{\ell,m}, \quad \text{for } m = 1, \dots, k_\ell - 1,$$

and $F_{\ell,\varepsilon}(\mathcal{D}) = (f_{\ell,k_\ell,\varepsilon} \circ f_{\ell,k_\ell-1,\varepsilon} \circ \dots \circ f_{\ell,1,\varepsilon})(\mathcal{D})$ is a graph of some Q^ε -disc \tilde{h}^ε in N_{ℓ,k_ℓ} ; i.e. $\tilde{h}^\varepsilon(\bar{B}^{n_u}) = F_{\ell,\varepsilon}(\mathcal{D})$.

When applying Theorem 9 we shall say that the Q^ε -disc h^ε is propagated (or moved) through the connecting sequence to become the Q^ε -disc \tilde{h}^ε .

Remark 20 From Remark 19 we know that horizontal discs are ‘slim’ along the central coordinates. The sizes of successive windows in a connecting sequence can grow along central coordinates. After propagating a horizontal disc through such sequence we obtain a horizontal disc, which remains ‘slim’ in the central coordinates. We can then enclose it in another window, which is again ‘slim’ in the central coordinates, and propagate once more through another connecting sequence. We can repeat such procedure infinitely many times. The fact that the propagated horizontal discs do not grow along the central coordinates is the key feature that allows to topologically control the central coordinate and obtain infinite orbits. For this, we require both correct alignment of windows as well as cone conditions. The latter ensure that the discs remain ‘slim’.

7 Existence of diffusing orbits

In this section we will give the proof of Theorem 2. We first give a version of this theorem in terms of Q^ε -discs – Theorem 10 – from which we derive Theorem 2.

7.1 Diffusion under conditions on Q^ε -discs

Consider an iterated function system (10) as described in Section 3.1, and the strip $\mathbf{S}^u \subset \Sigma_0$ defined in (16). We formulate the following condition.

Condition A1. There exists a constant $0 < c$, such that for every $\varepsilon \in (0, \varepsilon_0]$ and every Q^ε -disc $h^\varepsilon \subseteq \mathbf{S}^u$, the following hold:

(A1.1) There exist $F_{\ell, \varepsilon}$ in \mathcal{F}_ε and a Q^ε -disc $\tilde{h}^\varepsilon : \bar{B}^{n_u} \rightarrow \mathbf{S}^u$ satisfying

$$\tilde{h}^\varepsilon \subseteq F_{\ell, \varepsilon}(h^\varepsilon);$$

(A1.2) For each $z \in h^\varepsilon$ and $\tilde{z} = F_{\ell, \varepsilon}(z) \in \tilde{h}^\varepsilon$, we have that

$$\pi_I(\tilde{z}) - \pi_I(z) > c\varepsilon. \quad (56)$$

Theorem 10 *Assume that the IFS \mathcal{F}_ε satisfies Condition A1.*

Then, for every $M > 0$, and every $\varepsilon \in (0, \varepsilon_0]$, there exist $z \in \mathbf{S}^u$, $m \leq M/(c\varepsilon)$, and a sequence of functions $F_{\ell_1, \varepsilon}, \dots, F_{\ell_m, \varepsilon}$ in the IFS \mathcal{F}_ε , such that $\tilde{z} = (F_{\ell_m, \varepsilon} \circ \dots \circ F_{\ell_1, \varepsilon})(z)$ satisfies

$$\pi_I(\tilde{z}) - \pi_I(z) > M. \quad (57)$$

Proof. Fix $\varepsilon \in (0, \varepsilon_0]$.

We start with any Q^ε -disk $h_0^\varepsilon : \bar{B}^{n_u} \rightarrow \mathbf{S}^u$. (We can let, for instance, $h_0^\varepsilon(x) = (x, y_0, I_0, \theta_0)$ for some $y_0 \in \bar{B}^{n_s}, I_0 \in \mathbb{R}$ and $\theta_0 \in S_\theta^u$.) By our assumptions, there exists a Q^ε -disk $h_1^\varepsilon \subseteq F_{\ell_1, \varepsilon}(h_0^\varepsilon)$ as in (A1.1). The set of points $z_0 \in h_0^\varepsilon$ for which $z_1 = F_{\ell_1, \varepsilon}(h_0^\varepsilon(z_0)) \in h_1^\varepsilon$ forms a n_u -dimensional topological disk $\mathcal{D}_0^\varepsilon \subseteq h_0^\varepsilon$, which is the image under h_0^ε of a n_u -dimensional disk in \bar{B}^{n_u} . By (A1.2) we have $\pi_I(z_1) - \pi_I(z_0) > c\varepsilon$.

Inductively, at the n -th step, there exist a topological disc $\mathcal{D}_{n-1}^\varepsilon \subseteq h_0^\varepsilon$, a Q^ε -disk h_n^ε , and some functions $F_{\ell_1, \varepsilon}, \dots, F_{\ell_n, \varepsilon}$ in the IFS \mathcal{F}_ε such that $z_n = (F_{\ell_n, \varepsilon} \circ \dots \circ F_{\ell_1, \varepsilon})(z_0) \in h_n^\varepsilon$ for every $z_0 \in \mathcal{D}_{n-1}^\varepsilon$, with the disc $\mathcal{D}_{n-1}^\varepsilon$ satisfying

$$\mathcal{D}_{n-1}^\varepsilon \subseteq \mathcal{D}_{n-2}^\varepsilon \subseteq \dots \subseteq \mathcal{D}_0^\varepsilon,$$

where $\mathcal{D}_{n-2}^\varepsilon, \dots, \mathcal{D}_0^\varepsilon$ are the discs constructed at the previous steps. Also, $\pi_I(z_n) - \pi_I(z_0) > n\varepsilon \cdot c$.

For the induction step, there exists a Q^ε -disc

$$h_{n+1}^\varepsilon \subseteq F_{\ell_{n+1}, \varepsilon}(h_n^\varepsilon).$$

The set of points $z_{n+1} = F_{\ell_{n+1}, \varepsilon}(z_n) \in h_{n+1}^\varepsilon$ with $z_n \in h_n^\varepsilon$ of the form $z_n = (F_{\ell_n, \varepsilon} \circ \dots \circ F_{\ell_1, \varepsilon})(z_0)$ corresponds to a set of points $z_0 \in \mathcal{D}_n^\varepsilon \subseteq \mathcal{D}_{n-1}^\varepsilon$. We also have $\pi_I(z_{n+1}) - \pi_I(z_n) > c\varepsilon$. We obtain that

$$z_{n+1} = F_{\ell_{n+1}, \varepsilon} \circ F_{\ell_n, \varepsilon} \circ \dots \circ F_{\ell_1, \varepsilon}(z_0)$$

for $z_0 \in \mathcal{D}_n^\varepsilon$, and $\pi_I(z_{n+1}) - \pi_I(z_0) > c(n+1)\varepsilon$.

Repeating the iterative procedure for m -steps, with $m \leq M/(c\varepsilon)$, yields an orbit along which the change in the action I is more than M , which concludes the proof of the theorem.

For future reference, note that the points $z_0 \in h_0^\varepsilon$, for which $z_m = (F_{\ell_m, \varepsilon} \circ \dots \circ F_{\ell_1})(z)$ is as in the statement of the theorem, form a disc $\mathcal{D}_{m-1}^\varepsilon$, and we have $\mathcal{D}_{m-1}^\varepsilon \subseteq \mathcal{D}_{m-2}^\varepsilon \subseteq \dots \subseteq \mathcal{D}_0^\varepsilon$. ■

7.2 Diffusion under conditions on connecting sequences

In this section we give the proof of Theorem 2 and make a remark how it can be generalized to the setting when action angle coordinates are higher dimensional.

Proof of Theorem 2. The result follows from an analogous construction to the proof of Theorem 10, which is based on propagating Q^ε -discs from \mathbf{S}^u to \mathbf{S}^u . There are some technical differences though that we will point out below. In this new construction, we choose the initial Q^ε -disc h_0^ε to be $h_0^\varepsilon : \bar{B}^{n_u} \rightarrow \mathbf{S}^u$ (see proof of Theorem 10), defined as $h_0^\varepsilon(x) := (x, y_0, \theta_0, I_0)$, for some (arbitrary) fixed $y_0 \in \bar{B}^{n_s}$, $\theta_0 \in S_\theta^u$ and for $I_0 = 0$.

By Theorem 9, assumption (A1.1) from Theorem 10 follows from (C1.i–C1.iii). In more detail, by Remark 19 any Q^ε -disc h^ε in $\mathbf{S}^u \cap \{I \in [0, 1]\}$ is contained in a multi-dimensional rectangle $\bar{B}^{n_u} \times \bar{B}^{n_s} \times \bar{B}(I^*, \varepsilon_0 a_I) \cap [0, 1] \times \bar{B}(\theta^*, a_\theta) \cap [\theta^{a,1}, \theta^{a,2}]$ for $I^* = \pi_I h^\varepsilon(0)$ and $\theta^* = \pi_\theta h^\varepsilon(0)$. Condition (C1.ii) combined with (C1.iii) implies that the multi dimensional rectangle is in some set $N_{\ell,0}$. (In case that $(I^*, \theta^*) \in \pi_{I,\theta} N_{\ell,0}$ for just one $\ell \in L$ we use (C1.iii) with $\ell = \ell'$.) This ensures that we can enclose h^ε in some set $N_{\ell,0}$, and use Theorem 9 to obtain $\tilde{h}^\varepsilon = F_{\ell, \varepsilon}(\mathcal{D})$.

We note that by (C1.ii) we can only ensure that \tilde{h}^ε is in $N_{\ell, k_\ell} \subset \mathbf{S}^u$; we can not ensure that $\pi_I \tilde{h}^\varepsilon \subset [0, 1]$. This means that it is possible that after repeatedly propagating the Q^ε -disc h^ε the resulting Q^ε -disc \tilde{h}^ε is no longer contained in $\mathbf{S}^u \cap \{I \in [0, 1]\}$. In that case, we might not be able to keep propagating h^ε further along another connecting sequence. Having $\tilde{h}^\varepsilon \not\subset \mathbf{S}^u \cap \{I \in [0, 1]\}$ implies that, for some $z \in \tilde{h}^\varepsilon$ we have $\pi_I z > 1$, in which case (21) is obtained, and we do not need to propagate further. In short, for any Q^ε -disc h^ε in $\mathbf{S}^u \cap \{I \in [0, 1]\}$ we can either obtain the Q^ε -disc \tilde{h}^ε in $\mathbf{S}^u \cap \{I \in [0, 1]\}$, as in condition (A1.1) from Theorem 10, which enables us to continue with another step of the construction, or the Q^ε -disc \tilde{h}^ε contains a point outside of $\{I \leq 1\}$, implying that we have already achieved the required change in I and we do not need to propagate the Q^ε -disc any more.

Condition (C1.iv) is equivalent to condition (A1.2) from Theorem 10. It implies that the Q^ε -discs which are propagated from \mathbf{S}^u to \mathbf{S}^u by our construction must exit $\{I \leq 1\}$ after a finite number of iterates of the maps.

Now we will show how we obtain the bound on the Lebesgue measure for orbits which diffuse the distance $\frac{1}{3}$ in I . Take a Q^ε -disc $h_0^\varepsilon(x) = (x, y_0, I_0, \theta_0)$ with $y_0 \in \bar{B}^{n_s}$, $I_0 \in [0, 1/3]$, $\theta_0 \in S_\theta^u$. By the construction from our proof, we know that there exists an m , a sequence $\ell_1, \dots, \ell_m \in L$, a topological disc $\mathcal{D} \subset h_0^\varepsilon$, and a Q^ε -disc $\tilde{h}^\varepsilon = F_{\ell_m, \varepsilon} \circ \dots \circ F_{\ell_1, \varepsilon}(\mathcal{D})$ such that $\pi_I \tilde{h}^\varepsilon > 2/3$. Since as we propagate h_0^ε with each transition we gain more than εc in I , we see that $m \leq 2/(3\varepsilon c)$.

Let us now take two points $z_0, z_1 \in \mathcal{D}$ such that $F_{\ell_m, \varepsilon} \circ \dots \circ F_{\ell_1, \varepsilon}(z_1) = \tilde{z} \in \tilde{h}^\varepsilon(\partial B^{n_u})$,

and $F_{\ell_m, \varepsilon} \circ \dots \circ F_{\ell_1, \varepsilon}(z_0) = \tilde{h}^\varepsilon(0)$. From (22), by the mean value theorem,

$$\begin{aligned} 1 &= \|\pi_x(\tilde{z} - \tilde{h}^\varepsilon(0))\| \\ &= \|\pi_x(F_{\ell_m, \varepsilon} \circ \dots \circ F_{\ell_1, \varepsilon}(z_1) - F_{\ell_m, \varepsilon} \circ \dots \circ F_{\ell_1, \varepsilon}(z_0))\| \\ &\leq \alpha^m \|z_1 - z_0\|, \end{aligned}$$

which means that $B^{n_u}(z_0, \alpha^{-m}) \subset \pi_x \mathcal{D} \subset h_0^\varepsilon$. This holds for any choice of $y_0 \in \bar{B}^{n_s}$, $I_0 \in [0, 1/3]$, $\theta \in S_\theta^u$, which since $\alpha^{-m} \leq \alpha^{-2/(3\varepsilon c)}$ implies the claim; the n_u in the bound $\alpha^{-2n_u/(3\varepsilon c)}$ in the statement of the theorem comes from the fact that for any $r > 0$ we have $\mu(B^{n_u}(z_0, r)) = r^{n_u} \mu(B^{n_u})$. ■

Remark 21 Theorems 10 and 2 can be generalized to a setting where the action angle coordinates are higher dimensional $(I_1, \dots, I_{n_c}, \theta_1, \dots, \theta_{n_c})$.

To obtain a higher dimensional version of Theorem 10 we can proceed as follows. We define the strip $\mathbf{S}^u = \bar{B}^{n_u} \times \bar{B}^{n_s} \times \mathbb{R}^{n_c} \times S_\theta^u$ with $S_\theta^u = \prod_{i=1}^{n_c} [\theta_i^{u,1}, \theta_i^{u,2}]$. Under the conditions as in Theorem 10, if (56) holds for one of the action variable I_{i_*} , for $i_* \in \{1, \dots, d\}$, i.e., $\pi_{I_{i_*}}(\tilde{z}) - \pi_{I_{i_*}}(z) > c\varepsilon$, then we obtain diffusion along I_{i_*} .

For Theorem 2, to obtain diffusion of length $\frac{1}{2}$ in one of the actions, we can proceed as follows. We define the strip \mathbf{S}^u as above, and consider $I \in [0, 1]^{n_c}$. We need the condition **C1**, but it is enough that (20) holds for one action I_{i_*} that is, $\pi_{I_{i_*}} F_{i, \varepsilon}(z) - \pi_{I_{i_*}}(z) > c\varepsilon$. We can then repeat the construction from the proof of Theorem 2 taking $h^\varepsilon(x) = (x, y_0, I_0, \theta_0)$ for arbitrary $y_0 \in \bar{B}^{n_s}$, $I_0 = (\frac{1}{2}, \dots, \frac{1}{2})$ and any $\theta_0 \in S_\theta^u$. As we propagate h^ε through successive connecting sequences we increase in I_{i_*} . There is a possibility that as we propagate the discs some of them will leave $\{I \in [0, 1]^{n_c}\}$ along some other action than I_{i_*} . Nevertheless, for this to happen we also achieve a change of order $O(1)$ in the I_{i_*} -direction. In such case we obtain diffusion in the I_{i_*} -direction as well as in some other action direction.

8 Symbolic dynamics

In this section we prove Theorem 3. We do so by first formulating a version of this theorem in terms of Q^ε -discs – Theorem 11 – which we then use for the proof of Theorem 3. We also discuss how the results can be generalized to higher dimensional I .

8.1 Symbolic dynamics under conditions on Q^ε -discs

Here we introduce a theorem which establishes the symbolic dynamics under assumptions on propagation of Q^ε -discs. As before, for $\ell \in L$ we let $F_{\ell, \varepsilon} = f_{\ell, k_{\ell, \varepsilon}} \circ \dots \circ f_{\ell, 1, \varepsilon} \in \mathcal{F}_\varepsilon$, where \mathcal{F}_ε is our IFS from (10). We formulate the following condition.

Condition A2. There exist constants $0 < c < C$, such that for every $\varepsilon \in (0, \varepsilon_0]$ and every Q^ε -disk $h^\varepsilon \subseteq \mathbf{S}^u \cup \mathbf{S}^d$ the following holds:

(A2.1) For each $\kappa \in \{u, d\}$ there exist $F_{\ell, \varepsilon}$ in \mathcal{F}_ε and a Q^ε -disk $\tilde{h}^\varepsilon : \bar{B}^u \rightarrow \mathbf{S}^\kappa$ with

$$\tilde{h}^\varepsilon \subseteq F_{\ell, \varepsilon}(h^\varepsilon).$$

(A2.2) For $h^\varepsilon, \tilde{h}^\varepsilon$ as in (1), for all pairs of points $z \in h^\varepsilon, \tilde{z} \in \tilde{h}^\varepsilon$ with $\tilde{z} = F_{\ell,\varepsilon}(z)$ we have the following

$$(A2.2.i) \quad |\pi_I(\tilde{z}) - \pi_I(z)| < C\varepsilon. \quad (58)$$

(A2.2.ii) If $h^\varepsilon \subseteq \mathbf{S}^u$ (resp. \mathbf{S}^d) and $\tilde{h}^\varepsilon \subseteq \mathbf{S}^u$ (resp. \mathbf{S}^d) we have the following

$$\begin{aligned} c\varepsilon &< \pi_I(\tilde{z}) - \pi_I(z) \\ (\text{resp. } c\varepsilon &< \pi_I(z) - \pi_I(\tilde{z})). \end{aligned} \quad (59)$$

Theorem 11 *Assume that the IFS \mathcal{F}_ε satisfies Condition A2. Let $\eta = 2a_I + C$.*

Then for every $\varepsilon \in (0, \varepsilon_0]$ and every infinite sequence of I -level sets $(I^n)_{n \in \mathbb{N}} \subseteq \mathbb{R}$, with $|I^{n+1} - I^n| > 2\eta\varepsilon$ there exists an orbit $(z_n)_{n \in \mathbb{N}}$ of the IFS, and an increasing sequence $(k_n)_{n \in \mathbb{N}} \subseteq \mathbb{N}$, such that for every $n \in \mathbb{N}$ we have

$$|\pi_I(z_{k_n}) - I^n| < \varepsilon\eta. \quad (60)$$

Proof. The main idea is the following. If we want to increase the I -coordinate we move the Q^ε -disc by iterating from the energy strip \mathbf{S}^u to itself. If we want to decrease the I -coordinate we propagate the disk from the energy strip \mathbf{S}^d to itself. If we want to switch from increasing the I -coordinate to decreasing the I -coordinate, or from decreasing the I -coordinate to increasing the I -coordinate, we propagate the Q^ε -disc from \mathbf{S}^u to \mathbf{S}^d , or from \mathbf{S}^d to \mathbf{S}^u , respectively. We provide the details below.

Case 1.A. Assume $I^0 < I^1$. Start with any Q^ε -disk h_0^ε in \mathbf{S}^u such that $\pi_I(h_0^\varepsilon) \subseteq (I^0 - \eta, I^0 + \eta)$. By assumption (A2.1) there is a map $F_{\ell,\varepsilon} \in \mathcal{F}_\varepsilon$ and a Q^ε -disk \tilde{h}^ε in \mathbf{S}^u such that $\tilde{h}^\varepsilon \subseteq F_{\ell,\varepsilon}(h_0^\varepsilon)$. By (A2.2.i) and (A2.2.ii) for each point $z_0 \in h_0^\varepsilon$ with $\tilde{z} = F_{\ell,\varepsilon}(z_0) \in \tilde{h}^\varepsilon$ we have

$$\varepsilon c < \pi_I(\tilde{z}) - \pi_I(z_0) < \varepsilon C.$$

That is, moving the Q^ε -disk h_0^ε along the composition of maps to a Q^ε -disk \tilde{h}^ε , each point on h_0^ε that lands on \tilde{h}^ε changes its I -coordinate by at least εc and at most εC . This means that, by repeating this procedure for finitely many times we can obtain a Q^ε -disk h_1^ε such that, for some point $z_* \in h_1^\varepsilon$ we have $|\pi_I(z_*) - I^1| < C\varepsilon$. Then by Remark 19 for any $z_1 \in h_1^\varepsilon$,

$$|\pi_I(z_1) - I^1| \leq |\pi_I(z_1) - \pi_I(z_*)| + |\pi_I(z_*) - I^1| < 2\varepsilon a_I + \varepsilon C \leq \varepsilon\eta, \quad (61)$$

as required for (60).

Case 1.B. If $I^0 > I^1$, we proceed with a similar construction starting with any Q^ε -disk h_0^ε contained in \mathbf{S}^d , and moving the disk from \mathbf{S}^d to \mathbf{S}^d , until we obtain a Q^ε -disk h_1^ε satisfying $|\pi_I(z_1) - I^1| \leq \varepsilon\eta$ for all $z_1 \in h_1^\varepsilon$.

Case 2.A. Assume that we are as in *Case 1.A*, and that $I^1 < I^2$. Then, starting with the Q^ε -disk h_1^ε obtained at the end of the construction, we proceed in the same way as in *Case 1.A*, moving the disk h_1^ε repeatedly by passing from \mathbf{S}^u to \mathbf{S}^u (by doing so we increase I), until we obtain a Q^ε -disk h_2^ε satisfying $|\pi_I(z_2) - I^2| < \varepsilon\eta$, for all $z_2 \in h_2^\varepsilon$.

If we are as in *Case 1.B*, and $I^1 > I^2$, we proceed in a similar fashion.

Case 2.B. Assume that we are as in *Case 1.A*, that is $I^0 < I^1$, and that $I^1 > I^2$. Consider the Q^ε -disk h_1^ε obtained at the end of the construction of *Case 1.A*. If for some

$z \in h_1^\varepsilon$ we have $\pi_I(z) - I^2 < C\varepsilon$, then we propagate the disc h_1^ε by passing from \mathbf{S}^u to \mathbf{S}^u (by doing so we increase I) until we end up with a Q^ε -disc $h_1^{\varepsilon,*}$ such that for any $z \in h_1^{\varepsilon,*}$, $\pi_I(z) - I^2 > C\varepsilon$. Once this is achieved, we choose a mapping $F_{\ell,\varepsilon}$ in \mathcal{F}_ε satisfying (A2.1), (A2.2) with $\kappa = d$ and obtain a Q^ε -disc \tilde{h} in \mathbf{S}^d , $\tilde{h}^\varepsilon \subseteq F_{\ell,\varepsilon}(h_1^{\varepsilon,*})$. For any $\tilde{z} \in \tilde{h}^\varepsilon$, $\tilde{z} = F_{\ell,\varepsilon}(z)$ for some $z \in h_1^{\varepsilon,*}$, we have

$$\pi_I(\tilde{z}) - I^2 = (\pi_I(\tilde{z}) - \pi_I(z)) + (\pi_I(z) - I^2) > (-C\varepsilon) + (C\varepsilon) = 0.$$

If for all $z \in \tilde{h}^\varepsilon$ we have $|\pi_I(z) - I^2| < \varepsilon\eta$, then we take $h_2^\varepsilon = \tilde{h}^\varepsilon$, and the step is finished. If not, then we proceed with the construction from *Case 1.B*. i.e., propagate the disc \tilde{h}^ε by passing from \mathbf{S}^d to \mathbf{S}^d , as in Case 1.B (by doing so we decrease I) until we end up with h_2^ε for which for all $z_2 \in h_2^\varepsilon$ we have $|\pi_I(z_2) - I^2| < \varepsilon\eta$.

If we are as in *Case 1.B*, and $I^1 < I^2$, that is $I^0 > I^1$ and $I^2 > I^1$, we proceed in a similar fashion, but switching from the energy strip \mathbf{S}^d to the energy strip \mathbf{S}^u .

Repeating these constructions for all $\{I^n\}_{\sigma \in \mathbb{N}}$, we obtain at each step a Q^ε -disc h_n^ε such that for all $z_n \in h_n^\varepsilon$ we have $|\pi_I(z_n) - I^n| < \varepsilon\eta$. We reach a Q^ε -disc h_n^ε by iterating the Q^ε -disc h_{n-1}^ε by successively applying some maps of the IFS \mathcal{F}_ε , i.e., $h_n^\varepsilon \subseteq F_{\ell_{i_n},\varepsilon}^\circ \circ \dots \circ F_{\ell_1,\varepsilon}^\circ(h_{n-1}^\varepsilon)$, for some $\ell_1^n, \dots, \ell_{i_n}^n \in L$. This means that there exists a topological disc $\mathcal{D}_n^\varepsilon \subset h_0^\varepsilon$ such that

$$h_n^\varepsilon = \left(\left(F_{\ell_{i_n},\varepsilon}^\circ \circ \dots \circ F_{\ell_1,\varepsilon}^\circ \right) \circ \dots \circ \left(F_{\ell_1^1,\varepsilon}^\circ \circ \dots \circ F_{\ell_1^1,\varepsilon}^\circ \right) \right) (\mathcal{D}_n^\varepsilon).$$

Since $\mathcal{D}_n^\varepsilon \subseteq \dots \subseteq \mathcal{D}_1^\varepsilon \subseteq \mathcal{D}_0^\varepsilon$, using the Nested Compact Set Theorem, we obtain an orbit $(z_n)_{n \in \mathbb{N}}$ of the IFS together with the sequence $k_n = i_1 + \dots + i_n$ as in the statement of the theorem. ■

8.2 Symbolic dynamics under conditions on connecting sequences

In this section we give the proof of Theorem 3, and later comment how it can be generalized to higher dimensional I .

Proof of Theorem 3. The proof follows from the same construction as the proof of Theorem 11.

As in the proof of Theorem 2, condition (A2.1) of Theorem 11 follow from (C2.i–C2.iii), combined with Theorem 9. Conditions (A2.2.i) and (A2.2.ii) of Theorem 11 follow from (C2.iv), (C2.v), combined with Theorem 9. The shadowing of I^n is therefore obtained identically as in the proof of Theorem 11.

Conditions (C2.i–C2.iii) ensure that any Q^ε -disc in $\mathbf{S}^\kappa \cap \{I \in [0, 1]\}$, for $\kappa \in \{u, d\}$, can be propagated to \mathbf{S}^u and to \mathbf{S}^d .

One technical detail is to show that we can obtain Q^ε -discs whose I -coordinates $(\varepsilon\eta)$ -shadow the given action level sets so that these discs never leave $(\mathbf{S}^u \cup \mathbf{S}^d) \cap \{I \in [0, 1]\}$. More precisely, we need to ensure that we can propagate these discs through connecting sequences such that the successive iterates of the discs under $F_{\ell,\varepsilon}$ return to $(\mathbf{S}^u \cup \mathbf{S}^d)$ without leaving $\{I \in [0, 1]\}$.

Assume that the Q^ε -disc h^ε is such that $\pi_I h^\varepsilon \subset (I^n - \varepsilon\eta, I^n + \varepsilon\eta)$. Since $(I_n)_{n \in \mathbb{N}} \subseteq [2\varepsilon\eta, 1 - 2\varepsilon\eta]$, it follows that

$$\pi_I(h^\varepsilon) \subseteq (\varepsilon\eta, 1 - \varepsilon\eta). \tag{62}$$

Let \tilde{h}^ε be the image of h^ε in $\mathbf{S}^u \cup \mathbf{S}^d$ under some appropriate mapping $F_{\ell,\varepsilon}$ from \mathcal{F}_ε . Since $\eta = 2a_I + C$, we have

$$\pi_I \tilde{h}^\varepsilon > \min_{z \in h^\varepsilon} \pi_I z - \varepsilon C > \varepsilon \eta - \varepsilon C > 0, \quad (63)$$

$$\pi_I \tilde{h}^\varepsilon < \max_{z \in h^\varepsilon} \pi_I z + \varepsilon C < 1 - \varepsilon \eta + \varepsilon C < 1. \quad (64)$$

If in our construction we have a Q^ε -disc in \mathbf{S}^u (resp. in \mathbf{S}^d), and we need to increase its I -coordinate from an $(\varepsilon\eta)$ -neighborhood of I^n to an $(\varepsilon\eta)$ -neighborhood of I^{n+1} , with $I^n < I^{n+1}$, (resp. to decrease its I -coordinate from an $(\varepsilon\eta)$ -neighborhood of I^n to an $(\varepsilon\eta)$ -neighborhood of I^{n+1}), then we propagate the Q^ε -disc from \mathbf{S}^u to \mathbf{S}^u (resp. from \mathbf{S}^d to \mathbf{S}^d). By (62) we can do that without the discs having to leave $\{I \in (\varepsilon\eta, 1 - \varepsilon\eta)\}$.

If in our construction we have a Q^ε -disc in \mathbf{S}^u and we need to decrease its I -coordinate from an $(\varepsilon\eta)$ -neighborhood of I^n to an $(\varepsilon\eta)$ -neighborhood of I^{n+1} , with $I^n > I^{n+1}$, we first propagate the disc to \mathbf{S}^d without leaving $\{I \in [0, 1]\}$, which is ensured by (63–64). Then we continue to propagate the disc from \mathbf{S}^d to \mathbf{S}^d . This means that the successive Q^ε -discs will be in $\{I \in [0, 1]\}$ and they will subsequently return to $\{I \in (\varepsilon\eta, 1 - \varepsilon\eta)\}$.

By mirror arguments, if we have a Q^ε -disc in \mathbf{S}^d and we need to increase its I -coordinate from an $(\varepsilon\eta)$ -neighborhood of I^n to an $(\varepsilon\eta)$ -neighborhood of I^{n+1} , with $I^n < I^{n+1}$, we first propagate the disc to \mathbf{S}^u without leaving $\{I \in [0, 1]\}$, which is ensured by (63–64). Then we propagate from \mathbf{S}^u to \mathbf{S}^u . This means that the successive Q^ε -discs will be in $\{I \in [0, 1]\}$ and they will subsequently return to $\{I \in (\varepsilon\eta, 1 - \varepsilon\eta)\}$. ■

Remark 22 *Theorem 11 can be generalized to the higher dimensional case where the action angle coordinates are $(I_1, \dots, I_{n_c}, \theta_1, \dots, \theta_{n_c})$, by taking the strip $\mathbf{S}^\kappa = \bar{B}^{n_u} \times \bar{B}^{n_s} \times \mathbb{R}^{n_c} \times S_\theta^\kappa$ with $S_\theta^\kappa = \prod_{i=1}^{n_c} [S_i^{\kappa,1}, S_i^{\kappa,2}]$, for $\kappa \in \{u, d\}$, and assuming conditions (A2.1), (A2.2.i), (A2.2.ii) from Theorem 11, with the difference that conditions (58–59) are needed only for one of the components I_{i_*} of I . Then sequence of I_{i_*} -level sets $(I_{i_*}^n)_{n \in \mathbb{N}}$ with $|I_{i_*}^{n+1} - I_{i_*}^n| > 2\eta\varepsilon$ we can find an orbit $(z_n)_{n \in \mathbb{N}}$ of the IFS, which $\varepsilon\eta$ shadows the sequence of the IFS, i.e. such that for every $n \in \mathbb{N}$ we have $|\pi_{I_{i_*}}(z_n) - I_{i_*}^n| < \varepsilon\eta$.*

Generalizing Theorem 3 to the setting of higher dimensional I is more subtle. In the case when $n_c = 1$, condition C2 ensures that Q^ε -discs can be propagated as long as we have $I \in [0, 1]$ for all points on these disc. In higher dimensions we need an analogue of this. We restrict to the setting of $n_c = 2$. This is enough to demonstrate the ideas with which we can achieve this, without getting too technical.

When $n_c = 2$ we define the strips $\mathbf{S}^{uu}, \mathbf{S}^{ud}, \mathbf{S}^{du}, \mathbf{S}^{dd}$ with

$$\mathbf{S}^{i_1 i_2} = \bar{B}^u \times \bar{B}^s \times \mathbb{R}^2 \times S_\theta^{i_1 i_2}, \quad S_\theta^{i_1 i_2} = \prod_{k=1}^2 [\theta_k^{i_1 i_2, 1}, \theta_k^{i_1 i_2, 2}], \text{ for } i_1, i_2 \in \{u, d\}.$$

The role of these strips will be that propagating a Q^ε -disc from $\mathbf{S}^{i_1 i_2}$ to $\mathbf{S}^{i_1 i_2}$ will increase the coordinate I_k if $i_k = u$ and decrease I_k if $i_k = d$, for $k = 1, 2$.) We define

$$L = \bigcup_{i_1, i_2, j_1, j_2 \in \{u, d\}} L^{i_1 i_2, j_1 j_2}$$

and make the following modification of condition C2.

Condition C2'.

(C2'.i) For each $\ell \in L^{i_1 i_2, j_1 j_2}$, $i_1, i_2, j_1, j_2 \in \{u, d\}$, and each $\varepsilon \in (0, \varepsilon_0]$, there is a connecting sequence $(N_{\ell,0}, \dots, N_{\ell, k_\ell})$ from $\mathbf{S}^{i_1 i_2}$ to $\mathbf{S}^{j_1 j_2}$;

(C2'.ii) On the I, θ -coordinate we have

$$\bigcup_{\ell \in L^{i_1 i_2, j_1 j_2}} \pi_{I, \theta}(N_{\ell,0}) = [0, 1]^2 \times S_\theta^{i_1 i_2}, \quad \text{for } i_1, i_2, j_1, j_2 \in \{u, d\};$$

(C2'.iii) Whenever $N_{\ell,0} \cap N_{\ell',0} \neq \emptyset$ for $\ell, \ell' \in L^{i_1 i_2, j_1 j_2}$, for every $(I^*, \theta^*) \in \pi_{I, \theta}(N_{\ell,0} \cap N_{\ell',0})$ the multi dimensional rectangle $\bar{B}^{n_u} \times \bar{B}^{n_s} \times \bar{B}(I^*, \varepsilon_0 a_I) \cap [0, 1]^2 \times \bar{B}(\theta^*, a_\theta) \cap S_\theta^{i_1 i_2}$ is contained in $N_{\ell,0}$ or $N_{\ell',0}$;

(C2'.iv) There exists a constant $C > 0$, such that if z passes through a connecting sequence $(N_{\ell,0}, \dots, N_{\ell, k_\ell})$ we have

$$|\pi_I F_{\ell, \varepsilon}(z) - \pi_I(z)| < \varepsilon \cdot C;$$

(C2'.v) There exists a $c > 0$ such that for z passing through a connecting sequence

$$\begin{aligned} \varepsilon \cdot c &< \pi_{I_1} F_{\ell, \varepsilon}(z) - \pi_{I_1}(z), & \text{if } \ell \in L^{uu, uu}, L^{ud, ud}, \\ \varepsilon \cdot c &< \pi_{I_2} F_{\ell, \varepsilon}(z) - \pi_{I_2}(z), & \text{if } \ell \in L^{uu, uu}, L^{du, du}, \\ \varepsilon \cdot c &< \pi_{I_1}(z) - \pi_{I_1} F_{\ell, \varepsilon}(z), & \text{if } \ell \in L^{dd, dd}, L^{du, du}, \\ \varepsilon \cdot c &< \pi_{I_2}(z) - \pi_{I_2} F_{\ell, \varepsilon}(z), & \text{if } \ell \in L^{dd, dd}, L^{ud, ud}. \end{aligned}$$

Using analogous arguments to the proof Theorem 3, for $\eta \geq 2a_I + C$ we can $\varepsilon\eta$ shadow any sequence $I^n = (I_1^n, I_2^n) \subset [2\eta\varepsilon, 1 - 2\eta\varepsilon]^2$, $n \in \mathbb{N}$, for which $\|I^{n+1} - I^n\|_{\max} > 2\eta\varepsilon$. The idea is that we can move in any desired I_1 or I_2 direction, depending on the choice of the strips between which we propagate the Q^ε -discs, while keeping them inside $\{I \in [0, 1]^2\}$ at the same time.

9 Hausdorff dimension

For $V \subset \mathbb{R}^n$ let $\dim_H(V)$ denote the Hausdorff dimension of V (see [82] for the definition and basic properties). If π stands for the orthogonal projection on some selection of Cartesian coordinates of \mathbb{R}^n , it is a standard result that

$$\dim_H(V) \geq \dim_H(\pi V). \quad (65)$$

Proof of Theorem 4.. Let $\varepsilon \in (0, \varepsilon_0]$ be fixed and let **C2** hold.

For any given sequence of action levels $\mathcal{I} = (I^n)_{n \in \mathbb{N}} \subset (2\varepsilon\eta, 1 - 2\varepsilon\eta)$ satisfying $|I^{n+1} - I^n| > 2\varepsilon\eta$, let $\mathbf{z} = \mathbf{z}(\mathcal{I}) = (z^n(\mathcal{I}))_{n \in \mathbb{N}}$ be an orbit of the IFS that $(\eta\varepsilon)$ -shadows the sequence as in (60). The existence of such an orbit follows from Theorem 11. Denote

$$V_{\mathcal{I}} := \{z^0(\mathcal{I}) \in \mathbf{S}^u \cup \mathbf{S}^d : z^0(\mathcal{I}) \text{ is an initial point of } \mathbf{z}(\mathcal{I}), \text{ for which (60) holds}\}.$$

As in the proof of Theorem 11, for every Q^ε -disk h_0^ε of the form

$$h_0^\varepsilon(x) = h_{y^*, I^*, \theta^*}^\varepsilon(x) = (x, y^*, I^*, \theta^*), \quad (66)$$

with fixed $y^* \in \bar{B}^{n_s}$, $I^* \in (I^0 - \varepsilon\eta, I^0 + \varepsilon\eta)$, and $\theta^* \in S_\theta^u \cup S_\theta^d$, there exists an initial point $z^0(I)$ on that disc that is in $V_{\mathcal{I}}$. This implies that

$$\pi_{y, I, \theta} V_{\mathcal{I}} \supset \bar{B}^{n_s} \times (I^0 - \varepsilon\eta, I^0 + \varepsilon\eta) \times S_\theta^u \cup S_\theta^d,$$

hence from (65) we conclude

$$\dim_H(V_{\mathcal{I}}) \geq \dim_H(\pi_{y, I, \theta} V_{\mathcal{I}}) = n_s + 2.$$

We now assume the special case when $n_u = n_s = 1$ and prove the second part of Theorem 4. i.e., that the Hausdorff dimension of the set of orbits which follow a prescribed sequence of actions is strictly greater than $n_s + 2 = 3$. This special case corresponds to the setting of the PER3BP.

We will construct a family of 1-dimensional Cantor sets inside of $V_{\mathcal{I}}$. We will use Lemma 6 below to show that each Cantor set has positive Hausdorff measure. Then we will apply Lemma 7 below to show that $V_{\mathcal{I}}$ has Hausdorff dimension strictly greater than $n_s + 2 = 3$.

Lemma 6 [82] *Consider a one dimensional Cantor set \mathcal{D} , which is formed by creating $m_k - 1 \geq 1$ gaps in each interval at the k -th step of the construction. Assume that gaps created at the k -th step are of length at least δ_k , with $0 < \delta_{k+1} < \delta_k$ for each k . Then*

$$\dim_H(\mathcal{D}) \geq \liminf_{k \rightarrow \infty} \frac{\log(m_1 \cdots m_{l-1})}{-\log(m_l \delta_l)}.$$

Lemma 7 [82] *Let V be a Borel subset of \mathbb{R}^n . For $y \in \mathbb{R}^{n-1}$ let $L_y \subset \mathbb{R}^n$ be $L_y = \{(x, y) : x \in \mathbb{R}\}$. If $n - 1 \leq s \leq n$, then*

$$\int_{\mathbb{R}^{n-1}} \mathcal{H}^{s-(n-1)}(V \cap L_y) dy \leq \mathcal{H}^s(V).$$

Let N be an integer satisfying

$$N > \frac{2}{c\varepsilon}, \quad (67)$$

where c is as in (59). This choice ensures that by taking N applications of maps $F_{\ell, \varepsilon}$ from the IFS, any Q^ε -disk can be moved both up and down in action by 1.

Consider the following compact sets

$$\begin{aligned} A_{uu, uu} &= \bigcup_{\ell_1, \ell_2 \in L^{uu}} F_{\ell_1, \varepsilon}^{-1} \circ F_{\ell_2, \varepsilon}^{-1}(\mathbf{S}^u \cap \{I \in [0, 1]\}), \\ A_{dd, dd} &= \bigcup_{\ell_1, \ell_2 \in L^{dd}} F_{\ell_1, \varepsilon}^{-1} \circ F_{\ell_2, \varepsilon}^{-1}(\mathbf{S}^d \cap \{I \in [0, 1]\}), \\ A_{ud, du} &= \bigcup_{\ell_1 \in L^{ud}, \ell_2 \in L^{du}} F_{\ell_1, \varepsilon}^{-1} \circ F_{\ell_2, \varepsilon}^{-1}(\mathbf{S}^u \cap \{I \in [0, 1]\}), \\ A_{du, ud} &= \bigcup_{\ell_1 \in L^{du}, \ell_2 \in L^{ud}} F_{\ell_1, \varepsilon}^{-1} \circ F_{\ell_2, \varepsilon}^{-1}(\mathbf{S}^d \cap \{I \in [0, 1]\}). \end{aligned}$$

By condition **C3** there exists a δ satisfying

$$0 < \delta = \min \{ \text{dist} (A_{uu,uu}, A_{ud,du}), \text{dist} (A_{dd,dd}, A_{du,ud}) \}. \quad (68)$$

By the compactness of $(\mathbf{S}^u \cup \mathbf{S}^d) \cap \{I \in [0, 1]\}$ there exist $\lambda > 1$ such that

$$\lambda > \sup \{ \|D(F_{\ell_n, \varepsilon} \circ \dots \circ F_{\ell_1, \varepsilon})(z)\| \}, \quad (69)$$

where the supremum is taken over all

$$z \in (F_{\ell_n, \varepsilon} \circ \dots \circ F_{\ell_1, \varepsilon})^{-1} ((\mathbf{S}^u \cup \mathbf{S}^d) \cap \{I \in [0, 1]\}), \quad \text{for } \ell_i \in L \text{ and } n \leq N.$$

Suppose that $I^1 > I^0$ (the case $I^1 < I^0$ is similar). As in the proof of Theorem 11, start with a Q^ε -disc $h_0^\varepsilon(x)$ of the form (66), with $\pi_I h_0^\varepsilon \subset (I^0 - \eta\varepsilon, I^0 + \eta\varepsilon)$. We can propagate this disc until we obtain an image disc h_1^ε with $\pi_I(h_1^\varepsilon) \subseteq (I^1 - \eta\varepsilon, I^1 + \eta\varepsilon)$ in two different ways: (i) by propagating the disc only through \mathbf{S}^u up to $(I^1 - \eta\varepsilon, I^1 + \eta\varepsilon)$, or (ii) by propagating the disc through \mathbf{S}^d , switching back to \mathbf{S}^u , and propagating it through \mathbf{S}^u up to $(I^1 - \eta\varepsilon, I^1 + \eta\varepsilon)$. The choice in (67) ensures that each of these propagations can be achieved by applying at most N applications of maps $F_{\ell, \varepsilon}$ from the IFS. The points in h_0^ε that get propagated in these two ways yield two disjoint sub-discs $\mathcal{D}^0, \mathcal{D}^1$ of h_0^ε . By (68) and (69), the distance between \mathcal{D}^0 and \mathcal{D}^1 is at least $\delta_1 = \lambda^{-1}\delta$.

Continuing this procedure, we obtain recursively a nested sequence of finite unions of discs, such that the gaps between the discs at step k are at least $\delta_k = \lambda^{-k}\delta$. The resulting Cantor set $\mathcal{D}(y^*, I^*, \theta^*)$ depends on the choice of the initial Q^ε -disc h_0^ε given by (66). From Lemma 6

$$\dim_H(\mathcal{D}(y^*, I^*, \theta^*)) \geq \lim_{k \rightarrow \infty} \frac{\log(2^k)}{-\log(2\lambda^{-(k+1)}\delta)} = \log_\lambda 2 > 0.$$

By Lemma 7

$$\mathcal{H}^{s+2d+\log_\lambda 2}(V_{\mathcal{I}}) \geq \int_{\bar{B}^{n_s} \times (I^0 - \varepsilon\eta, I^0 + \varepsilon\eta) \times (S_\theta^u \cup S_\theta^d)} \mathcal{H}^{\log_\lambda 2}(\mathcal{D}(y, I, \theta)) dy dI d\theta > 0,$$

so $\dim_H(V) \geq n_s + 2d + \log_\lambda 2$, proving our claim. \blacksquare

10 Stochastic behavior

Our proof will be based on the Donsker's functional central limit theorem. We start by recalling the result.

Consider a sequence Y_n of independent identically distributed random variables with $\mathbb{E}(Y_n) = 0$ and $\text{Var}(Y_n) = 1$ and define

$$\begin{aligned} S_n &= Y_1 + \dots + Y_n, \\ S(t) &= S_{[t]} + (t - [t]) (S_{[t]+1} - S_{[t]}) \quad \text{for } t \in [0, +\infty), \\ S_n^*(t) &= \frac{S(nt)}{\sqrt{n}} \quad \text{for } t \in [0, 1]. \end{aligned}$$

Theorem 12 [83] (*Donsker's functional central limit theorem*) *On the space $C[0,1]$ of continuous functions on the unit interval with the metric induced by the sup-norm, the sequence S_n^* converges in distribution⁷ to a standard Brownian motion W_t .*

10.1 Stochastic behavior under conditions on Q^ε -disks

Let $\Omega_\varepsilon \subset \mathbb{R}^u \times \mathbb{R}^s \times \mathbb{R}^2 \times \mathbb{T}$ be a set of positive Lebesgue measure. (We add the subscript ε in Ω_ε since in the result stated below the choice of this set will depend on ε .) On Ω_ε we define a probability space $(\Omega_\varepsilon, \mathbb{F}_\varepsilon, \mathbb{P}_\varepsilon)$ by taking \mathbb{F}_ε to be the sigma field of Borel sets on Ω_ε and

$$\mathbb{P}_\varepsilon(B) := \frac{|B|}{|\Omega_\varepsilon|}. \quad (70)$$

We introduce the following notation. For a point z in the extended phase space we denote by $\pi_t(z)$ the time-coordinate t of the point z , where t is the covering space \mathbb{R} of \mathbb{T}^1 . Thus the 'angle' coordinate θ is given by $\theta = t \pmod{2\pi}$. The quantity $\pi_t(\Phi_\tau^\varepsilon(z)) - \pi_t(z)$ represents the time τ it takes for a point z to flow to $\Phi_\tau^\varepsilon(z)$. For $\tilde{h}^\varepsilon \subseteq F_{\ell,\varepsilon}(h^\varepsilon)$ as in Condition (A2.1), for each pair of points $z \in h^\varepsilon$, $\tilde{z} = F_{\ell,\varepsilon}(z) \in \tilde{h}^\varepsilon$, there is an associated time $\pi_t(\tilde{z}) - \pi_t(z)$. We denote by $\pi_t(\tilde{h}^\varepsilon) - \pi_t(h^\varepsilon)$ the time interval consisting of all $\pi_t(\tilde{z}) - \pi_t(z)$ for all z, \tilde{z} as above.

Below we define some uniformity conditions for all pairs of Q^ε -disks $h^\varepsilon, \tilde{h}^\varepsilon$ as in Condition **A2**.

Condition A3.

(A3.1) There exists $T_0 > 0$ such that for every pair of points z, \tilde{z} as in Condition **A2** we have

$$\pi_t(\tilde{z}) - \pi_t(z) < T_0. \quad (71)$$

(A3.2) There exists $M_0 > 0$ such that for every $z \in \mathbf{S}^u \cup \mathbf{S}^d$ and $t \in [0, T_0]$

$$|\pi_I(\Phi_t^\varepsilon(z)) - \pi_I(z)| < M_0\varepsilon. \quad (72)$$

Condition (A3.1) says that the first-return times to $\mathbf{S}^u \cup \mathbf{S}^d$ via any of the maps $F_{\ell,\varepsilon}$ in \mathcal{F}_ε , for any $\ell \in L$, are uniformly bounded for $z \in \mathbf{S}^u \cup \mathbf{S}^d$. Condition (A3.2) says that the change in I along the flow Φ_t^ε is uniformly bounded for the length of time it takes a point $z \in \mathbf{S}^u \cup \mathbf{S}^d$ to return to $\mathbf{S}^u \cup \mathbf{S}^d$.

We recall that $\mathbf{S}^u \cup \mathbf{S}^d$ is non-compact. If we restrict to the dynamics on a compact subset of $\mathbf{S}^u \cup \mathbf{S}^d$, for instance to $(\mathbf{S}^u \cup \mathbf{S}^d) \cap \{I \in [0,1]\}$, then both assumptions in Condition **A3** are automatically satisfied.

The theorem below will be used in the subsequent section to prove Theorem 5.

Theorem 13 *Assume that the IFS \mathcal{F}_ε satisfies the conditions **A2** and **A3**. Let $I = H_0 - h_0$, and let μ, σ, X_0 be any fixed real numbers and let $\gamma > 3/2$. Then for sufficiently small ε there is a set $\Omega_\varepsilon \subset \mathbb{R}^{n_u} \times \mathbb{R}^{n_s} \times \mathbb{R}^2 \times \mathbb{T}$ of positive Lebesgue measure, such that*

⁷See Section 4.4 for more details on the convergence.

$\pi_{y,I,\theta}\Omega_\varepsilon = \pi_{y,I,\theta}(\mathbf{S}^u \cup \mathbf{S}^d) \cap \{I \in [X_0 - \varepsilon, X_0 + \varepsilon]\}$, and the stochastic processes defined as energy paths⁸

$$\begin{aligned} X_t^\varepsilon &: \Omega_\varepsilon \rightarrow \mathbb{R}, \\ X_t^\varepsilon(z) &: = I(\Phi_{\varepsilon^{-\gamma t}}^\varepsilon(z)), \quad \text{for } t \in [0, 1], \end{aligned} \quad (73)$$

have the following limit in distribution on $C[0, 1]$

$$\lim_{\varepsilon \rightarrow 0} X_t^\varepsilon = X_0 + \mu t + \sigma W_t. \quad (74)$$

For the proof of Theorem 13 we will need two technical lemmas.

Lemma 8 *Assume that the IFS \mathcal{F}_ε satisfies the conditions **A2** and **A3**, and let η be a constant as given by Theorem 11. Then there exist constants $T > 0$ and $M > 1$, such that for every $k \in \mathbb{N}$, every $\varepsilon \in (0, \varepsilon_0]$ and every Q^ε -disc h^ε in $\mathbf{S}^u \cup \mathbf{S}^d$ satisfying*

$$\pi_I h^\varepsilon \subset [I_0 - \varepsilon\eta, I_0 + \varepsilon\eta],$$

there exists a sequence $\ell_1, \dots, \ell_m \in L$ (m depends on k, ε and h^ε) and a disc $D \subset \bar{B}^u$ such that

$$h^{\varepsilon'} = F_{\ell_m, \varepsilon} \circ \dots \circ F_{\ell_1, \varepsilon} \circ h^\varepsilon(D)$$

is a Q^ε -disc satisfying

$$\begin{aligned} \pi_I h^{\varepsilon'} &\subset (I_0 - \varepsilon M, I_0 + \varepsilon M), \quad \text{and} \\ \pi_t h^{\varepsilon'} - \pi_t h^\varepsilon &\subset [kT, (k+1)T]. \end{aligned}$$

Moreover, for every $z \in h^\varepsilon(D)$ and $\tilde{z} = F_{\ell_m, \varepsilon} \circ \dots \circ F_{\ell_1, \varepsilon}(z) \in h^{\varepsilon'}$ we have

$$\pi_I \Phi_t(z) \in (-\varepsilon M, \varepsilon M) \quad \text{for every } t \in [0, \pi_t \tilde{z} - \pi_t z].$$

Proof. The idea behind the proof is depicted in Figure 9.

Consider a sequence $\{I^n\}_{n \in \mathbb{N}}$ of I -level sets whose values alternate between I_0 and $I_0 + 3\eta$, i.e.,

$$I_0, I_0 + 3\eta\varepsilon, I_0, I_0 + 3\eta\varepsilon, \dots \quad (75)$$

Note that the consecutive values are more than $(2\eta\varepsilon)$ apart. By Theorem 11 there exists a trajectory whose I -coordinate $(\varepsilon\eta)$ -shadows $\{I^n\}$. Following the construction from the proof of Theorem 11 we start with a Q^ε -disc h^ε whose I -projection is contained in $[I_1 - \eta\varepsilon, I_1 + \eta\varepsilon]$ and take successive iterates of this disc under the IFS \mathcal{F}_ε .

In order to move from I^n to I^{n+1} , we make repeated transitions from \mathbf{S}^u to \mathbf{S}^u , in the case $I^n < I^{n+1}$, or from \mathbf{S}^d to \mathbf{S}^d , in the case $I^n > I^{n+1}$. Each transition corresponds to one application of some return map $F_{\ell, \varepsilon}$ to $\mathbf{S}^u \cup \mathbf{S}^d$. From the lower bounds from Condition (A2.2.ii) there exists an upper bound K for the number of transitions necessary to move from I^n to I^{n+1} , where K is independent of ε and of the initial Q^ε -disc h^ε . By Condition (A3.1), the time t for each transition is upper bounded by T_0 . Hence the time to move

⁸Alternatively we can define the energy paths as $X_t^\varepsilon(z) := I(\Phi_{\varepsilon^{-3/2t}}^\varepsilon(z))$, by taking $\gamma \in \mathbb{R}$ which satisfies $\gamma > T_0\sigma/c$, where c and T_0 are the constants from the conditions **A2** and **A3**, respectively. We highlight this alternative in footnotes while giving the proof.

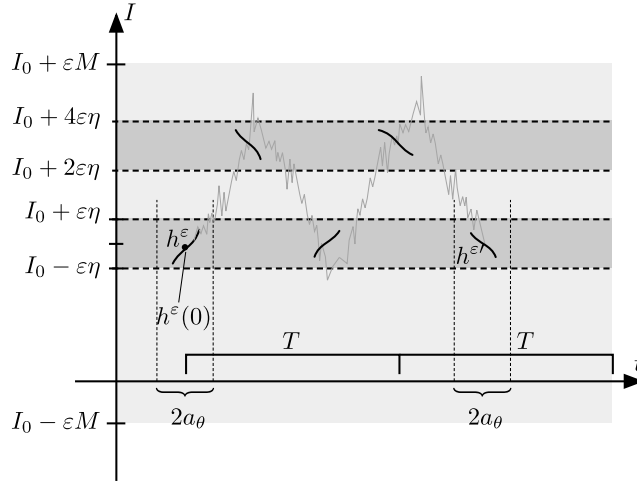


Figure 9: The Q^ε -disc h^ε is moved to $h^{\varepsilon'}$, by constructing successive Q^ε -discs which travel up and down between the two regions in darker grey. Any trajectory which passes through the full excursion stays within the light grey area. This plot is a sketch of what is happening in Lemma 8 for $k = 1$.

from I^n to I^{n+1} is upper bounded by $T_1 := KT_0$, where T_1 is independent of ε and of the initial Q^ε -disc h^ε .

By Condition (A3.2) there exists $M_0 > 0$ such that the change in I along the flow Φ_t^ε between successive returns to $\mathbf{S}^u \cup \mathbf{S}^d$ is upper bounded by $M_0\varepsilon$. Therefore, the change in I along the flow as we move from I^n to I^{n+1} is upper bounded by εKM_0 . We note that the change in I by each return map $F_{\ell,\varepsilon}$ is at most $5\eta\varepsilon$, since each level set I^n is visited within a distance of $\varepsilon\eta$, and two successive level sets I^n and I^{n+1} are $3\eta\varepsilon$ apart. Note that by Condition (A3.2) we must have $5\varepsilon\eta < \varepsilon KM_0$.

We let M be a number bigger than KM_0 and bigger than one. Thus, when we move Q^ε -discs between I^n and I^{n+1} the I -coordinate along the trajectory stays in $(I_0 - \varepsilon M, I_0 + \varepsilon M)$.

For each Q^ε -disc in our construction by (15) its t -projection has diameter less than or equal to $2a_\theta$. Let $T_2 = 2T_1 = 2KT_0$ which is an upper bound for the time needed to move from I^n to I^{n+1} and then to I^{n+2} . Let $T = T_2 + 4a_\theta$.

Our result now follows from the following construction. We start with our Q^ε -disc h^ε . This disc is already in $[I^1 - \varepsilon\eta, I^1 + \varepsilon\eta] = [I_0 - \varepsilon\eta, I_0 + \varepsilon\eta]$, so we move this disc up in I (using transitions from \mathbf{S}^u to \mathbf{S}^u) to reach $[I^2 - \varepsilon\eta, I^2 + \varepsilon\eta] = [I_0 + 2\varepsilon\eta, I_0 + 4\varepsilon\eta]$, and then down in I (using transitions from \mathbf{S}^d to \mathbf{S}^d) to return to $[I^3 - \varepsilon\eta, I^3 + \varepsilon\eta] = [I_0 - \varepsilon\eta, I_0 + \varepsilon\eta]$. We repeat such trips until we obtain a Q^ε -disc $h^{\varepsilon'}$ with $\pi_t h^{\varepsilon'} > kT + \pi_t h^\varepsilon(0)$, where k is given in the statement of the lemma. The last transition to reach $h^{\varepsilon'}$ takes less time than T_2 and the t -projection of every Q^ε -disc has diameter no bigger than $2a_\theta$. This implies $\pi_t h^{\varepsilon'} < (k+1)T + \pi_t h^\varepsilon$. From our construction we already know that the I -coordinate along the trajectory of the flow for the points that start in h^ε and arrive in $h^{\varepsilon'}$ is between $(I_0 - \varepsilon M, I_0 + \varepsilon M)$. We define D as the set of points that start in h^ε and arrive in $h^{\varepsilon'}$

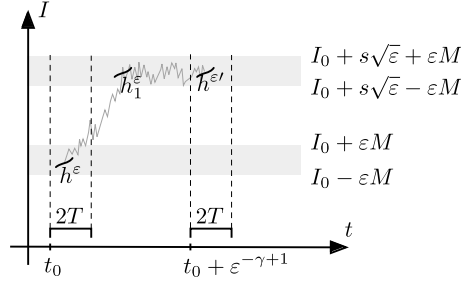


Figure 10: A schematic plot for Lemma 9 with $c > 0$. The disc h^ε is moved to $h^{\varepsilon'}$, by being moved up and then being propagated within the upper grey region.

through this construction. The I -coordinate along the trajectory of the flow for the points that start in h^ε and arrive in $h^{\varepsilon'}$ is between $(I_0 - \varepsilon M, I_0 + \varepsilon M)$. This concludes the proof. ■

Lemma 9 *Assume that the IFS $\widehat{\mathcal{F}}_\varepsilon$ satisfies the conditions **A2** and **A3**. Let T and M be constants as in Lemma 8. Let $\gamma > 3/2$ and $s \in \mathbb{R}$ be fixed constants.*

Then, for every sufficiently small $\varepsilon > 0$, and every Q^ε -disc h^ε satisfying

$$\begin{aligned} \pi_t h^\varepsilon &\subset t_0 + [0, 2T], \\ \pi_I h^\varepsilon &\subset (I_0 - \varepsilon M, I_0 + \varepsilon M), \end{aligned}$$

there exists $\ell_1, \dots, \ell_m \in L$ and a set $D \subset \bar{B}^u$ such that

$$\pi_I \{ \Phi_{t_0 + \varepsilon^{-\gamma+1} - \pi_t z}^\varepsilon(z) : z \in h^\varepsilon(D) \} \subset I_0 + s\sqrt{\varepsilon} + (-\varepsilon M, \varepsilon M), \quad (76)$$

and

$$h^{\varepsilon'} = F_{\ell_m, \varepsilon} \circ \dots \circ F_{\ell_1, \varepsilon} \circ h^\varepsilon(D)$$

*is a Q^ε -disc satisfying*⁹

$$\begin{aligned} \pi_t h^{\varepsilon'} &\subset t_0 + \varepsilon^{-\gamma+1} + [0, 2T], \\ \pi_I h^{\varepsilon'} &\subset I_0 + s\sqrt{\varepsilon} + (-\varepsilon M, \varepsilon M). \end{aligned}$$

Proof. The idea behind the proof is depicted in Figure 10.

Here we conduct the proof for $s > 0$. For $s < 0$ the proof will be analogous and we comment on the difference at the end of the proof. If $s = 0$ the result follows directly from Lemma 8.

Let η be a constant as given by Theorem 11. Consider a sequence $\{I^n\}_{n \in \mathbb{N}}$ of I -level sets whose values alternate between $I_0 + s\sqrt{\varepsilon}$ and $I_0 + s\sqrt{\varepsilon} + 3\eta\varepsilon$, i.e.,

$$I^1 = I_0 + s\sqrt{\varepsilon}, I^2 = I_0 + s\sqrt{\varepsilon} + 3\eta\varepsilon, I^3 = I_0 + s\sqrt{\varepsilon}, I^4 = I_0 + s\sqrt{\varepsilon} + 3\eta\varepsilon, \dots \quad (77)$$

⁹If we consider instead the energy paths $X_t^\varepsilon(z) := I(\Phi_{\gamma\varepsilon^{-3/2t}}^\varepsilon(z))$, then here we require that $\pi_t h' \subset t_0 + \gamma\varepsilon^{-1/2} + [0, 2T]$, by taking $\gamma \in \mathbb{R}$ such that $\gamma > T_0 s/c$. This enters in (78) during the course of the proof.

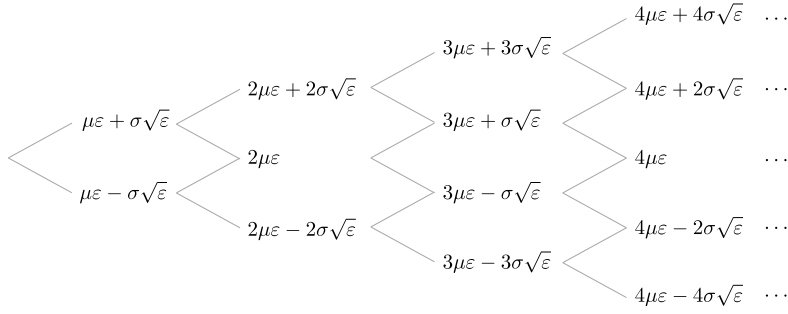


Figure 11: The idea behind the proof of Theorem 13 is to shadow the changes of I so that they would follow a random walk from the above tree.

By Theorem 3 we know that we can $(\varepsilon\eta)$ -shadow this sequence. To reach $I^1 = I_0 + c\sqrt{\varepsilon}$ we move h^ε up using transitions from \mathbf{S}^u to \mathbf{S}^u . We reach this level by moving h^ε to a Q^ε -disc which we denote here as h_1^ε (see Figure 10). By Condition (A2.2.ii), this requires no more than $s\sqrt{\varepsilon}/(c\varepsilon)$ applications of maps $F_{\ell,\varepsilon}$. Recall that T_0 is an upper bound on the time along the flow to follow an application of a map $F_{\ell,\varepsilon}$. The time needed to reach h_1^ε is less than or equal to $(T_0s/c)\varepsilon^{-1/2}$. Since $\gamma > \frac{3}{2}$, for sufficiently small ε we have

$$\varepsilon^{-\gamma+1} - (T_0s/c)\varepsilon^{-1/2} = \varepsilon^{-1/2} \left(\varepsilon^{-\gamma+\frac{3}{2}} - (T_0s/c) \right) > 0. \quad (78)$$

This means that we reach h_1^ε in a time less than $\varepsilon^{-\gamma+1}$. We now apply Lemma 8 which ensures that we can stay in $I_0 + s\sqrt{\varepsilon} + (-\varepsilon M, \varepsilon M)$ as we shadow I^n . By Lemma 8 we can move h_1^ε to obtain a Q^ε -disc $h^{\varepsilon'}$ with

$$\pi_t h^{\varepsilon'} \subset [\pi_t h_1^\varepsilon(0) + kT, \pi_t h_1^\varepsilon(0) + (k+1)T],$$

with any $k \in \mathbb{N}$ of our choosing; this interval has length T . We can choose k so that above interval is within the interval $t_0 + \varepsilon^{-\gamma+1} + [0, 2T]$, which has length $2T$. By Lemma 8 we also know that the trajectories of points leading from h_1^ε to $h^{\varepsilon'}$ remain in $I_0 + s\sqrt{\varepsilon} + (-\varepsilon M, \varepsilon M)$. This in particular implies that at time $t_0 + \varepsilon^{-\gamma+1}$ (see Figure 10) we obtain the condition (76). This concludes the proof for $s > 0$.

For $s < 0$ the argument is almost identical, with the only difference that to reach I^1 instead of going up we move down using transitions from \mathbf{S}^d to \mathbf{S}^d . ■

Proof of Theorem 13.

The intuition behind the proof is to define Ω_ε as a set of points in $\mathbf{S}^u \cup \mathbf{S}^d$ for which the I -coordinate $O(\varepsilon)$ -shadows the random walk in Figure 11.

Let M be the constant from Lemma 8 and consider the following two sets¹⁰

$$A_u^\varepsilon = \{z \in \mathbb{R}^{n_u+n_s+2} \times \mathbb{T} : \pi_I \Phi_{\varepsilon^{-\gamma+1}}^\varepsilon(z) \in X_0 + \mu\varepsilon + \sigma\sqrt{\varepsilon} + (-\varepsilon M, \varepsilon M)\},$$

$$A_d^\varepsilon = \{z \in \mathbb{R}^{n_u+n_s+2} \times \mathbb{T} : \pi_I \Phi_{\varepsilon^{-\gamma+1}}^\varepsilon(z) \in X_0 + \mu\varepsilon - \sigma\sqrt{\varepsilon} + (-\varepsilon M, \varepsilon M)\}.$$

¹⁰If we consider instead the energy paths $X_t^\varepsilon(z) := I(\Phi_{\gamma\varepsilon^{-3/2t}}^\varepsilon(z))$, as indicated in the footnote for Theorem 13, then in the remainder of the proof we have: in A_u^ε and A_d^ε we have $\gamma\varepsilon^{-1/2}$ instead of $\varepsilon^{-\gamma+1}$; in $A_{uu}^\varepsilon, A_{ud}^\varepsilon, A_{du}^\varepsilon, A_{dd}^\varepsilon$ we have $2\gamma\varepsilon^{-1/2}$ instead of $2\varepsilon^{-\gamma+1}$; in $A_{\kappa\omega}^\varepsilon$ we have $k\gamma\varepsilon^{-1/2}$ instead of $k\varepsilon^{-\gamma+1}$, with mirror changes carried throughout the argument.

The subscript u in A_u^ε is meant to suggest that for $z \in A_u^\varepsilon$ the trajectory moves ‘up’ in I . Similarly, d in A_d^ε is meant to suggest that for $z \in A_d^\varepsilon$ the trajectory moves ‘down’ in I .

By Lemma 9 A_u^ε and A_d^ε are nonempty. (We apply the lemma with $I_0 = X_0$, $s = \mu\varepsilon/\sqrt{\varepsilon} + \sigma$ for A_u^ε , and with $s = \mu\varepsilon/\sqrt{\varepsilon} - \sigma$ for A_d^ε . We restrict to $\varepsilon < (\sigma/M)^2$ so that $A_u^\varepsilon \cap A_d^\varepsilon = \emptyset$.) We obtain in fact more. For every fixed $y_0 \in \bar{B}^{n_s}$, $I_0 \in (X_0 - \varepsilon M, X_0 + \varepsilon M)$, and $\theta_0 \in S_\theta^u \cup S_\theta^d$, choose an initial Q^ε -disc h^ε of the form

$$h^\varepsilon(x) = (x, y_0, I_0, \theta_0), \quad x \in \bar{B}^{n_u}. \quad (79)$$

Applying Lemma 9 yields a point $z \in h^\varepsilon$ so that $z \in A_u^\varepsilon$. For such a point z we have $\pi_{y, I, \theta}(z) = (y_0, I_0, \theta_0)$. This implies that $\pi_{y, \theta}(A_u^\varepsilon) = \pi_{y, \theta}(\mathbf{S}^u \cup \mathbf{S}^d)$ and $\pi_I(A_u^\varepsilon) = (X_0 - \varepsilon M, X_0 + \varepsilon M)$. By mirror arguments $\pi_{y, \theta}(A_d^\varepsilon) = \pi_{y, \theta}(\mathbf{S}^u \cup \mathbf{S}^d)$ and $\pi_I(A_d^\varepsilon) = (X_0 - \varepsilon M, X_0 + \varepsilon M)$.

We now define the following subsets of $\mathbb{R}^{n_u+n_s+2} \times \mathbb{T}$:

$$\begin{aligned} A_{uu}^\varepsilon &= A_u^\varepsilon \cap \{z : \pi_I \Phi_{2\varepsilon^{-\gamma+1}}^\varepsilon(z) \in X_0 + 2\mu\varepsilon + 2\sigma\sqrt{\varepsilon} + (-M\varepsilon, M\varepsilon)\}, \\ A_{du}^\varepsilon &= A_u^\varepsilon \cap \{z : \pi_I \Phi_{2\varepsilon^{-\gamma+1}}^\varepsilon(z) \in X_0 + 2\mu\varepsilon + (-M\varepsilon, M\varepsilon)\}, \\ A_{ud}^\varepsilon &= A_d^\varepsilon \cap \{z : \pi_I \Phi_{2\varepsilon^{-\gamma+1}}^\varepsilon(z) \in X_0 + 2\mu\varepsilon + (-M\varepsilon, M\varepsilon)\}, \\ A_{dd}^\varepsilon &= A_d^\varepsilon \cap \{z : \pi_I \Phi_{2\varepsilon^{-\gamma+1}}^\varepsilon(z) \in X_0 + 2\mu\varepsilon - 2\sigma\sqrt{\varepsilon} + (-M\varepsilon, M\varepsilon)\}. \end{aligned}$$

The set A_{uu}^ε is the set of points which first go up to $\mu\varepsilon + \sigma\sqrt{\varepsilon}$ at time $\varepsilon^{-\gamma+1}$, and then go up again to $2\mu\varepsilon + 2\sigma\sqrt{\varepsilon}$ at time $2\varepsilon^{-\gamma+1}$. This is the reason for the subscript uu . The set A_{du}^ε is the set of points which first go up $\mu\varepsilon + \sigma\sqrt{\varepsilon}$ at time $\varepsilon^{-\gamma+1}$, and then go down to $2\mu\varepsilon$ at time $2\varepsilon^{-\gamma+1}$. This is the reason for the subscript du . Similar descriptions can be made for A_{ud}^ε and A_{dd}^ε .

We apply Lemma 9 twice for Q^ε -discs of the form (79), obtaining that the sets A_{uu}^ε , A_{ud}^ε , A_{du}^ε , A_{dd}^ε are nonempty. Due to (79), we have that $\pi_{y, \theta}(A_{\kappa\kappa'}^\varepsilon) = \pi_{y, \theta}(\mathbf{S}^u \cup \mathbf{S}^d)$, and $\pi_I(A_{\kappa\kappa'}^\varepsilon) = (X_0 - \varepsilon M, X_0 + \varepsilon M)$ for $\kappa, \kappa' \in \{u, d\}$.

We continue to subdivide these sets in a similar manner using an inductive procedure. First we introduce the following notation. For a given sequence of symbols $\omega = \omega_k \dots \omega_1$, where $\omega_i \in \{u, d\}$, we denote

$$\begin{aligned} |\omega| &:= k, \\ U(\omega) &:= \#\{\omega_i : \omega_i = u, i = 1, \dots, |\omega|\}, \\ D(\omega) &:= \#\{\omega_i : \omega_i = d, i = 1, \dots, |\omega|\}, \\ N(\omega) &:= U(\omega) - D(\omega). \end{aligned} \quad (80)$$

For each string ω , $|\omega|$ represents the length of ω , $U(\omega)$ the number of steps ‘up’, $D(\omega)$ the number of steps ‘down’, and $N(\omega)$ the ‘net’ number of ‘up-down’ steps.

For a given string $\omega = \omega_{k-1} \dots \omega_1$ and $\kappa \in \{u, d\}$ we now inductively define $A_{\kappa\omega}^\varepsilon \subset \mathbb{R}^{n_u+n_s+2} \times \mathbb{T}$ as

$$A_{\kappa\omega}^\varepsilon = A_\omega^\varepsilon \cap \{z : \pi_I \Phi_{k\varepsilon^{-\gamma+1}}^\varepsilon(z) \in X_0 + k\mu\varepsilon + N(\kappa\omega)\sigma\sqrt{\varepsilon} + (-M\varepsilon, M\varepsilon)\}. \quad (81)$$

By construction, the sets A_ω^ε with ω of the same length are disjoint, i.e., if $|\omega| = |\varpi|$ and $\omega \neq \varpi$ then $A_\omega^\varepsilon \cap A_\varpi^\varepsilon = \emptyset$. Also because we take the points in A_ω^ε by inductively applying Lemma 9, for $t \in [\varepsilon k, \varepsilon(k+1)]$ we obtain (see Figure 10)

$$\Phi_{\varepsilon^{-\gamma}t}^\varepsilon(z) \in \Phi_{\varepsilon^{-\gamma+1}k}^\varepsilon(z) + [-2\sigma\sqrt{\varepsilon}, 2\sigma\sqrt{\varepsilon}]. \quad (82)$$

Let

$$K_\varepsilon := \lfloor \varepsilon^{-1} \rfloor \in \mathbb{N}. \quad (83)$$

Let us consider paths of length $|\omega| = K_\varepsilon$ and let us define the set $B = (\mathbf{S}^u \cup \mathbf{S}^d) \cap \{I \in [X_0 - \varepsilon, X_0 + \varepsilon]\}$. The set B is compact and has finite Lebesgue measure. We will show that for a fixed ε we can restrict the sets A_ω^ε to $\tilde{A}_\omega^\varepsilon \subset A_\omega^\varepsilon \cap B$, so that

$$0 < \mu(\tilde{A}_\omega^\varepsilon) = \mu(\tilde{A}_{\varpi}^\varepsilon) < \infty \quad \text{for any } \omega, \varpi \text{ with } |\omega| = |\varpi| = K_\varepsilon, \quad (84)$$

$$\pi_{y,I,\theta}(\tilde{A}_\omega^\varepsilon) = \pi_{y,\theta}(\mathbf{S}^u \cup \mathbf{S}^d) \cap \{I \in [X_0 - \varepsilon, X_0 + \varepsilon]\}. \quad (85)$$

In order to show (84–85) let us fix ε and first consider a fixed ω of length $|\omega| = K_\varepsilon$. Since $M > 1$, $[X_0 - \varepsilon, X_0 + \varepsilon] \subset (X_0 - M\varepsilon, X_0 + M\varepsilon)$, so we know that for every $(y_0, I_0, \theta_0) \in \pi_{y,I,\theta}B$ there exists an x_0 such that $(x_0, y_0, I_0, \theta_0) \in A_\omega^\varepsilon$. By the continuity of the solutions of ODEs with respect to the initial conditions we can choose a small neighborhood of $(x_0, y_0, I_0, \theta_0)$ which will also be in A_ω^ε . We can take this neighborhood to be of the form $B^{n_u}(x_0, \delta) \times B^{n_s+2}((y_0, I_0, \theta_0), r) \cap B$, where δ, r are some small positive numbers depending on ω and y_0, I_0, θ_0 . By the compactness of $\pi_{y,I,\theta}B$ we can choose a finite sequences (y_i, I_i, θ_i) and r_i , for $i = 1, \dots, n$, such that

$$\pi_{y,I,\theta}B = \bigcup_{i=1}^n B^{n_s+2}((y_i, I_i, \theta_i), r_i) \cap \pi_{y,I,\theta}B. \quad (86)$$

Each (y_i, I_i, θ_i) has a $\delta_i = \delta(y_i, I_i, \theta_i)$ associated with it. For $\delta < \min_{i=1, \dots, n} \delta_i$ we define

$$\tilde{A}_\omega^\varepsilon(\delta) := \left(\bigcup_{i=1}^n B^{n_u}(x_0, \delta) \times B^{n_s+2}((y_i, I_i, \theta_i), r_i) \right) \cap B \subset A_\omega^\varepsilon. \quad (87)$$

The measure of this set depends continuously on δ . There is a finite number of ω of length K_ε . This means that we can choose a finite sequence of $\delta(\omega)$ such that $\tilde{A}_\omega^\varepsilon := \tilde{A}_\omega^\varepsilon(\delta(\omega))$ satisfy (84). Condition (85) follows from (86) and (87).

We now define the set Ω_ε that appears in the statement of Theorem 13:

$$\Omega_\varepsilon := \bigcup_{|\omega|=K_\varepsilon} \tilde{A}_\omega^\varepsilon.$$

By construction, $\mu(\Omega_\varepsilon) > 0$. Moreover, by (85), we also have

$$\pi_{y,I,\theta}(\Omega_\varepsilon) = \pi_{y,\theta}(\mathbf{S}^u \cup \mathbf{S}^d) \cap \{I \in [X_0 - \varepsilon, X_0 + \varepsilon]\}.$$

We now define a sequence of random variables $Y_n^\varepsilon : \Omega_\varepsilon \rightarrow \mathbb{R}$, for $n = 1, \dots, K_\varepsilon$ as

$$Y_n^\varepsilon(z) = \begin{cases} 1 & \text{if } z \in \tilde{A}_\omega^\varepsilon \text{ and } \omega_n = u, \\ -1 & \text{if } z \in \tilde{A}_\omega^\varepsilon \text{ and } \omega_n = d. \end{cases} \quad (88)$$

Since the sets $\tilde{A}_\omega^\varepsilon$ satisfy (84), the random variables Y_n^ε are independent and identically distributed with $\mathbb{P}_\varepsilon(Y_n^\varepsilon = 1) = \mathbb{P}_\varepsilon(Y_n^\varepsilon = -1) = \frac{1}{2}$, moreover $\mathbb{E}(Y_n^\varepsilon) = 0$, $Var(Y_n^\varepsilon) = 1$.

As in the setup for Theorem 12, we define $S_n^\varepsilon = Y_1^\varepsilon + \dots + Y_n^\varepsilon$ for $n \in \{1, \dots, K_\varepsilon\}$, define $S^\varepsilon(t) = S_{[t]}^\varepsilon + (t - [t])(S_{[t]+1}^\varepsilon - S_{[t]}^\varepsilon)$ for $t \in [0, K_\varepsilon]$, and define

$$S_n^{\varepsilon,*}(t) = \frac{S^\varepsilon(tn)}{\sqrt{n}} \quad \text{for } t \in [0, 1] \text{ and } n \in \{1, \dots, K_\varepsilon\}.$$

Since Y_n^ε have distribution independent of ε (for $n \leq K_\varepsilon$), we see that $S_n^{\varepsilon,*}(t)$ also have distribution independent of ε (for $n \leq K_\varepsilon$), hence by Theorem 12

$$\lim_{\varepsilon \rightarrow 0} S_{K_\varepsilon}^{\varepsilon,*}(t) = W_t, \quad (89)$$

where the limit is in distribution on $C[0, 1]$.

Our objective will be to use the process $S_{K_\varepsilon}^{\varepsilon,*}(t)$ for the proof of convergence of X_t^ε . Before that we need to prepare some auxiliary facts.

Firstly, from (88) we see that $S_n^\varepsilon(z)$ counts the ‘net’ number of ‘up-down’ steps along the trajectory starting from z , so for $z \in \tilde{A}_\omega$ with $|\omega| = n \leq K_\varepsilon$ we have (see (80))

$$N(\omega) = S_n^\varepsilon(z). \quad (90)$$

For $t \in [0, 1]$ let $k \in \mathbb{N}$ be a number such that $t \in [\varepsilon k, \varepsilon(k+1)]$. We then have

$$k\varepsilon \in [t - \varepsilon, t + \varepsilon], \quad (91)$$

and also, by (83) for such t and k it holds that $k \in [tK_\varepsilon - 1, tK_\varepsilon + 2]$, hence

$$S_k^\varepsilon(z) \in S^\varepsilon(tK_\varepsilon) + [-2, 2]. \quad (92)$$

Since $K_\varepsilon = \lfloor \varepsilon^{-1} \rfloor$,

$$\sqrt{\varepsilon} \in \frac{1}{\sqrt{K_\varepsilon}} + \left[\frac{-1}{2} K_\varepsilon^{-3/2}, \frac{1}{2} K_\varepsilon^{-3/2} \right]. \quad (93)$$

We are now ready for our proof of convergence of X_t^ε . We compute

$$\begin{aligned} X_t^\varepsilon(z) &= \pi_I \Phi_{\varepsilon^{-\gamma} t}^\varepsilon(z) \\ &\in \pi_I \Phi_{k\varepsilon^{-\gamma+1}}^\varepsilon(z) + [-2\sigma\sqrt{\varepsilon}, +2\sigma\sqrt{\varepsilon}] && \text{from (82)} \\ &\subset X_0 + k\mu\varepsilon + S_k^\varepsilon(z)\sigma\sqrt{\varepsilon} + [-M\varepsilon - 2\sigma\sqrt{\varepsilon}, M\varepsilon + 2\sigma\sqrt{\varepsilon}] && \text{from (81),(90)} \\ &\subset X_0 + \mu t + S_k^\varepsilon(z)\sigma\sqrt{\varepsilon} + [-(M+\mu)\varepsilon - 2\sigma\sqrt{\varepsilon}, (M+\mu)\varepsilon + 2\sigma\sqrt{\varepsilon}] \\ &&& \text{from (91)} \\ &\subset X_0 + \mu t + S_k^\varepsilon(z)\sigma\sqrt{\varepsilon} + [-3\sigma\sqrt{\varepsilon}, 3\sigma\sqrt{\varepsilon}] && \text{for small } \varepsilon \\ &\subset X_0 + \mu t + S_k^\varepsilon(tK_\varepsilon)(z)\sigma\sqrt{\varepsilon} + [-5\sigma\sqrt{\varepsilon}, 5\sigma\sqrt{\varepsilon}] && \text{from (92)} \\ &\subset X_0 + \mu t + \sigma S_{K_\varepsilon}^{\varepsilon,*}(t)(z) + \sigma S_{K_\varepsilon}^{\varepsilon,*}(t)(z) \left(\frac{-1}{2K_\varepsilon}, \frac{1}{2K_\varepsilon} \right) + \left[\frac{-6\sigma}{\sqrt{K_\varepsilon}}, \frac{6\sigma}{\sqrt{K_\varepsilon}} \right] \\ &&& \text{from (93)}. \end{aligned}$$

We have therefore shown that

$$X_t^\varepsilon = X_0 + \mu t + \sigma (S_{K_\varepsilon}^{\varepsilon,*}(t) + Z_\varepsilon(t)) \quad (94)$$

where

$$|Z_\varepsilon(t)| \leq \frac{1}{K_\varepsilon} |S_{K_\varepsilon}^{\varepsilon,*}(t)| + \frac{6}{\sqrt{K_\varepsilon}}.$$

Since $Z_\varepsilon(t)$ converges to zero in probability and $S_{K_\varepsilon}^{\varepsilon,*}(t)$ converges in distribution to W_t we obtain that $S_{K_\varepsilon}^{\varepsilon,*}(t) + Z_\varepsilon(t)$ converges in distribution to W_t . This means that from (94) we obtain (74), which concludes our proof. ■

Remark 23 *By a modification of the proof of Theorem 13, by shadowing a random walk with time dependent coefficients, we can obtain convergence to $\mu(t) + \sigma(t)W_t$ for deterministic, continuous functions $\mu(t), \sigma(t)$, $t \in [0, 1]$.*

10.2 Stochastic behavior under conditions on connecting sequences

Proof of Theorem 5. By Theorem 3 we know that we can $\eta\varepsilon$ shadow any sequence of $I^\sigma \in [2\eta\varepsilon, 1 - 2\eta\varepsilon]$. As long as we remain in $\{I \in [2\eta\varepsilon, 1 - 2\eta\varepsilon]\}$ we can shadow the energy levels from the binomial process from Figure 11. Our result follows from the same construction as the proof of Theorem 13 with the only difference that once X_t^ε leaves the set $\{I \in [0, 1]\}$ the assumption **C2** can no longer be used to propagate Q^ε -discs. This is why we stop the considered processes as soon as we exit this set.

One issue we can comment on is the existence of T_0 and M_0 from Condition **A3**, which is part of the assumption of Theorem 13. The T_0 exists, since any map $F_{\ell,\varepsilon}$ associated with the connecting sequence with $\ell \in L$ has a compact domain. We have a finite number of such maps, hence the time needed for the flow to pass through these maps is finite.

For $T_0 > 0$ since the set

$$A(T_0) := [0, T_1] \times [0, \varepsilon_0] \times ((\mathbf{S}^u \cup \mathbf{S}^d) \cap \{I \in [0, 1]\})$$

is compact, we can find $M_0 = M_0(T_0)$ such that

$$\pi_I \Phi_t^\varepsilon(z) - \pi_I z \in [-M_0\varepsilon, M_0\varepsilon] \quad \text{for } (t, \varepsilon, z) \in A(T_0).$$

Such M_0 will be the bound for (72). ■

11 Appendix

11.1 Proof of Lemma 2

Proof. To establish (29) it is enough to show that for all $\varepsilon \in E$ and $z_1, z_2 \in N$ satisfying $Q_a^\varepsilon(z_1 - z_2) > 0$ we have

$$\frac{\|f_\kappa(\varepsilon, z_1) - f_\kappa(\varepsilon, z_2)\|}{\|f_x(\varepsilon, z_1) - f_x(\varepsilon, z_2)\|} < b_\kappa \quad \text{for } \kappa \in \{y, \theta\}, \quad (95)$$

$$\frac{\|f_I(\varepsilon, z_1) - f_I(\varepsilon, z_2)\|}{\|f_x(\varepsilon, z_1) - f_x(\varepsilon, z_2)\|} < \varepsilon b_I. \quad (96)$$

Take $Q_a^\varepsilon(z_1 - z_2) > 0$. Let $z_1 - z_2 = (x, y, I, \theta)$. This means that $\|x\| \neq 0$ and

$$\|y\| / \|x\| \leq a_y, \quad \|I\| / \|x\| \leq \varepsilon a_I, \quad \|\theta\| / \|x\| \leq a_\theta. \quad (97)$$

For $\kappa \in \{x, y, \theta\}$ we compute

$$f_\kappa(\varepsilon, z_1) - f_\kappa(\varepsilon, z_2) = \left(\int_0^1 \frac{\partial f_\kappa}{\partial z}(\varepsilon, z_2 + s(z_1 - z_2)) ds \right) (z_1 - z_2). \quad (98)$$

Using (98) and (97), for $\kappa \in \{y, \theta\}$ we have

$$\begin{aligned} & \frac{\|\pi_\kappa(f_\kappa(\varepsilon, z_1) - f(\varepsilon, z_2))\|}{\|\pi_x(f(\varepsilon, z_1) - f(\varepsilon, z_2))\|} \\ & \leq \frac{\sum_{h \in \{x, y, I, \theta\}} \left\| \left[\frac{\partial f_\kappa}{\partial h} \right] \right\| \|h\|}{m \left(\frac{\partial f_x}{\partial x} \right) \|x\| - \sum_{h \in \{y, I, \theta\}} \left\| \left[\frac{\partial f_\kappa}{\partial h} \right] \right\| \|h\|} \\ & \leq \frac{\left\| \left[\frac{\partial f_\kappa}{\partial x} \right] \right\| + \left\| \left[\frac{\partial f_\kappa}{\partial y} \right] \right\| a_y + \left\| \left[\frac{\partial f_\kappa}{\partial I} \right] \right\| \varepsilon_0 a_I + \left\| \left[\frac{\partial f_\kappa}{\partial \theta} \right] \right\| a_\theta}{m \left(\frac{\partial f_x}{\partial x} \right) - \left\| \left[\frac{\partial f_x}{\partial y} \right] \right\| a_y - \left\| \left[\frac{\partial f_x}{\partial I} \right] \right\| \varepsilon_0 a_I - \left\| \left[\frac{\partial f_x}{\partial \theta} \right] \right\| a_\theta} < b_\kappa \end{aligned}$$

We now turn to establishing (96). We compute

$$\begin{aligned} & f_I(\varepsilon, z_1) - f_I(\varepsilon, z_2) \\ & = f_I(0, z_1) - f_I(0, z_2) + \varepsilon \int_0^1 \left(\frac{\partial f_I}{\partial \varepsilon}(\varepsilon u, z_1) - \frac{\partial f_I}{\partial \varepsilon}(\varepsilon u, z_2) \right) du \\ & = \pi_I(z_1 - z_2) + \varepsilon \left(\int_0^1 \int_0^1 \frac{\partial f_I}{\partial \varepsilon \partial z}(\varepsilon u, z_2 + s(z_1 - z_2)) duds \right) (z_1 - z_2) \end{aligned}$$

This gives

$$\begin{aligned} & \frac{\|f_I(\varepsilon, z_1) - f_I(\varepsilon, z_2)\|}{\|f_x(\varepsilon, z_1) - f_x(\varepsilon, z_2)\|} \\ & \leq \frac{\|I\| + \varepsilon \sum_{h \in \{x, y, I, \theta\}} \left\| \left[\frac{\partial f_I}{\partial \varepsilon \partial h} \right] \right\| \|h\|}{m \left(\frac{\partial f_x}{\partial x} \right) \|x\| - \sum_{h \in \{y, I, \theta\}} \left\| \left[\frac{\partial f_x}{\partial h} \right] \right\| \|h\|} \\ & \leq \varepsilon \frac{a_I + \left\| \left[\frac{\partial f_I}{\partial \varepsilon \partial x} \right] \right\| + \left\| \left[\frac{\partial f_I}{\partial \varepsilon \partial y} \right] \right\| a_y + \left\| \left[\frac{\partial f_I}{\partial \varepsilon \partial I} \right] \right\| a_I \varepsilon_0 + \left\| \left[\frac{\partial f_I}{\partial \varepsilon \partial \theta} \right] \right\| a_\theta}{m \left(\frac{\partial f_x}{\partial x} \right) - \sum_{h \in \{y, \theta, I\}} \left\| \left[\frac{\partial f_x}{\partial h} \right] \right\| a_h} < \varepsilon b_I. \end{aligned}$$

We have established (95–96), which concludes our proof. ■

References

- [1] V.I. Arnold, *Instability of dynamical systems with several degrees of freedom*, Sov. Math. Doklady **5** (1964), 581–585.
- [2] Boris V. Chirikov, *A universal instability of many-dimensional oscillator systems*, Phys. Rep. **52** (1979), no. 5, 264–379. MR536429 (80h:70022)
- [3] M. J. Capiński, M. Gidea, and R. De la Llave, *Arnold diffusion in the planar elliptic restricted three-body problem: mechanism and numerical verification*, Nonlinearity **30** (2017), no. 1, 329–360.

- [4] Piotr Zgliczyński, *Covering relations, cone conditions and the stable manifold theorem*, J. Differential Equations **246** (2009), no. 5, 1774–1819. MR2494688
- [5] Piotr Zgliczyński and Marian Gidea, *Covering relations for multidimensional dynamical systems*, J. Differential Equations **202** (2004), no. 1, 32–58. MR2060531 (2005c:37019a)
- [6] L. Chierchia and G. Gallavotti, *Drift and diffusion in phase space*, Ann. Inst. H. Poincaré Phys. Théor. **60** (1994), no. 1, 144. MR1259103 (95b:58056)
- [7] Ugo Bessi, *An approach to Arnold's diffusion through the calculus of variations*, Nonlinear Anal. **26** (1996), no. 6, 1115–1135. MR1375654
- [8] Massimiliano Berti and Philippe Bolle, *A functional analysis approach to Arnold diffusion*, Ann. Inst. H. Poincaré Anal. Non Linéaire **19** (2002), no. 4, 395–450. MR1912262
- [9] S. Bolotin and D. Treschev, *Unbounded growth of energy in nonautonomous Hamiltonian systems*, Nonlinearity **12** (1999), no. 2, 365–388. MR1677779 (99m:58086)
- [10] D. Treschev, *Trajectories in a neighbourhood of asymptotic surfaces of a priori unstable Hamiltonian systems*, Nonlinearity **15** (2002), no. 6, 2033–2052. MR1938480 (2003j:37093)
- [11] ———, *Evolution of slow variables in a priori unstable Hamiltonian systems*, Nonlinearity **17** (2004), no. 5, 1803–1841. MR2086152 (2005g:37116)
- [12] ———, *Arnold diffusion far from strong resonances in multidimensional a priori unstable Hamiltonian systems*, Nonlinearity **25** (2012), no. 9, 2717–2757. MR2967122
- [13] Amadeu Delshams, Rafael de la Llave, and Tere M. Seara, *A geometric approach to the existence of orbits with unbounded energy in generic periodic perturbations by a potential of generic geodesic flows of \mathbf{T}^2* , Comm. Math. Phys. **209** (2000), no. 2, 353–392. MR1737988 (2001a:37086)
- [14] Ernest Fontich and Pau Martín, *Arnold diffusion in perturbations of analytic integrable Hamiltonian systems*, Discrete and Continuous Dynamical Systems **7** (2001), no. 1, 61–84.
- [15] Amadeu Delshams, Rafael de la Llave, and Tere M Seara, *A geometric mechanism for diffusion in Hamiltonian systems overcoming the large gap problem: heuristics and rigorous verification on a model*, Mem. Amer. Math. Soc. **179** (2006), no. 844, viii+141. MR2184276 (2009m:37170)
- [16] ———, *Orbits of unbounded energy in quasi-periodic perturbations of geodesic flows*, Adv. Math. **202** (2006), no. 1, 64–188. MR2218821 (2007a:37070)
- [17] Vassili Gelfreich and Dmitry Turaev, *Unbounded energy growth in Hamiltonian systems with a slowly varying parameter*, Comm. Math. Phys. **283** (2008), no. 3, 769–794. MR2434747 (2009j:37092)
- [18] G. N. Piftankin, *Diffusion speed in the Mather problem*, Dokl. Akad. Nauk **408** (2006), no. 6, 736–737. MR2350915 (2008m:37102)
- [19] V. Kaloshin, *Geometric proofs of Mather's connecting and accelerating theorems*, Topics in dynamics and ergodic theory, 2003, pp. 81–106. MR2052276 (2005c:37114)
- [20] Patrick Bernard, Vadim Kaloshin, and Ke Zhang, *Arnold diffusion in arbitrary degrees of freedom and normally hyperbolic invariant cylinders*, Acta Math. **217** (2016), no. 1, 1–79. MR3646879
- [21] V. Kaloshin and K. Zhang, *Normally hyperbolic invariant manifolds near strong double resonance*, 2012.
- [22] ———, *A strong form of Arnold diffusion for two and a half degrees of freedom*, 2012.
- [23] Ke Zhang, *Speed of Arnold diffusion for analytic Hamiltonian systems*, Invent. Math. **186** (2011), no. 2, 255–290. MR2845619
- [24] Abed Bounemoura, *An example of instability in high-dimensional Hamiltonian systems*, Int. Math. Res. Not. IMRN **3** (2012), 685–716. MR2885986
- [25] Chong-Qing Cheng and Jun Yan, *Existence of diffusion orbits in a priori unstable Hamiltonian systems*, J. Differential Geom. **67** (2004), no. 3, 457–517. MR2153027 (2006d:37110)
- [26] ———, *Arnold diffusion in Hamiltonian systems: a priori unstable case*, J. Differential Geom. **82** (2009), no. 2, 229–277. MR2520793
- [27] C.-Q. Cheng, *Arnold diffusion in nearly integrable Hamiltonian systems*, ArXiv e-prints (July 2012), available at 1207.4016.

- [28] C.-Q. Cheng and J. Xue, *Arnold diffusion in nearly integrable hamiltonian systems of arbitrary degrees of freedom*, 2015.
- [29] M. Gidea and C. Robinson, *Diffusion along transition chains of invariant tori and Aubry-Mather sets*, *Ergodic Theory Dynam. Systems* **33** (2013), 1401–1449.
- [30] Jean-Pierre Marco, *Arnold diffusion for cusp-generic nearly integrable convex systems on \mathbb{A}^3* , arXiv preprint arXiv:1602.02403 (2016).
- [31] ———, *Chains of compact cylinders for cusp-generic nearly integrable convex systems on \mathbb{A}^3* , arXiv preprint arXiv:1602.02399 (2016).
- [32] Marian Gidea and Jean-Pierre Marco, *Diffusion along chains of normally hyperbolic cylinders*, arXiv preprint arXiv:1708.08314 (2017).
- [33] Amadeu Delshams, Rafael de la Llave, and Tere M. Seara, *Instability of high dimensional Hamiltonian systems: multiple resonances do not impede diffusion*, *Adv. Math.* **294** (2016), 689–755. MR3479576
- [34] Marian Gidea, Rafael de la Llave, and Tere M-Seara, *A general mechanism of diffusion in hamiltonian systems: Qualitative results*, *Communications on Pure and Applied Mathematics* **73** (2020), no. 1, 150–209, available at <https://onlinelibrary.wiley.com/doi/pdf/10.1002/cpa.21856>.
- [35] JL Tennyson, MA Lieberman, and AJ Lichtenberg, *Diffusion in near-integrable hamiltonian systems with three degrees of freedom*, *Aip conference proceedings*, 1980, pp. 272–301.
- [36] Jeffrey Tennyson, *Resonance transport in near-integrable systems with many degrees of freedom*, *Phys. D* **5** (1982), no. 1, 123–135. MR83k:70027
- [37] M. A. Lieberman and Jeffrey L. Tennyson, *Chaotic motion along resonance layers in near-integrable Hamiltonian systems with three or more degrees of freedom*, *Long-time prediction in dynamics* (Lake-way, Tex., 1981), 1983, pp. 179–211. MR714724 (84i:58081)
- [38] A. J. Lichtenberg and M. A. Lieberman, *Regular and chaotic dynamics*, Second, *Applied Mathematical Sciences*, vol. 38, Springer-Verlag, New York, 1992. MR1169466 (93c:58071)
- [39] Jacques Laskar, *Frequency analysis for multi-dimensional systems. Global dynamics and diffusion*, *Phys. D* **67** (1993), no. 1-3, 257–281. MR1234445 (94k:58087)
- [40] George M Zaslavsky and Georgij Moisevič Zaslavskij, *Hamiltonian chaos and fractional dynamics*, Oxford University Press on Demand, 2005.
- [41] Claude Froeschlé, Elena Lega, and Massimiliano Guzzo, *Analysis of the chaotic behaviour of orbits diffusing along the Arnold web*, *Periodic, quasi-periodic and chaotic motions in celestial mechanics: Theory and applications*, 2006, pp. 141–153.
- [42] Massimiliano Guzzo, Elena Lega, and Claude Froeschle, *A numerical study of Arnold diffusion in a priori unstable systems*, *Communications in Mathematical Physics* **290** (2009), no. 2, 557–576.
- [43] Massimiliano Guzzo, Elena Lega, and Claude Froeschlé, *First numerical evidence of global Arnold diffusion in quasi-integrable systems*, *Discrete Contin. Dyn. Syst. Ser. B* **5** (2005), no. 3, 687–698. MR2151727 (2005m:37139)
- [44] John N. Mather, *Arnol'd diffusion. I. Announcement of results*, *J. Math. Sci. (N. Y.)* **124** (2004), no. 5, 5275–5289. MR2129140 (2005m:37142)
- [45] ———, *Arnold diffusion by variational methods*, *Essays in mathematics and its applications*, 2012, pp. 271–285. MR2975591
- [46] Pablo M Cincotta, *Arnold diffusion: an overview through dynamical astronomy*, *New Astronomy Reviews* **46** (2002), no. 1, 13–39.
- [47] Jacques Laskar, ACM Correia, Mickael Gastineau, Frédéric Joutel, Benjamin Levrard, and Philippe Robutel, *Long term evolution and chaotic diffusion of the insolation quantities of Mars*, *Icarus* **170** (2004), no. 2, 343–364.
- [48] Alejandro Luque and Daniel Peralta-Salas, *Arnold diffusion of charged particles in ABC magnetic fields*, *J. Nonlinear Sci.* **27** (2017), no. 3, 721–774. MR3638320
- [49] Zhihong Xia, *Arnold diffusion in the elliptic restricted three-body problem*, *Journal of Dynamics and Differential Equations* **5** (1993), no. 2, 219–240.

- [50] Richard Moeckel, *Transition tori in the five-body problem*, Journal of Differential Equations **129** (1996), no. 2, 290–314.
- [51] Joseph Galante and Vadim Kaloshin, *Destruction of invariant curves in the restricted circular planar three-body problem by using comparison of action*, Duke mathematical Journal **159** (2011), no. 2, 275–327.
- [52] Jacques Féjoz, Marcel Guardia, Vadim Kaloshin, and Pablo Roldán, *Kirkwood gaps and diffusion along mean motion resonances in the restricted planar three-body problem*, J. Eur. Math. Soc. **18** (2016), 2315–2403, available at [1109.2892](#).
- [53] Maciej J Capiński and Piotr Zgliczyński, *Transition tori in the planar restricted elliptic three-body problem*, Nonlinearity **24** (2011), no. 5, 1395.
- [54] A. Delshams, M. Gidea, and P. Roldan, *Transition map and shadowing lemma for normally hyperbolic invariant manifolds*, Discrete and Continuous Dynamical Systems. Series A. **3** (2013), no. 33, 1089–1112.
- [55] Jinxin Xue, *Arnold diffusion in a restricted planar four-body problem*, Nonlinearity **27** (2014), no. 12, 2887.
- [56] Amadeu Delshams, Vadim Kaloshin, Abraham de la Rosa, and Tere M. Seara, *Global instability in the restricted planar elliptic three body problem*, Comm. Math. Phys. **366** (2019), no. 3, 1173–1228. [MR3927089](#)
- [57] Massimiliano Berti and Philippe Bolle, *Fast Arnold diffusion in systems with three time scales*, Discrete Contin. Dyn. Syst. **8** (2002), no. 3, 795–811. [MR1897882](#)
- [58] Massimiliano Berti, Luca Biasco, and Philippe Bolle, *Drift in phase space: a new variational mechanism with optimal diffusion time*, J. Math. Pures Appl. (9) **82** (2003), no. 6, 613–664. [MR1996776](#)
- [59] Ugo Bessi, Luigi Chierchia, and Enrico Valdinoci, *Upper bounds on Arnold diffusion times via Mather theory*, J. Math. Pures Appl. (9) **80** (2001), no. 1, 105–129. [MR2002a:37093](#)
- [60] Marian Gidea and Rafael de la Llave, *Topological methods in the instability problem of Hamiltonian systems*, Discrete Contin. Dyn. Syst. **14** (2006), no. 2, 295–328. [MR2163534 \(2006i:37130\)](#)
- [61] Pierre Lochak and Jean-Pierre Marco, *Diffusion times and stability exponents for nearly integrable analytic systems*, Cent. Eur. J. Math. **3** (2005), no. 3, 342–397 (electronic). [MR2152466 \(2006i:37131\)](#)
- [62] Marian Gidea and Rafael de la Llave, *Perturbations of geodesic flows by recurrent dynamics*, Journal of the European Mathematical Society **19** (2017), no. 3, 905–956.
- [63] Massimiliano Guzzo, Christos Efthymiopoulos, and Rocío I Paez, *Semi-analytic computations of the speed of Arnold diffusion along single resonances in a priori stable Hamiltonian systems*, Journal of Nonlinear Science (2019), 1–51.
- [64] Anton Gorodetski and Vadim Kaloshin, *Hausdorff dimension of oscillatory motions in the restricted planar circular three body problem and in Sitnikov problem*, 2011. preprint.
- [65] D Sauzin, *Ergodicity and conservativity in the random iteration of standard maps*, preprint (2006).
- [66] David Sauzin, *Exemples de diffusion d’Arnold avec convergence vers un mouvement brownien*, preprint (2006).
- [67] Oriol Castejón, Marcel Guardia, and Vadim Kaloshin, *Random iteration of cylinder maps and diffusive behavior away from resonances*, arXiv preprint [arXiv:1705.09571](#) (2017).
- [68] Vadim Kaloshin, Jianlu Zhang, and Ke Zhang, *Normally hyperbolic invariant laminations and diffusive behaviour for the generalized Arnold example away from resonances*, arXiv preprint [arXiv:1511.04835](#) (2015).
- [69] Allan J Lichtenberg and Michael A Lieberman, *Regular and stochastic motion*, Vol. 38, Springer Science & Business Media, 2013.
- [70] V. Kaloshin and P. Roldan, *Numerical evidence of stochastic diffusive behavior for Arnold’s example and the 3:1 Kirkwood gap*. in preparation.
- [71] V. Szebehely, *Theory of orbits: The restricted problem of three bodies*, Academic Press, 1967.
- [72] Craig B Agnor and Douglas P Hamilton, *Neptune’s capture of its moon Triton in a binary–planet gravitational encounter*, Nature **441** (2006), no. 7090, 192.

- [73] R Easton, *Orbit structure near trajectories biasymptotic to invariant tori*, Classical mechanics and dynamical systems **70** (1981).
- [74] Patrick Billingsley, *Convergence of probability measures*, Wiley, 1999.
- [75] Siegfried M. Rump, *Verification methods: rigorous results using floating-point arithmetic*, Acta Numer. **19** (2010), 287–449. MR2652784
- [76] R. Lohner and E. Adams, *Einschließung der Lösung gewöhnlicher Anfangs- und Randwertaufgaben*, Z. Angew. Math. Mech. **64** (1984), no. 5, 295–297. MR754513
- [77] Piotr Zgliczyński, *C^1 Lohner algorithm*, Found. Comput. Math. **2** (2002), no. 4, 429–465. MR1930946
- [78] Daniel Wilczak and Piotr Zgliczyński, *C^r Lohner algorithm*, Schedae Informaticae **20** (2012), 9–42.
- [79] Tomasz Kapela, Marian Mrozek, Daniel Wilczak, and Piotr Zgliczyński, *CAPD::DynSys: a flexible C++ toolbox for rigorous numerical analysis of dynamical systems.*, To appear in: Commun. Nonlinear Sci. (2020).
- [80] Warwick Tucker, *A rigorous ODE solver and Smale’s 14th problem*, Foundations of Computational Mathematics **2** (2002), no. 1, 53–117.
- [81] Amadeu Delshams, Rafael de la Llave, and Tere M. Seara, *Geometric properties of the scattering map of a normally hyperbolic invariant manifold*, Adv. Math. **217** (2008), no. 3, 1096–1153. MR2383896 (2008m:37100)
- [82] Kenneth Falconer, *Fractal geometry*, Second, John Wiley & Sons, Inc., Hoboken, NJ, 2003. Mathematical foundations and applications. MR2118797
- [83] Peter Mörters and Yuval Peres, *Brownian motion*, Cambridge Series in Statistical and Probabilistic Mathematics, vol. 30, Cambridge University Press, Cambridge, 2010. With an appendix by Oded Schramm and Wendelin Werner. MR2604525